BioMed Research International

Bioenergy and Biomass Utilization

Guest Editors: Guangli Cao, Dexun Zou, Ximing Zhang, Lei Zhao, and Guojun Xie

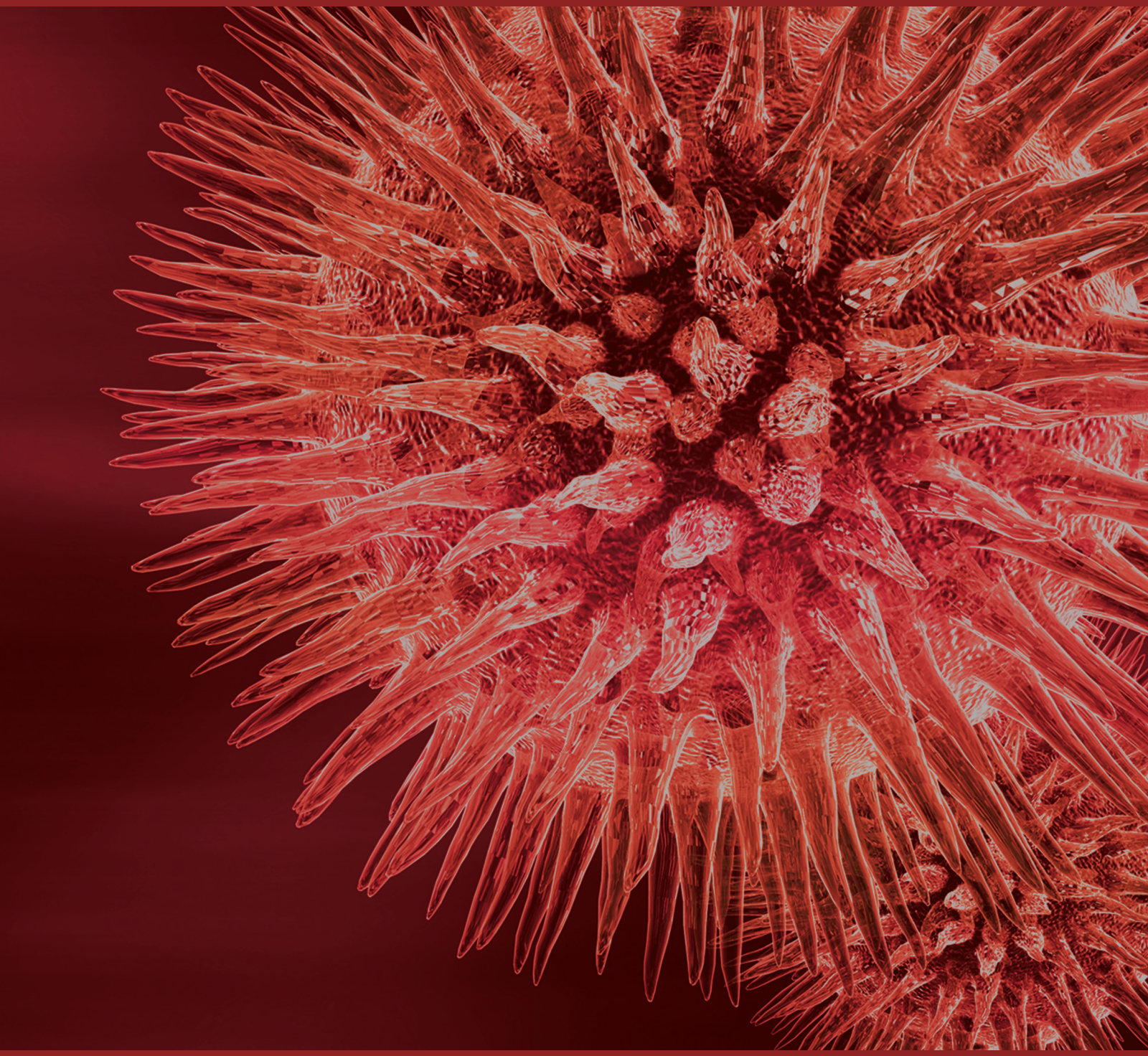

Bioenergy and Biomass Utilization

BioMed Research International

Bioenergy and Biomass Utilization

Guest Editors: Guangli Cao, Dexun Zou, Ximing Zhang, Lei Zhao, and Guojun Xie

Contents

Hindawi Publishing Corporation
BioMed Research International
Volume 2015, Article ID 857568, 2 pages
http://dx.doi.org/10.1155/2015/857568

Editorial

Bioenergy and Biomass Utilization

Guangli Cao,[1] Dexun Zou,[2] Ximing Zhang,[3] Lei Zhao,[4] and Guojun Xie[5]

[1]*School of Life Science and Technology, Harbin Institute of Technology, Harbin 150001, China*
[2]*College of Chemical Engineering, Beijing University of Chemical Technology, Beijing 100029, China*
[3]*Laboratory of Renewable Resources Engineering, Purdue University, West Lafayette, IN 47907-2032, USA*
[4]*State Key Laboratory of Urban Water Resource and Environment, Harbin Institute of Technology, Harbin 150090, China*
[5]*Advanced Water Management Centre, The University of Queensland, Brisbane, QLD 4072, Australia*

Correspondence should be addressed to Guangli Cao; caogl@hit.edu.cn

Received 20 April 2015; Accepted 20 April 2015

Bioenergy is of increasing interest as a renewable, environmentally friendly alternative to energy derived from fossil fuels. Through a variety of processes, biomass can be converted to solid, liquid, or gaseous biofuels. However, various challenges persist to the maintenance and development of biomass-to-energy utilization. This special issue focuses on the most recent advances in the frontier research of bioenergy and biomass utilization and features six selected papers with high quality.

The paper titled "Nanofibrillated Cellulose and Copper Nanoparticles Embedded in Polyvinyl Alcohol Films for Antimicrobial Applications" by T. Zhong et al. develops a method to produce hybrids of TEMPO nanofibrillated cellulose (TNFC) and copper nanoparticles. The hybrid material is embedded in polyvinyl alcohol thermoplastic resin and the films are produced using a solvent casting method. The authors evaluate the films in terms of its morphology and thermal and antimicrobial properties and prove that TNFC-copper nanoparticles as antimicrobial nanofillers are valuable for PVA applications.

The paper titled "Response of Arbuscular Mycorrhizal Fungi to Hydrologic Gradients in the Rhizosphere of *Phragmites australis* (Cav.) Trin ex. Steudel Growing in the Sun Island Wetland" by L. Wang et al. assesses the variations of hydrologic gradients in the relationships among AM fungi, reed, and rhizospheric microorganisms. The authors discover water content in soil and reed growth parameters are both positively associated with AM fungi colonization, but only the positive correlations between reed biomass parameters and the colonization could be expected, or both the host plant biomass and the AM fungi could be beneficial. This study could shed light on the mechanisms inside AM fungi-reed symbioses and would be referred to for optimizing the combined phytorhizoremediation.

The paper titled "Production by Tobacco Transplastomic Plants of Recombinant Fungal and Bacterial Cell-Wall Degrading Enzymes to Be Used for Cellulosic Biomass Saccharification" by L. Paolo et al. presents work on saccharification of plant biomass. The authors express in tobacco chloroplasts microbial genes encoding five cellulases and a polygalacturonase. Leaf extracts containing the recombinant enzymes show the ability to degrade various cell-wall components under different conditions. In addition, a thermostable xylanase is also tested in combination with a cellulase and a polygalacturonase to study the cumulative effect on the depolymerization of a complex plant substrate. Results demonstrate the feasibility of using transplastomic tobacco leaf extracts to convert cell-wall polysaccharides into reducing sugars, fulfilling a major prerequisite of large scale availability of a variety of cell-wall degrading enzymes for biofuel industry.

The paper titled "Enzymatic Saccharification of Lignocellulosic Residues by Cellulases Obtained from Solid State Fermentation Using *Trichoderma viride*" by T. Sartori et al. presents an approach that uses cellulolytic complex produced by *Trichoderma viride* in solid state fermentation to hydrolyze lignocellulosic residues. This produced enzyme shows viability in comparison with the commercial cellulase enzyme. The

synthesis of cellulases by microorganisms from lignocellulosic residues is a process of great interest, representing the search for renewable sources to replace the fossil energetic matrix.

The paper titled "Improving Biomethane Production and Mass Bioconversion of Corn Stover Anaerobic Digestion by Adding NaOH Pretreatment and Trace Elements" by C. Liu et al. describes an approach to improve biomethane production from corn stover. The authors use NaOH pretreatment and trace elements supplementation as a strategy to enhance the biodegradability of corn stover for biomethane production. The approach is compared with only NaOH-pretreated and untreated corn stover, and the paper highlights the supplementation of trace elements.

The paper titled "Biochemical Modulation of Lipid Pathway in Microalgae *Dunaliella* sp. for Biodiesel Production," by A. F. Talebi et al., explores the use of myoinositol to modulate LP and biodiesel quality. Inclusion of myoinositol in the media indeed improves the total lipid accumulation and biodiesel quality parameters, and this work highlights the fact that the biochemical modulation strategies should be progressively considered in the hope of finding more efficient and economically feasible strategies leading to more viable production systems.

Acknowledgment

The guest editors are thankful to the reviewers for their efforts in reviewing the manuscripts.

Guangli Cao
Dexun Zou
Ximing Zhang
Lei Zhao
Guojun Xie

Hindawi Publishing Corporation
BioMed Research International
Volume 2015, Article ID 810124, 9 pages
http://dx.doi.org/10.1155/2015/810124

Research Article

Response of Arbuscular Mycorrhizal Fungi to Hydrologic Gradients in the Rhizosphere of *Phragmites australis* (Cav.) Trin ex. Steudel Growing in the Sun Island Wetland

Li Wang, Jieting Wu, Fang Ma, Jixian Yang, Shiyang Li, Zhe Li, and Xue Zhang

State Key Lab of Urban Water Resource and Environment, School of Municipal and Environmental Engineering, Harbin Institute of Technology, Harbin 150090, China

Correspondence should be addressed to Fang Ma; mafang@hit.edu.cn

Received 29 September 2014; Accepted 6 January 2015

Academic Editor: Guo-Jun Xie

Within the rhizosphere, AM fungi are a sensitive variable to changes of botanic and environmental conditions, and they may interact with the biomass of plant and other microbes. During the vegetative period of the *Phragmites australis* growing in the Sun Island Wetland (SIW), the variations of AM fungi colonization were studied. Root samples of three hydrologic gradients generally showed AM fungi colonization, suggesting that AM fungi have the ability for adaptation to flooded habitats. There were direct and indirect hydrological related effects with respect to AM fungi biomass, which interacted simultaneously in the rhizosphere. Though water content in soil and reed growth parameters were both positively associated with AM fungi colonization, only the positive correlations between reed biomass parameters and the colonization could be expected, or both the host plant biomass and the AM fungi could be beneficial. The variations in response of host plant to the edaphic and hydrologic conditions may influence the effectiveness of the plant-mycorrhizal association. This study included a hydrologic component to better assess the role and distribution of AM fungi in wetland ecosystems. And because of that, the range of AM fungi was extended, since they actually showed a notable adaptability to hydrologic gradients.

1. Introduction

Interactions between plants and their rhizosphere microorganisms can significantly affect the corresponding ecosystem function. One key microbial component of the rhizosphere is the arbuscular mycorrhizal fungi (AM fungi), which can form symbiotic relationships with the majority of terrestrial plant roots [1]. These ubiquitous fungi are grouped into the phylum *Glomeromycota*. They can form living root-soil links and a specific zone of soil, which is called mycorrhizosphere [2]. The AM fungi can have an effect on rhizosphere through various mechanisms, such as alterations in soil properties, microbial community, and/or root exudates [3–5]. The symbiosis may help plants to thrive by colonizing a wide soil volume, accelerating photosynthesis, protecting plants against plant pathogens and pests in soil, absorbing resources efficiently, and dissipating of pollutants from the soil [4, 6–8]. They also have the ability for adaptation to different conditions and being synergistic with indigenous soil microorganisms [9]. It has also been proposed that AM fungi can increase the solubility of some immobile nutrients by releasing certain enzymes [10].

AM fungi can form symbiotic relationships with the majority of terrestrial plant biomass. But because the soils of wetlands are often saturated and subsequently lack available oxygen for aerobic soil microorganisms, AM fungi were historically thought to be rare in wetland ecosystem [1, 11]. As a result, although the effects of AM fungi on plant and soil in terrestrial ecosystems are well known [12, 13], these fungi in aquatic and wetland habitats have gotten little attention [14, 15]. Recently, an increasing number of studies have revealed that AM fungi exist in wetland habitats [16, 17]. Stevens et al. [17] found AM fungi colonization in 31 plant species in a bottomland hardwood forest. Besides, several wetland plant species that were thought to be nonmycorrhizal have been found to have high levels of AM fungi colonization

[18]. It is now recognized that AM fungi are prevalent in wetlands [14]. It has been also suggested that the success of ecosystem reforestation efforts is likely to depend on the establishment of mycorrhizas, and AM fungi should receive special attention in indigenous plant biomass production and restoration [19]. However, the factors which affect the levels of AM fungi colonization and the relationships between plant biomass, native rhizospheric microorganism communities, and AM fungi in wetland habitats are poorly understood [15].

Because *Phragmites australis* (Cav.) Trin ex. Steudel is a widespread helophyte characteristic of the ecotone between terrestrial and aquatic environments in freshwater to brackish water bodies [20], exhibiting a wide tolerance to the conditions [21], especially to water depth [22], it was chosen as the object plant of this research. AM fungi have been reported on reed [1], and one of the important reasons may be that reed can vent its underground tissues [23]. However, previous researchers have rarely clarified the relationship between AM fungi and reed establishment in wetlands and investigated whether this symbiotic phenomenon depended on the habitat conditions [24]. Though these studies differ greatly with respect to sampling time and venue, it is still difficult to identify which is the primary factor influencing the patterns of AM fungi colonization across different hydrologic gradients, because the fungi in aquatic and wetland habitats have been paid little attention for the reasons mentioned above. Therefore, the specific aims were (1) to assess the variations of hydrologic gradients in the relationships among AM fungi, reed, and rhizospheric microorganisms; (2) to investigate the possible factors that affect AM fungi colonization and determine the primary one among them. The main findings could shed some light on the mechanisms inside AM fungi-reed symbioses and would be referred to optimize the application of phyto-rhizoremediation.

2. Materials and Methods

2.1. Sample Collection and Analysis. The Sun Island Wetland (SIW) is located at 126°31′–126°36′E, 45°41′–45°47′N on the north shore of Songhua River (Harbin, China). SIW is in the temperate continental monsoon climate zone. During June (summer) and October (autumn) of both 2010 and 2011, the mean daily air temperatures ranged from 16.0 to 26.0°C in June and from 2.6 to 11.2°C in October, while the mean daily relative humidity ranged from 46.7 to 88.7% in June and from 48.2 to 80.7% in October. The Sun Island Wetland is in a triple functional zone overlapped by urbanization areas, development zones, and scenic spots [25].

Three sampling areas were chosen along the hydrologic gradients of SIW (about 50 meters apart). Point SIW1 is flooded with water, the reeds growing in this area are frequently submerged to a depth of up to 15 cm and the soil is always waterlogged. Point SIW2 is located in the river bank, where flooding rarely occurs but where the soil is frequently waterlogged during the wet period. Point SIW3, only water saturated, is located at the outermost bank of the river, where the reeds still have a sufficient water supply from the river during the dry period. During the summer and autumn of 2010-2011, ten samples (including reed plant and rhizospheric soil) were selected from each of the three sampling areas randomly, and each sample was collected within a plot (about $30 \times 30 \times 30\,\text{cm}^3$).

Sampling was conducted during 2010 and 2011, the samples were analyzed immediately after they were collected and the backup samples were temporarily stored in a refrigerator to keep them fresh. Each rhizospheric soil sample was divided into 3 parts; one part was stored in 4°C to keep fresh for Biolog, the second part was stored in −20°C for DGGE, and the third part was dried to a constant weight for element analysis. Each plant sample was divided into two parts; one part was stored in refrigerator temporarily to keep fresh and the other part was dried to a constant weight for element analysis. Fine fresh roots were carefully separated from the soil and fixed in ethanol for later studies of AM fungi colonization. The organic matter content of soil was determined by the wet combustion method [26]. The content of organic C was determined by Total Organic Carbon Analyzer (SSM-5000A; Shimadzu Corp., Kyoto, Japan). The content of total N and total S in the soil was determined by a Carbon/Nitrogen/Oxygen/Sulphur Analyzer (Vario EL; Elementar Analysensysteme GmbH, Hanau, Germany). The dried samples were homogenized and subsequently mineralized with HNO_3 (67%)-HCl (30%)-HF (49%) acids (5 : 2 : 2, V/V/V) in Microwave Digestion System (MARS-5; CEM, Matthews, North Carolina), and then the mineralized samples were analyzed for total P, K, Ca, and Mg, using Inductively Coupled Plasma-Atomic Emission Spectrometry (ICP-AES) (Perkin Elmer Optima 5300DV, Waltham, Massachusetts).

2.2. Rhizospheric Microbial Characteristics Analysis. Community level physiological profiles (CLPPs) were assessed by the Biolog EcoPlateTM system (Biolog Inc., CA, USA) as described by Gomez et al. [27]. The color development in each well was recorded as optical density (OD) at 590 nm and 750 nm with a plate reader at regular 24-hour intervals [28]. All work during plate preparation was done under a laminar-flow hood to minimize the risk of contamination.

Microbial activity in each microplate, expressed as average well-color development (AWCD), was determined as follows [27]:

$$\text{AWCD} = \frac{\sum \text{OD}_i}{31}, \tag{1}$$

where OD_i is the optical density value from each well [28].

The Shannon-Weaver diversity index (H) and richness index (S) were calculated using an OD of 0.25 as threshold for positive response, which was described by Garland and Derry et al. [29, 30]:

$$H = -\sum p_i \left(\ln p_i\right), \tag{2}$$

where p_i is the ratio of the activity on each substrate to the sum of activities on all substrates.

The DGGE profiles were assessed by the DCode system (BioRad Co., Ltd., USA). The DNA of rhizospheric microbes was extracted with a FastDNA Spin Kit for Soil

Table 1: Characteristics of arbuscular mycorrhizal fungi colonization of *Phragmites australis*. Area SW1 is flooded with water sometimes; the reeds growing in this area are frequently submerged to a depth of up to 15 cm and the soil is always waterlogged. Area SW2 is located in the river bank, where flooding rarely occurs but the soil is always saturated during the wet period. Area SW3, only humid, is located at the outermost bank of the river, where the reeds still have a sufficient water supply from the river during the dry period. S: summer; A: autumn.

	S			A		
	SIW1	SIW2	SIW3	SIW1	SIW2	SIW3
Hyphae	19.2 ± 3.56^{A}	17.7 ± 2.18^{A}	13.2 ± 2.19^{A}	21.6 ± 3.51^{b}	16.6 ± 2.34^{b}	9.3 ± 2.2^{a}
Vesicles	5.6 ± 0.65^{B}	3.7 ± 0.45^{A}	2.9 ± 0.29^{A}	4.7 ± 0.59^{c}	3.6 ± 0.53^{b}	2.3 ± 0.38^{a}
Arbuscules	3.5 ± 0.35^{B}	2.9 ± 0.3^{AB}	2.7 ± 0.35^{A}	7.9 ± 1.1^{a}	7.2 ± 1.33^{a}	6.3 ± 0.9^{a}
Frequency	26.3 ± 2.38^{B}	23.2 ± 3.64^{B}	16.1 ± 2.7^{A}	33.2 ± 4.92^{b}	27.2 ± 4.29^{a}	16.9 ± 1.99^{a}
Intensity	7.4 ± 0.62^{B}	6.3 ± 0.95^{AB}	5.4 ± 0.78^{A}	11.7 ± 2.5^{b}	9.2 ± 1.76^{a}	5.5 ± 0.91^{a}

Different letters in uppercase indicate significant difference between three hydrologic gradients in summer (S) ($\alpha = 0.05$) after one-way ANOVA (Duncan test). Different letters in lowercase indicate significant difference between three hydrologic gradients in autumn (A) ($\alpha = 0.05$) after one-way ANOVA (Duncan test). Data are mean ± SD ($n = 30$).

(Q-Biogene, Vista, CA, USA). The extracted DNA was used as a template for PCR. The primers of bacteria, actinomycetes, and fungi for the PCR amplification were designed, respectively, and the corresponding thermocycling conditions were set. Genes of bacteria were amplified with primers GC-341F (5′-CCTACGGGAGGCAGCAG-3′) and 534R (5′-ATTACCGCGGCTGCTGG-3′). The thermocycling conditions were (touchdown PCR) 3 min at 95°C, followed by 20 cycles of 30 s at 95°C (annealing for 30 s with a 0.5°C/cycle decrement until the 56°C is reached), 1 min at 72°C, 35 cycles of 30 s at 95°C and 30 s at 56°C and 1 min at 72°C, and a final extension for 5 min at 72°C [31, 32]. Genes of fungi were amplified with primers GC-FR1 (5′-AICCATTCAATCGGTAIT-3′) and FF390 (5′-CGATAACGAACGAGACCT-3′). The thermocycling conditions were 8 min at 95°C, followed by 30 cycles of 30 s at 95°C and 45 s at 50°C, 2 min at 72°C, and a final extension for 10 min at 72°C [33]. Electrophoresis was performed in a DCode system (Bio-Rad Co., Ltd., Hercules, California). The DGGE profiles were analyzed by software "Quantity One version 4.6.2" (BIO-RAD Laboratories, Inc., USA).

The Shannon-Weaver diversity index (H) and richness index (S) were determined according to the following equation as described by Yang et al. [34]:

$$H = -\sum p_i (\ln p_i) = -\sum \left(\frac{N_i}{N}\right) \ln \left(\frac{N_i}{N}\right), \quad (3)$$

where p_i is the percentage of the DGGE band gray degree to each DNA sample, N_i is the net gray degree quantity (subtracted by the background gray degree quantity of a gel) of the DGGE band to each DNA sample, N is the total net gray degree quantity, and S is the number of DGGE bands to each DNA sample (richness index).

2.3. Assessment of AM Fungi Colonization. Samples of fine roots were cleared in 10% w/v KOH and stained with 0.5% acid fuchsin as described by Li et al. [35]. Root colonization described as the percentage of root length with hyphae or vesicles was estimated using a line intercept approach and determined using procedures described by McGonigle et al. [36]. Root segments were examined under a microscope (Olympus CX31, Olympus). For assessment of AM colonization levels, the variables considered to characterize AM colonization were the percentages of arbuscules (A%), hyphae (H%), vesicles (V%), mycorrhizal frequency (F%), and mycorrhizal intensity (M%) [37]. Hyphae were only scored if attached to other AM fungi structures [38]. Thirty root fragments of each plant individuals were used to estimate AM fungi colonization parameters of reed.

2.4. Statistics and Data Analyses. Standard error (SD) was used as a measure of variance. One-way ANOVA (Duncan test) was performed to ascertain whether parameters were significantly different among treatments ($\alpha = 0.05$). The bivariate correlations (Pearson correlation coefficient) were performed, via using SPSS Statistical Software Package (version 17.0) (SPSS Inc., Chicago, Illinois) for Windows.

3. Results

AM fungi colonization was observed through a microscope (Figure 1). Regardless of the hydrologic gradient, mean values for the proportion of root segment colonized by hypha ranged from 13% to 20%, which were less variable than the vesicle colonization (ranged from 2% to 6%) and the arbuscules colonization (ranged from 2% to 8%) (Table 1). Despite the AM fungi structures (hypha, vesicle, and arbuscules) intensity in roots of *Ph. australis* was not high, it showed a tendency to change along with the hydrologic gradient, with the general order: SIW1 > SIW2 > SIW3. The AM fungi hypha colonization varied significantly between SIW1 and SIW3 (autumn), but no significant difference was found between SIW1 and SIW2 (autumn). In contrast, the AM fungi arbuscules colonization varied significantly between SIW1 and SIW3 (summer), but no significant difference was found between SIW1 and SIW2 (summer). In addition, the frequency and intensity of AM fungi colonization also varied significantly between SIW1 and SIW3 both in summer and autumn, but there were no significant differences between SIW1 and SIW2 (summer).

Correlation analyses were performed between the AM fungi colonization and the rhizosphere soil physicochemical properties of *Ph. australis* (Table 2). Note that the moisture content had significant positive relationships with arbuscular

Table 2: Coefficients of Pearson's correlations between the characteristics of arbuscular mycorrhizal fungi colonization and the rhizosphere soil physicochemical properties of *Phragmites australis* (MC: moisture content; OM: organic matter; OC: organic carbon).

	pH	MC (%)	OM (%)	OC (%)	N ($mg\,kg^{-1}$)	P ($mg\,kg^{-1}$)	S ($mg\,kg^{-1}$)	K ($mg\,kg^{-1}$)	Ca ($mg\,kg^{-1}$)	Mg ($mg\,kg^{-1}$)
SIW1	8.23	28.13	15.73	13551	957	413.3	396.7	20523	12145	992
SIW2	8.26	20.87	16.69	15327	1065	432.1	287.9	22367	14003	1132
SIW3	8.28	12.52	12.24	18256	1193	481.2	271.1	23579	13795	1171
AIW1	7.69	27.51	13.52	11095	836	262.9	357.3	19333	8753	1272
AIW2	7.71	23.01	13.75	12337	893	331.9	230.1	20471	8886	1333
AIW3	7.76	11.05	11.86	14511	997	396.7	219.9	23451	11795	1354
Hyphae	ns	**	ns	ns	ns	ns	ns	ns	ns	ns
Vesicles	ns	**	ns	ns	ns	ns	ns	ns	ns	ns
Arbuscules	−**	ns	ns	ns	ns	ns	ns	ns	−*	ns
Frequency	ns	**	ns	−*	−*	−*	ns	−*	ns	ns
Intensity	ns	ns	ns	−*	−*	−*	ns	−*	−*	ns

ns: no significant correlation at the 0.05 level (2-tailed).
*Correlation is significant at the 0.05 level (2-tailed).
**Correlation is significant at the 0.01 level (2-tailed).

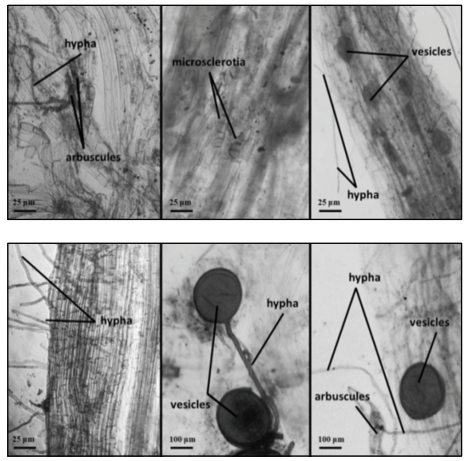

Figure 1: Arbuscular mycorrhizal structures in the roots of *Phragmites australis*.

Table 3: Coefficients of Pearson's correlations between the characteristics of arbuscular mycorrhizal fungi colonization and the characteristics of the rhizospheric microbial community of *Phragmites australis*. ((*H*): Shannon-Weaver diversity index; (*S*): Shannon-Weaver richness index; B: bacteria; A: actinomycetes; F: fungi).

	Genetic characteristics				Metabolic characteristics		
	(*H*)-B	(*H*)-F	(*S*)-B	(*S*)-F	AWCD	(*H*)	(*S*)
SIW1	3.2	2.91	25	19	0.64	2.62	3.2
SIW2	3.45	3.06	32	22	0.67	2.89	3.45
SIW3	3.46	3.1	32	23	0.65	2.73	3.46
AIW1	2.98	2.18	20	9	0.57	2.29	2.98
AIW2	3.08	2.47	22	12	0.63	2.55	3.08
Hyphae	ns	ns	ns	ns	ns	ns	ns
Vesicles	ns	ns	ns	ns	ns	ns	ns
Arbuscules	−**	−*	−**	−*	−*	−*	−*
Frequency	ns	−*	ns	−*	ns	ns	ns
Intensity	ns	−**	ns	−**	ns	ns	ns

ns: no significant correlation at the 0.05 level (2-tailed).
*Correlation is significant at the 0.05 level (2-tailed).
**Correlation is significant at the 0.01 level (2-tailed).

mycorrhizal fungi colonization (hyphae, vesicles and the mycorrhizal frequency). In contrast, pH, organic carbon, total N, total P, total K, and Ca had significant negative relationships with arbuscular mycorrhizal fungi colonization. In addition, compared to the arbuscular mycorrhizal structures (hyphae, vesicles, and arbuscules), the frequency and intensity have relationships with more physicochemical properties.

Correlation analyses were also performed between the AM fungi colonization and the characteristics of the rhizospheric microbial community of *Ph. australis* (Table 3). Note that the rhizospheric microbial biomass had significant negative relationships with the frequency and intensity of arbuscular mycorrhizal fungi colonization, especially the arbuscules. In contrast, hyphae and vesicles had no significant negative relationships with arbuscular mycorrhizal fungi colonization. Besides, compared to the frequency and intensity, the arbuscules have relationships with more physicochemical properties.

In addition, correlation analyses were performed between the AM fungi colonization and the growth parameters of *Ph. australis* (Table 4). The results indicated that the biomass of *Ph. australis* had significant positive relationships with the arbuscules, the arbuscular mycorrhizal frequency and intensity. In contrast, hyphae and vesicles had no significant relationships with arbuscular mycorrhizal fungi colonization. Besides, the frequency and intensity have relationships with all the related physicochemical properties.

Table 4: Coefficients of Pearson's correlations between the characteristics of arbuscular mycorrhizal fungi colonization and the growth parameters of *Phragmites australis*. (ShL: shoot length; BD: basal diameter; LA: leaf area; RaL: rachis length; ShW: shoot dry weight).

	ShL (cm)	BD (mm)	LA (cm^2)	RaL (cm)	ShW (g)
SIW1	174.37	8.73	325.62	21.3	8.49
SIW2	128.36	8.43	301.35	18.2	7.09
SIW3	116.35	7.73	171.03	15.6	5.69
AIW1	265.49	9.47	399.24	27.2	19.06
AIW2	225.46	8.93	382.32	25.2	15.55
SIW1	207.51	8.53	260.22	22.9	11.38
Hyphae	ns	ns	ns	ns	ns
Vesicles	ns	ns	ns	ns	ns
Arbuscules	**	ns	ns	ns	**
Frequency	*	*	**	**	*
Intensity	*	*	*	**	*

ns: no significant correlation at the 0.05 level (2-tailed).
*Correlation is significant at the 0.05 level (2-tailed).
**Correlation is significant at the 0.01 level (2-tailed).

4. Discussion

AM fungi have the ability for adaptation to different conditions [9]. The variations of hydrologic gradients in the relationships among the components of reed rhizosphere were studied, which showed that AM fungi were present along hydrologic gradients in the wetland of Northeast China. The maximum colonization occurred at the sampling point with the highest moisture content (SW1) and was minimal in the rhizosphere with the lowest moisture content (SWA3), which suggested that AM fungi not only have the ability for adaptation to aquatic and wetland habitats, but also have preferential colonization with respect to hydrologic gradient. Observed variations in the dynamics of different AM fungi structures were significant in this research. Previous studies proved that AM fungi dynamics are strongly affected by their capacity to colonize in roots and scavenge carbohydrates and minerals, respectively. These direct and indirect effects with respect to AM fungi interact simultaneously in the rhizosphere [39]. Consequently, we hypothesize that both habitat condition (living matter and nonliving matter) and host plant growth can affect the dynamics of AM fungi. However, we still need to know whose effect is greater.

One of the possible factors affecting AM fungi colonization was water level changing. However, there is no consensus about the effect of moisture content on AM fungi growth. The effect of increase in moisture content in soil on AM fungi colonization has been generally documented: when plants become submerged, a decrease in AM fungi colonization is usually found [1], because the saturated soil subsequently lacks available oxygen for aerobic soil microorganisms, such as AM fungi [11]. But some studies proved that there are no relationships between AM fungi colonization and moisture content [40]. As reported by some researchers, once AM fungi symbiosis was established, subsequent increase in water level or even permanent flooding did not affect their colonization in the roots [1, 41]. In addition, although the growth of external mycelium of AM fungi is thought to be improved by organic matter content [42], the carbon incorporated into AM fungi biomass actually originates from plant photosynthates rather than the surrounding organic matter [43]. But the organic matter could still act as an important source of other nutrients, such as P, for AM fungi [44]. The results suggested that soil organic matter content maybe not the principal promoter of AM fungi colonization. In addition, the trend that moisture content in soil was positively associated with AM fungi root colonization probably could explain the fact that AM fungi growth was suppressed by certain environmental factors which were decreasing with moisture content, such as P. P was proved to have negative effects on AM fungi growth [45, 46]. In such an intermittent ecosystem, the amount of plant available nutrients depends on soil moisture and oxygen availability, which may disguise the relationships between soil properties and AM fungi colonization [1]. Moreover, the AM fungi biomass could also affect the properties of rhizosphere through indirect mechanisms including altering soil acidity [3] and producing more root exudates [47]. Thus, we still requires more details to determine how the variations of soil parameters and water level combinedly affect AM fungi colonization on the Sun Island Wetland.

Moisture content in soil was associated with AM fungi colonization, which also suggested that moisture content possibly affected AM fungi through changing their symbiotic partners: the indigenous rhizospheric microorganisms and host plant. Therefore, another possible factors affecting AM fungi colonization could be rhizospheric microorganisms. The plant rhizosphere is a dynamic complex system in which many parameters may influence the population structure, diversity, and activity of the microbial community [48]. Therefore, the interactions between AM fungi and other indigenous soil organisms are complex. The reciprocal effect of AM fungi and rhizospheric microorganisms has also been widely examined, but principally using in vitro systems [49, 50]. For instance, Filion et al. [51] showed that exudates from the hyphae of *Glomus intraradices* could stimulate the

growth of certain microorganisms on agar. In this study, DGGE and Biolog were used to assess the microbial community characteristics in the rhizosphere of reed in different ways. It is well known that AM fungi are synergistic with mycorrhizal helper bacteria and plant growth-promoting rhizobacteria [52, 53]. Though beneficial interactions have been frequently mentioned [54], other evidence has also suggested antagonistic interactions with bacteria, fungi, and microarthropods that may affect the functioning of the AM fungi symbioses [55–57]. We expected to find that the AM fungi influenced the indigenous microbial community and benefited from it. However, the results did not support this synergistic relationship. What we found was that AM fungi growth was seemly reduced by certain indigenous soil microorganisms and the presence of AM fungi did not increase the diversity and richness of the microbial community. Several authors also reported that AM fungi may play a role in controlling soil microbial communities [58]. Either the competition for resources between AM fungi and other microorganisms or the suppressive effects of certain types of microorganisms on AM fungi growth may lead to reduction in the growth of AM fungi. Competition between AM fungi and soil microorganisms may attribute to the so-called Gadgil effect [59]. Leigh et al. [60] found that the absence of live bacterial inoculums could increase the P concentration in AM fungi hyphae colonized root, because the competition between AM fungi and bacteria inhibited the ability of AM fungi to acquire resources directly from organic matter. Other researchers also suggested that the effects of microbial community on AM fungi growth and function were greater than the reciprocal impact [60]. de Jaeger et al. [61] demonstrated that *Trichoderma harzianum* was able to impact the viability of AM fungi by feeding on its intra- and extraradical mycelium under in vitro controlled conditions. In natural ecosystems, the rhizosphere effects may be the dominant influence [62, 63]. However, there is no consensus about the effect of microbial communities on AM fungi growth [64].

The lack of positive correlation between AM fungi colonization and the habitat (living and nonliving matter) of *Ph. australis* rhizosphere was possibly due to the fact that plant growth exerted relatively dominant effect on mycorrhizal colonization. The results suggest that more vigorous plants could maintain higher AM fungi colonization rate. Since *Ph. australis* is a kind of well-adapted helophyte to water level fluctuation, the phenomenon that AM fungi colonized reed under flooded conditions is not illogical. Their ability to survive in such conditions is mainly due to the aerenchyma in the stems and roots, through which the host plants can ventilate their own underground tissues by pressurized gas flow [23]. From this perspective, the more vigorously host plants grow, the better their stems and roots develop. As a result, the more oxygen can be delivered to promote the AM fungi dynamics in the root system. Vice versa, the results also suggest the converse that AM fungi colonization could promote plant growth. A positive in situ correlation between reed biomass and AM fungi can be expected in this research, but whether the enhanced plant sturdiness is the consequence or the promoter of AM fungi colonization is difficult to establish. AM fungi can form symbiotic associations with the roots of most terrestrial plants and provide many benefits including improved nutrient uptake, flood and drought resistance, and herbivore resistance [13, 65]. It is well known that arbuscules are the major site for the transfer of minerals and carbohydrates between both partners of the symbiosis [13]. Because AM fungi can promote decomposition of organic material [66] and acquire substantial amounts of N that can be transferred to plant partners [67], AM fungi are antagonistic to pathogenic microorganisms and synergistic with plant growth-promoting rhizobacteria [53, 68]. The effects of AM fungi on biomass of various plant species have been reported mainly in studies under experimental conditions with controlled environmental and soil parameters [41, 69, 70]. Field studies that have focused on the benefits of AM fungi for plant biomass are rarely documented [71]. Therefore, further studies should be conducted to ascertain these results under controlled conditions.

In conclusion, this study included hydrologic components to better assess the dynamics, distribution, and role of AM fungi in wetland ecosystems. Although moisture content in soil and reed growth parameters were both positively associated with AM fungi colonization, only the correlation between reed biomass and AM fungi can be expected. Since AM fungi showed a response to the conditions of their host plant and performed as a tie of the tripartite correspondence between the symbiotic partners of plant biomass and rhizospheric microbial biomass, its application as a biomonitor should be considered in further research.

Conflict of Interests

The authors declare that there is no conflict of interests regarding the publication of this paper.

Acknowledgments

This work was supported by National Natural Science Foundation of China (51179041), the Major Science and Technology Program for Water Pollution Control and Treatment (2012ZX07201003), the National Creative Research Group from the National Natural Science Foundation of China (51121062), and the State Key Lab of Urban Water Resource and Environment, Harbin Institute of Technology, China (HIT) (2014TS05).

References

[1] N. Dolinar and A. Gaberščik, "Mycorrhizal colonization and growth of *Phragmites australis* in an intermittent wetland," *Aquatic Botany*, vol. 93, no. 2, pp. 93–98, 2010.

[2] D. Redecker and P. Raab, "Phylogeny of the *Glomeromycota* (arbuscular mycorrhizal fungi): recent developments and new gene markers," *Mycologia*, vol. 98, no. 6, pp. 885–895, 2006.

[3] X.-L. Li, E. George, and H. Marschner, "Phosphorus depletion and pH decrease at the root-soil and hyphae- soil interfaces of VA mycorrhizal white clover fertilized with ammonium," *New Phytologist*, vol. 119, no. 3, pp. 397–404, 1991.

[4] L. Lioussanne, F. Perreault, M. Jolicoeur, and M. St-Arnaud, "The bacterial community of tomato rhizosphere is modified by inoculation with arbuscular mycorrhizal fungi but unaffected by soil enrichment with mycorrhizal root exudates or inoculation with *Phytophthora nicotianae*," *Soil Biology and Biochemistry*, vol. 42, no. 3, pp. 473–483, 2010.

[5] K. H. Söderberg, P. A. Olsson, and E. Bååth, "Structure and activity of the bacterial community in the rhizosphere of different plant species and the effect of arbuscular mycorrhizal colonisation," *FEMS Microbiology Ecology*, vol. 40, no. 3, pp. 223–231, 2002.

[6] R. M. Dunham, A. M. Ray, and R. S. Inouye, "Growth, physiology, and chemistry of mycorrhizal and nonmycorrhizal *Typha latifolia* seedlings," *Wetlands*, vol. 23, no. 4, pp. 890–896, 2003.

[7] E. J. Joner, A. Johansen, A. P. Loibner et al., "Rhizosphere effects on microbial community structure and dissipation and toxicity of polycyclic aromatic hydrocarbons (PAHs) in spiked soil," *Environmental Science and Technology*, vol. 35, no. 13, pp. 2773–2777, 2001.

[8] R. T. Koide and B. Mosse, "A history of research on arbuscular mycorrhiza," *Mycorrhiza*, vol. 14, no. 3, pp. 145–163, 2004.

[9] M. Miransari, H. A. Bahrami, F. Rejali, and M. J. Malakouti, "Effects of soil compaction and arbuscular mycorrhiza on corn (*Zea mays* L.) nutrient uptake," *Soil and Tillage Research*, vol. 103, no. 2, pp. 282–290, 2009.

[10] H. Marschner and B. Dell, "Nutrient uptake in mycorrhizal symbiosis," *Plant and Soil*, vol. 159, no. 1, pp. 89–102, 1994.

[11] B. E. Wolfe, D. L. Mummey, M. C. Rillig, and J. N. Klironomos, "Small-scale spatial heterogeneity of arbuscular mycorrhizal fungal abundance and community composition in a wetland plant community," *Mycorrhiza*, vol. 17, no. 3, pp. 175–183, 2007.

[12] H. Evelin, R. Kapoor, and B. Giri, "Arbuscular mycorrhizal fungi in alleviation of salt stress: a review," *Annals of Botany*, vol. 104, no. 7, pp. 1263–1280, 2009.

[13] S. E. Smith, E. Facelli, S. Pope, and F. A. Smith, "Plant performance in stressful environments: interpreting new and established knowledge of the roles of arbuscular mycorrhizas," *Plant and Soil*, vol. 326, no. 1, pp. 3–20, 2010.

[14] K. J. Stevens and R. L. Peterson, "Relationships among three pathways for resource acquisition and their contribution to plant performance in the emergent aquatic plant *Lythrum salicaria* (L.)," *Plant Biology*, vol. 9, no. 6, pp. 758–765, 2007.

[15] K. J. Stevens, C. B. Wall, and J. A. Janssen, "Effects of arbuscular mycorrhizal fungi on seedling growth and development of two wetland plants, *Bidens frondosa* L., and *Eclipta prostrata* (L.) L., grown under three levels of water availability," *Mycorrhiza*, vol. 21, no. 4, pp. 279–288, 2011.

[16] D. Kandalepas, K. J. Stevens, G. P. Shaffer, and W. J. Platt, "How abundant are root-colonizing fungi in Southeastern Louisiana's degraded marshes?" *Wetlands*, vol. 30, no. 2, pp. 189–199, 2010.

[17] K. J. Stevens, M. R. Wellner, and M. F. Acevedo, "Dark septate endophyte and arbuscular mycorrhizal status of vegetation colonizing a bottomland hardwood forest after a 100 year flood," *Aquatic Botany*, vol. 92, no. 2, pp. 105–111, 2010.

[18] A. M. Hirsch and Y. Kapulnik, "Signal transduction pathways in mycorrhizal associations: comparisons with the Rhizobium-legume symbiosis," *Fungal Genetics and Biology*, vol. 23, no. 3, pp. 205–212, 1998.

[19] T. Wubet, I. Kottke, D. Teketay, and F. Oberwinkler, "Mycorrhizal status of indigenous trees in dry Afromontane forests of Ethiopia," *Forest Ecology and Management*, vol. 179, no. 1–3, pp. 387–399, 2003.

[20] A. Mauchamp and M. Méthy, "Submergence-induced damage of photosynthetic apparatus in *Phragmites australis*," *Environmental and Experimental Botany*, vol. 51, no. 3, pp. 227–235, 2004.

[21] C. Hudon, P. Gagnon, and M. Jean, "Hydrological factors controlling the spread of common reed (*Phragmites australis*) in the St. Lawrence River (Québec, Canada)," *Ecoscience*, vol. 12, no. 3, pp. 347–357, 2005.

[22] A. I. Engloner and M. Papp, "Vertical differences in *Phragmites australis* culm anatomy along a water depth gradient," *Aquatic Botany*, vol. 85, no. 2, pp. 137–146, 2006.

[23] H. Brix, B. K. Sorrell, and H. H. Schierup, "Gas fluxes achieved by in situ convective flow in *Phragmites australis*," *Aquatic Botany*, vol. 54, no. 2-3, pp. 151–163, 1996.

[24] S. G. R. Wirsel, "Homogenous stands of a wetland grass harbour diverse consortia of arbuscular mycorrhizal fungi," *FEMS Microbiology Ecology*, vol. 48, no. 2, pp. 129–138, 2004.

[25] J. Wu, L. Wang, F. Ma, J. Yang, S. Li, and Z. Li, "Effects of vegetative-periodic-induced rhizosphere variation on the uptake and translocation of metals in *Phragmites australis* (Cav.) Trin ex. Steudel growing in the Sun Island Wetland," *Ecotoxicology*, vol. 22, no. 4, pp. 608–618, 2013.

[26] E. Kandeler, "Organic matter by wet combustion," in *Methods in Soil Biology*, F. Schinner, R. Öhlinger, E. Kandeler, and R. Margesin, Eds., pp. 397–398, Springer, Berlin, Germany, 1st edition, 1995.

[27] E. Gomez, L. Ferreras, and S. Toresani, "Soil bacterial functional diversity as influenced by organic amendment application," *Bioresource Technology*, vol. 97, no. 13, pp. 1484–1489, 2006.

[28] A. T. Classen, S. I. Boyle, K. E. Haskins, S. T. Overby, and S. C. Hart, "Community-level physiological profiles of bacteria and fungi: plate type and incubation temperature influences on contrasting soils," *FEMS Microbiology Ecology*, vol. 44, no. 3, pp. 319–328, 2003.

[29] A. M. Derry, W. J. Staddon, P. G. Kevan, and J. T. Trevors, "Functional diversity and community structure of microorganisms in three arctic soils as determined by sole-carbon-source-utilization," *Biodiversity & Conservation*, vol. 8, no. 2, pp. 205–221, 1999.

[30] J. L. Garland, "Analysis and interpretation of community-level physiological profiles in microbial ecology," *FEMS Microbiology Ecology*, vol. 24, no. 4, pp. 289–300, 1997.

[31] S. A. Huws, J. E. Edwards, E. J. Kim, and N. D. Scollan, "Specificity and sensitivity of eubacterial primers utilized for molecular profiling of bacteria within complex microbial ecosystems," *Journal of Microbiological Methods*, vol. 70, no. 3, pp. 565–569, 2007.

[32] G. Muyzer, E. C. De Waal, and A. G. Uitterlinden, "Profiling of complex microbial populations by denaturing gradient gel electrophoresis analysis of polymerase chain reaction-amplified genes coding for 16S rRNA," *Applied and Environmental Microbiology*, vol. 59, no. 3, pp. 695–700, 1993.

[33] E. J. Vainio and J. Hantula, "Direct analysis of wood-inhabiting fungi using denaturing gradient gel electrophoresis of amplified ribosomal DNA," *Mycological Research*, vol. 104, no. 8, pp. 927–936, 2000.

[34] Y.-H. Yang, J. Yao, S. Hu, and Y. Qi, "Effects of agricultural chemicals on DNA sequence diversity of soil microbial community: a study with RAPD marker," *Microbial Ecology*, vol. 39, no. 1, pp. 72–79, 2000.

[35] L.-F. Li, Y. Zhang, and Z.-W. Zhao, "Arbuscular mycorrhizal colonization and spore density across different land-use types

in a hot and arid ecosystem, Southwest China," *Journal of Plant Nutrition and Soil Science*, vol. 170, no. 3, pp. 419–425, 2007.

[36] T. P. McGonigle, M. H. Miller, D. G. Evans, G. L. Fairchild, and J. A. Swan, "A new method which gives an objective measure of colonization of roots by vesicular-arbuscular mycorrhizal fungi," *New Phytologist*, vol. 115, no. 3, pp. 495–501, 1990.

[37] N. Šraj-Kržič, P. Pongrac, M. Klemenc, A. Kladnik, M. Regvar, and A. Gaberščik, "Mycorrhizal colonisation in plants from intermittent aquatic habitats," *Aquatic Botany*, vol. 85, no. 4, pp. 331–336, 2006.

[38] A. M. Ray and R. S. Inouye, "Effects of water-level fluctuations on the arbuscular mycorrhizal colonization of *Typha latifolia* L," *Aquatic Botany*, vol. 84, no. 3, pp. 210–216, 2006.

[39] M. Ijdo, N. Schtickzelle, S. Cranenbrouck, and S. Declerck, "Do arbuscular mycorrhizal fungi with contrasting life-history strategies differ in their responses to repeated defoliation?" *FEMS Microbiology Ecology*, vol. 72, no. 1, pp. 114–122, 2010.

[40] K. E. Bohrer, C. F. Friese, and J. P. Amon, "Seasonal dynamics of arbuscular mycorrhizal fungi in differing wetland habitats," *Mycorrhiza*, vol. 14, no. 5, pp. 329–337, 2004.

[41] S. P. Miller and R. R. Sharitz, "Manipulation of flooding and arbuscular mycorrhiza formation influences growth and nutrition of two semiaquatic grass species," *Functional Ecology*, vol. 14, no. 6, pp. 738–748, 2000.

[42] T. V. St. John, D. C. Coleman, and C. P. P. Reid, "Association of vesicular-arbuscular mycorrhizal hyphae with soil organic particles," *Ecology*, vol. 64, no. 4, pp. 957–959, 1983.

[43] M. E. Gavito and P. A. Olsson, "Allocation of plant carbon to foraging and storage in arbuscular mycorrhizal fungi," *FEMS Microbiology Ecology*, vol. 45, no. 2, pp. 181–187, 2003.

[44] S. Ravnskov, J. Larsen, P. A. Olsson, and I. Jakobsen, "Effects of various organic compounds on growth and phosphorus uptake of an arbuscular mycorrhizal fungus," *New Phytologist*, vol. 141, no. 3, pp. 517–524, 1999.

[45] R. C. Anderson, A. E. Liberta, and L. A. Dickman, "Interaction of vascular plants and vesicular-arbuscular mycorrhizal fungi across a soil moisture-nutrient gradient," *Oecologia*, vol. 64, no. 1, pp. 111–117, 1984.

[46] M. Landwehr, U. Hildebrandt, P. Wilde et al., "The arbuscular mycorrhizal fungus *Glomus geosporum* in European saline, sodic and gypsum soils," *Mycorrhiza*, vol. 12, no. 4, pp. 199–211, 2002.

[47] F. Laheurte, C. Leyval, and J. Berthelin, "Root exudates of maize, pine and beech seedlings influenced by mycorrhizal and bacterial inoculation," *Symbiosis*, vol. 9, pp. 111–116, 1990.

[48] P. Garbeva, J. D. van Elsas, and J. A. van Veen, "Rhizosphere microbial community and its response to plant species and soil history," *Plant and Soil*, vol. 302, no. 1-2, pp. 19–32, 2008.

[49] V. Artursson, R. D. Finlay, and J. K. Jansson, "Combined bromodeoxyuridine immunocapture and terminal-restriction fragment length polymorphism analysis highlights differences in the active soil bacterial metagenome due to *Glomus mosseae* inoculation or plant species," *Environmental Microbiology*, vol. 7, no. 12, pp. 1952–1966, 2005.

[50] J. F. Toljander, B. D. Lindahl, L. R. Paul, M. Elfstrand, and R. D. Finlay, "Influence of arbuscular mycorrhizal mycelial exudates on soil bacterial growth and community structure," *FEMS Microbiology Ecology*, vol. 61, no. 2, pp. 295–304, 2007.

[51] M. Filion, M. St-Arnaud, and J. A. Fortin, "Direct interaction between the arbuscular mycorrhizal fungus *Glomus intraradices* and different rhizosphere microorganisms," *New Phytologist*, vol. 141, no. 3, pp. 525–533, 1999.

[52] E. Gamalero, A. Trotta, N. Massa, A. Copetta, M. G. Martinotti, and G. Berta, "Impact of two fluorescent pseudomonads and an arbuscular mycorrhizal fungus on tomato plant growth, root architecture and P acquisition," *Mycorrhiza*, vol. 14, no. 3, pp. 185–192, 2004.

[53] A. Marulanda-Aguirre, R. Azcón, J. M. Ruiz-Lozano, and R. Aroca, "Differential effects of a *Bacillus megaterium* strain on *Lactuca sativa* plant growth depending on the origin of the arbuscular mycorrhizal fungus coinoculated: physiologic and biochemical traits," *Journal of Plant Growth Regulation*, vol. 27, no. 1, pp. 10–18, 2008.

[54] P. Bonfante and I.-A. Anca, "Plants, mycorrhizal fungi, and bacteria: a network of interactions," *Annual Review of Microbiology*, vol. 63, pp. 363–383, 2009.

[55] M. Bonkowski, C. Villenave, and B. Griffiths, "Rhizosphere fauna: the functional and structural diversity of intimate interactions of soil fauna with plant roots," *Plant and Soil*, vol. 321, no. 1-2, pp. 213–233, 2009.

[56] M. Miransari, "Interactions between arbuscular mycorrhizal fungi and soil bacteria," *Applied Microbiology and Biotechnology*, vol. 89, no. 4, pp. 917–930, 2011.

[57] S. Purin and M. C. Rillig, "Parasitism of arbuscular mycorrhizal fungi: reviewing the evidence," *FEMS Microbiology Letters*, vol. 279, no. 1, pp. 8–14, 2008.

[58] C. Wamberg, S. Christensen, I. Jakobsen, A. K. Müller, and S. J. Sørensen, "The mycorrhizal fungus (*Glomus intraradices*) affects microbial activity in the rhizosphere of pea plants (*Pisum sativum*)," *Soil Biology and Biochemistry*, vol. 35, no. 10, pp. 1349–1357, 2003.

[59] R. L. Gadgil and P. D. Gadgil, "Mycorrhiza and litter decomposition," *Nature*, vol. 233, no. 5315, p. 133, 1971.

[60] J. Leigh, A. H. Fitter, and A. Hodge, "Growth and symbiotic effectiveness of an arbuscular mycorrhizal fungus in organic matter in competition with soil bacteria," *FEMS Microbiology Ecology*, vol. 76, no. 3, pp. 428–438, 2011.

[61] N. de Jaeger, S. Declerck, and I. E. de la Providencia, "Mycoparasitism of arbuscular mycorrhizal fungi: a pathway for the entry of saprotrophic fungi into roots," *FEMS Microbiology Ecology*, vol. 73, no. 2, pp. 312–322, 2010.

[62] J. F. Johansson, L. R. Paul, and R. D. Finlay, "Microbial interactions in the mycorrhizosphere and their significance for sustainable agriculture," *FEMS Microbiology Ecology*, vol. 48, no. 1, pp. 1–13, 2004.

[63] E. Paterson, "Importance of rhizodeposition in the coupling of plant and microbial productivity," *European Journal of Soil Science*, vol. 54, no. 4, pp. 741–750, 2003.

[64] L. J. C. Xavier and J. J. Germida, "Bacteria associated with Glomus clarum spores influence mycorrhizal activity," *Soil Biology & Biochemistry*, vol. 35, no. 3, pp. 471–478, 2003.

[65] M. Søndergaard and S. Laegaard, "Vesicular-arbuscular mycorrhiza in some aquatic vascular plants," *Nature*, vol. 268, no. 5617, pp. 232–233, 1977.

[66] A. Hodge, C. D. Campbell, and A. H. Fitter, "An arbuscular mycorrhizal fungus accelerates decomposition and acquires nitrogen directly from organic material," *Nature*, vol. 413, no. 6853, pp. 297–299, 2001.

[67] J. Leigh, A. Hodge, and A. H. Fitter, "Arbuscular mycorrhizal fungi can transfer substantial amounts of nitrogen to their host plant from organic material," *New Phytologist*, vol. 181, no. 1, pp. 199–207, 2009.

[68] H. H. Zhu, L. K. Long, S. Z. Yang, and Q. Yao, "Influence of AM fungus on *Ralstonia solanacearum* population and bacterial community structure in rhizosphere," *Mycosystema*, vol. 24, pp. 137–142, 2005 (Chinese).

[69] F. Ø. Andersen and T. Andersen, "Effects of arbuscular mycorrhizae on biomass and nutrients in the aquatic plant *Littorella uniflora*," *Freshwater Biology*, vol. 51, no. 9, pp. 1623–1633, 2006.

[70] K. Jayachandran and K. G. Shetty, "Growth response and phosphorus uptake by arbuscular mycorrhizae of wet prairie sawgrass," *Aquatic Botany*, vol. 76, no. 4, pp. 281–290, 2003.

[71] I. R. Sanders and A. H. Fitter, "The ecology and functioning of vesicular-arbuscular mycorrhizas in co-existing grassland species. II. Nutrient uptake and growth of vesicular-arbuscular mycorrhizal plants in a semi-natural grassland," *New Phytologist*, vol. 120, no. 4, pp. 525–533, 1992.

Hindawi Publishing Corporation
BioMed Research International
Volume 2015, Article ID 597198, 12 pages
http://dx.doi.org/10.1155/2015/597198

Research Article

Biochemical Modulation of Lipid Pathway in Microalgae *Dunaliella* sp. for Biodiesel Production

Ahmad Farhad Talebi,[1] Masoud Tohidfar,[2,3] Seyedeh Mahsa Mousavi Derazmahalleh,[4] Alawi Sulaiman,[2,5] Azhari Samsu Baharuddin,[6] and Meisam Tabatabaei[2,3]

[1]*Microbial Biotechnology Department, Semnan University, Semnan 35131-19111, Iran*
[2]*Microbial Biotechnology and Biosafety Department, Agricultural Biotechnology Research Institute of Iran (ABRII), Karaj 31359-33151, Iran*
[3]*Biofuel Research Team (BRTeam), Karaj 31438-44693, Iran*
[4]*Genomics Department, Agricultural Biotechnology Research Institute of Iran (ABRII), Karaj 31359-33151, Iran*
[5]*Tropical Agro-Biomass (TAB) Group, Faculty of Plantation and Agrotechnology, Universiti Teknologi MARA (UiTM), 40450 Shah Alam, Malaysia*
[6]*Faculty of Engineering, Universiti Putra Malaysia (UPM), 43400 Serdang, Malaysia*

Correspondence should be addressed to Azhari Samsu Baharuddin; azharis@eng.upm.edu.my and Meisam Tabatabaei; meisam_tab@yahoo.com

Received 31 October 2014; Revised 7 January 2015; Accepted 8 January 2015

Academic Editor: Ximing Zhang

Exploitation of renewable sources of energy such as algal biodiesel could turn energy supplies problem around. Studies on a locally isolated strain of *Dunaliella* sp. showed that the mean lipid content in cultures enriched by 200 mg L^{-1} myoinositol was raised by around 33% (1.5 times higher than the control). Similarly, higher lipid productivity values were achieved in cultures treated by 100 and 200 mg L^{-1} myoinositol. Fluorometry analyses (microplate fluorescence and flow cytometry) revealed increased oil accumulation in the Nile red-stained algal samples. Moreover, it was predicted that biodiesel produced from myoinositol-treated cells possessed improved oxidative stability, cetane number, and cloud point values. From the genomic point of view, real-time analyses revealed that myoinositol negatively influenced transcript abundance of *AccD* gene (one of the key genes involved in lipid production pathway) due to feedback inhibition and that its positive effect must have been exerted through other genes. The findings of the current research are not to interprete that myoinositol supplementation could answer all the challenges faced in microalgal biodiesel production but instead to show that "there is a there there" for biochemical modulation strategies, which we achieved, increased algal oil quantity and enhanced resultant biodiesel quality.

1. Introduction

Commercial and industrial microalgae cultivation is of growing interest for numerous applications, including production of food, fertilizer, bioplastics, and pharmaceuticals, as well as algal fuel [1, 2]. Among algal species, the microalga *Dunaliella* spp. are known as the best commercial natural source for the production of *cis*-β-carotene. Besides, several biochemical and genetical engineering investigations have demonstrated that different species of *Dunaliella* spp. are capable of accumulating significant amounts of valuable compound such as proteins, glycerol, and also lipids [3]. As a result, they are not only a promising feedstock for biofuel production, for example, biodiesel [4], but also could potentially be used for different biotechnological processes such as foreign proteins expression and β-carotene production at industrial level [5]. In order to fully and economically exploit these organisms, however, some existing barriers for their large-scale cultivation should be overcome. On such basis, low cost and high quality biomass production is of great significance. To achieve such goal for biodiesel production, for instance, the following strategies could be taken into consideration in

order to boost biomass productivity (BP) and volumetric lipid productivity (LP) [6].

(A) Introduction of new genes into algal cells by implementation of genetic engineering techniques stimulates some key metabolic pathways and consequently improves the energy production phenotypes in green microalgae [7] and ultimately produces biofuel at lower cost. However, despite the fact that the underlying principles laid out in this strategy are reasonable, there has been little achievement made to date. For instance, the very first genetic engineering attempts in order to increase microalgal lipid content (LC) by upregulating the first major steps of fatty acid synthesis through overexpression of acetyl-CoA carboxylase (*ACCase*) and malic enzyme were to some extent effective (12% increase in LC) [8]. Blocking-off competing pathways may also enhance the lipid accumulation in the cells. In an attempt, Picataggio and coworkers [9] blocked β-oxidation in *C. tropicalis* by knocking out the genes encoding acyl-CoA oxidase. Despite their expectation, it was observed that the growth of the cells was adversely affected. Therefore, enhanced lipid accumulation was rarely reported through overexpression of relevant enzymes and/or intermediate products such as FAs because of emerging a secondary rate-limiting step. Overall, given the existing obstacles facing gene transformation projects such as biosafety rules, correct introduction, and maintenance of transgenes, this strategy should not be considered as the first resort.

(B) The second strategy is the optimization of nutrient formulations [10, 11]. There have been reports that development of optimum growth condition variables [12, 13] has increased the lipid pool in some microalgal strains [14, 15]. Provision of biogenic elements, mainly nitrogen, is one of the main factors affecting algal metabolism. The change in the carbon/nitrogen ratio in a media is known to result in a change in the metabolism direction. In many algae species, increases in this ratio could contribute significantly to the accumulation of neutral lipids, mainly triacylglycerol [16–18]. On the other hand, unfortunately the conditions required for optimal production of algal biomass are different from those of lipid production; consequently, decreasing the cost through growth condition optimization approaches is not only time- and money-consuming but also, in most cases, will not significantly improve lipid accumulation [16].

(C) The last strategy would be biochemical engineering approaches, in which a variety of different plant growth regulators (PGR) could be used to support cell growth. It is generally assumed that the genetic background of a respective algal species would determine the composition of the produced lipids but the lipid amount is mainly a response to the growth conditions [19]. To channel metabolic flux generated in photobiosynthesis into lipid biosynthesis, implementation of some PGRs, vitamins, and lipid precursors could lead to an increase in total catabolism activation and lipid accumulation.

Myoinositol, as one of the nine stereoisomers of inositol, is classified as a member of the vitamin B complex and is required for the cell growth as well as other significant biological processes. Myoinositol was first used by Jacquiot [20] in order to favor bud formation and retard necrosis in elm when supplied at 20–1000 mg L^{-1}; however, the proliferation of the callus was not improved. Letham [21] reported that myoinositol acts as second messengers in the primary action of auxins in plants and its interaction with cytokinin stimulates cell division in carrot phloem explants [22]. Moreover, inositol is also known as a precursor for phospholipids such phosphatidylinositol (PI) in the cells. In an investigation, it was found out that inositol addition into the growth media of yeast led to changes in transcript abundance of over 100 genes, namely, the UAS_{ino}-containing genes. Many of these genes encode enzymes involved in lipid metabolism [23, 24]. For instance, in yeast, the expression of *ACCase* gene, a key gene in the synthesis of long chain fatty acids, is stimulated by inositol and choline [25].

The present study was set to investigate myoinositol-driven modulation of LP and quality (fatty acids (Fas) profile) in cultures of local *Dunaliella* sp. strain isolated from the north coast of Persian Gulf. Nile red staining using microplate fluorescence reading as well as epifluorescent microscopic and flow cytometer analyses was used to monitor the effect of the myoinositol supplementation on the algal cells. Moreover, real-time PCR analysis was performed to look into the impact of myoinositol on one of the key genes involved in lipid synthesis.

2. Methods

2.1. Strains Cultivation. A marine strain (*Dunaliella* sp.) isolated from Bandar Lengeh, a port city on the northern coast of the Persian Gulf, was used in this study. Green colonies were transferred into new flasks containing a media named Lake Media and was kept at 20°C and a constant (24 : 0) 3klux photon flux of white and red LED lamps [27]. The ingredients of Lake Media, developed during the course of the present study, are included: Lake salt sediment (60 g L^{-1}), NPK fertilizer (2 g L^{-1}), and $FeSO_4$ (0.05 g L^{-1}). The media's pH was set at 7.5 and the samples were constantly shaking at 120 rpm.

Beside the strain locally isolated in this study, one other local strain, *D. salina* (generously provided by Dr. Shariati, Isfahan University), and two standard stains, CCAP 19/18 and UTEX 200, purchased from the Culture Collection of Algae and Protozoa (Sams Research, Scotland), and University of Texas at Austin, (Austin, USA), respectively, were also included in the experiments. All the strains were cultivated in the Lake Media under the above-mentioned conditions. During the cultivation period, growth kinetic parameters were recorded for all the strains in triplicate. Data comparison was then carried out using the ANOVA test. The calculated growth parameters included BP, LC, and LP (mg L^{-1} day^{-1}). For BP determination, algal suspensions were centrifuged (3000 g, 10 min) and the wet weights were determined gravimetrically. LP was calculated according to the following equation:

$$\mathrm{LP} = \mathrm{BP} \times \mathrm{LC}. \quad (1)$$

Besides, to investigate the effect of myoinositol inclusion on lipid metabolism and biodiesel properties, only the Persian

Gulf strain was used and cultured in the Lake Media supplemented with 0, 50, 100, and 200 mg L^{-1} myoinositol.

2.2. Molecular Identification. Isolation of total DNA content from the studied strains was carried out by using the DNeasy plant minikit (QIAGENE, Germany). Species-specific oligonucleotides, namely, MA1 and MA3 (without any restriction site), corresponding to the conserved regions of 5′ and 3′ termini were used to amplify 18S rDNA gene. PCR reactions were performed according to the method described by Olmos and coworkers [26]. The molecular weights of PCR-amplified products were calculated and confirmed using a gel documentation system. PCR amplicons were purified using the PCR purification kit (Roche) according to the manufacturer's instructions. Then, the purified products were sequenced by Macrogen Company (Korea). Using BLAST software, the obtained sequences were compared with those deposited in NCBI GenBank as 18S rDNA and ITS regions of different *Dunaliella* species.

A neighbor-joining tree was constructed using the software MEGA version 4. Evolutionary distances were computed using the maximum composite likelihood model. For analysis, 1000 bootstrap replicates were performed to assess the statistical support for the tree. Phylogenetic studies included *Chlamydomonas pumilio*, as the outgroup.

2.3. RNA Extraction, Reverse Transcription, and Real-Time PCR Analysis. To extract RNA from algal cells, 50 mg wet biomass (28-day old culture) was harvested by centrifugation at 2000 ×g for 10 min. Separated algae cells in microtube were disrupted by glass rod in liquid nitrogen, then 500 μL TRIzol reagent (Invitrogen, Carlsbad, CA, USA) was added, and RNA was extracted according to the manufacturer's instructions. Concentrations and purity of the total RNA extracted were measured spectrophotometrically. The extracted RNAs were treated with DNase to eliminate genomic DNA contamination and continuously reverse transcription (RT) was carried out using QuantiTect Reverse Transcription kit (Qiagen). Real-time PCR was performed using a Bio-Rad iCycler iQ real-time PCR.

The first rate-limiting step in the FA biosynthesis pathway was regulated by ACCase [29]. Since AccD subunit overexpression leads to boosted ACCase activity, the effect of myoinositol on *AccD* transcript accumulation was studied. Gene-specific primer pairs of *AccD* and a housekeeping gene used for PCR are listed in Table 5. The 18S rRNA transcript was used to normalize the results by eliminating variations in the quantity and quality of mRNA and cDNA. A reaction mixture for each PCR run was prepared with the SYBR Green supermix (Bio-Rad). The cycle parameters consisted of one cycle of 100 s at 95°C and then 35 cycles of 30 s at 95°C followed by 30 s at 62°C and 20 s at 72°C. Data were collected at the end of each extension step. The relative quantification of gene expressions among the treatment groups was analyzed by the $2^{-\Delta\Delta Ct}$ method [30], where Ct is the cycle number at which the fluorescent signal rises statistically above the background.

2.4. Fluorescent Measurement of Microalgal Neutral Lipids. The intracellular neutral lipid distribution in microalgal cells was examined by staining the cells harvested from 500 μL cell suspension, with 300 μL working solution (1 μM) of Nile red fluorescent dye (Sigma-Aldrich, St. Louis, MO) diluted in Hanks and 20 mM Hepes buffer (HHBS), pH 7. The stock solution was first prepared by dissolving Nile red in anhydrous DMSO (1 mM). The cells were incubated at 37°C for 10 min and protected from light. To remove the Nile red working solution from the cells, the cells were washed and resuspended in HHBS. Cells were examined by an epifluorescent microscope Leica DMRXA with a Nikon (DXM 1200) digital camera (Nikon, Tokyo, Japan) with an excitation wavelength of 486 nm; the emission was measured at 570 nm, following the method of Cooney et al. [28].

For fluorescence-based quantification of the accumulated lipids, a high-throughput technique reported by Chen and coworkers [31] was followed with some modifications. The base procedure was performed in two models: (1) measuring total emitted fluorescence by staining same volume of cell suspension for different treatments (cells at the lag stationary phase), which would quantify total produced lipid volumetrically; (2) measuring emitted fluorescence by staining same cell number (10^5 cells) for different treatment, which would quantify stored lipid in cells. Both procedures involved staining the cell suspensions with Nile red as mentioned above. Fluorescence was measured on a Varian 96-well plate spectrofluorometer. The excitation and emission wavelengths of 522 and 628 nm were selected, based on a previously published report [28].

2.5. Flow Cytometry Study. To figure out the duration after which myoinositol supplementation would lead to an improving effect on lipid synthesis, flow cytometry analysis was used. To investigate that, 7- and 35-day cell suspensions, at linear growth phase and lag stationary phase, respectively, were analyzed. Cells were stained with working Nile red solution as explained earlier. The optical system used in the EPICS XL flow cytometer collects yellow light (575 band-pass filters) in the FL2 channel, corresponding to the Nile red fluorescence in a neutral lipid matrix. To remove nonalgal particles, chlorophyll fluorescence characteristics were considered. Approximately 10,000 cells were analyzed using a log amplification of the fluorescence signal. Unstained cells were used as autofluorescence control. The data used was the arithmetic mean of all cytometric events (10,000 cells) in 3 repeats and two independent experiments [32].

2.6. Oil Extraction and Fatty Acid Profile by Gas Chromatography (GC) Analysis. All cultures, by three replications, were allowed to grow for 35 days to reach the lag stationary phase and then cells were harvested for lipid profile analysis. By this means, the effects of growth phase on the total LC and FA profile were minimized [28]. LC reported as percentage of the total biomass (%dwt) was determined based on the Bligh and Dyer method [33] and was obtained in triplicate for the different strains. Data comparison was then carried out using the ANOVA test.

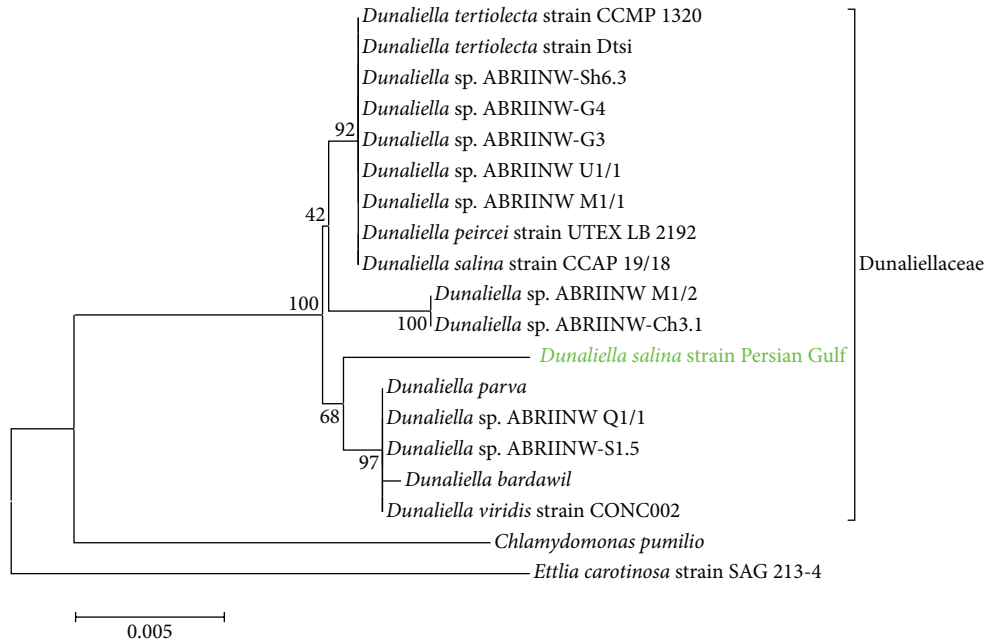

Figure 1: NJ bootstrap consensus tree showing the relationships among *Dunaliella salina* (Persian Gulf) and other standard and Iranian strains. Bootstrap values were calculated over 1000 replicates. *Chlamydomonas pumilio* and *Ettlia carotinosa* were considered as outgroups.

For GC analysis, the direct transesterification method was used based on the procedure reported by Lepage and Roy with minor modifications [34]. The samples containing hexane and FAME were used for GC analysis. The FAs determination was carried out on a Varian CP-3800 GC (Varian Inc., Palo Alto, CA) equipped with a CP-Sil88 fused silica column (100 m, 0.25 mm I.D., film thickness 0.25 μm). The oven temperature was programmed as our previous report [6]. Fatty acid peeks were identified by comparison of the retention time with FAME standards.

2.7. Biodiesel Properties by Bioprospection. Biodiesel quality parameters, that is, oxidation stability, cold performance (cloud point), and combustion characteristics (cetane number), were estimated based on the fact that they are directly influenced by the molecular structure of FAME like the carbon chain length and the amount and/or position of double bonds [35]. Oxidation stability parameters estimated were iodine value (IV), APE, and BAPE. All these parameters were calculated based on the FAME profile using empirical equations as detailed in previous report [36].

3. Result and Discussion

3.1. Identification. Molecular identification and discrimination of living eukaryotic organisms based on the comparison of 18S rDNA gene sequences are a promising method and have been frequently used for molecular identification of different species of *Dunaliella* [26, 37, 38]. Hereby, the chromosomal DNA of 18S using the forward primer MA1 and reverse primer MA3 was amplified. A single band representing the amplified DNA product of 1.7 kb was recorded, which could be used in the intron sizing method for the identification of *Dunaliella* genus [39]. The sequence was aligned with 18 different strains whose 18S sequences were previously submitted at NCBI. The 18S sequence of the *Dunaliella* sp., Persian Gulf strain, was registered in NCBI database with an accession number of KF477384. This sequence exhibited high similarities to other members of Dunaliellaceae. The highest similarity was observed with *Dunaliella* sp. ABRIINWQ1/1 at 98%, which was isolated from an ancient saline lake located in the middle of Iran plateau (Qum Salt Lake). This finding, coupled with the morphological features of the isolated strain (Figure 1), confirmed that the saline water isolate strain is a member of *Dunaliella* genus. The cells lack a cell wall and a well-developed apical papilla and two equal-long (25.0–30.0 μm) and smooth flagella also uphold this identification.

As for the size, number, and position of introns of the 18S rDNA gene, in the *Dunaliella* sp., three types of 18S rDNA structure have been reported by Olmos et al. [40]: no-intron genes with a size of ~1770 bp, one-intron gene with a size of ~2170 bp, and finally the genes with two introns and with a size of ~2570 bp. Interestingly, using intron-sizing method in this genus was applied to an indicator for selection of hyperproducing species [40]. Based on this method, the Persian Gulf strain belonged to the first group with no intron in the 18S rDNA gene. This strain never turned red, indicating that β-carotene was not hyperproduced by this strain. In order to properly explore the similarity observed among the obtained 18S sequences and, moreover, to determine their phylogenetic relationship, a phylogenetic tree was reconstructed using the neighbor-joining (NJ) method. NJ result along with the bootstrap coefficients (replication ×1000) is

Table 1: Biomass productivity, lipid content, and lipid productivity of the microalgae strains.

Strains	Parameters		
	Biomass productivity (BP, g L^{-1} day^{-1})	Lipid content (LC, %dwt)*	Volumetric lipid productivity Pb × LC × 1000 (LP, mg L^{-1} day^{-1})
Dunaliella salina (Shariati)	0.05^{A}	18.9 ± 1.1^{A}	10.26 ± 0.4^{A}
D. salina (UTEX)	0.15^{C}	24 ± 1.3^{B}	36.48 ± 0.6^{C}
D. salina (CCAP19/18)	0.14^{B}	25.1 ± 0.7^{B}	35.14 ± 0.2^{C}
Dunaliella sp. (Persian Gulf)	0.15^{C}	22 ± 2^{B}	33 ± 0.3^{B}
1#	0.14^{B}	25 ± 0.5^{C}	36.15 ± 0.9^{C}
2#	0.14^{B}	27 ± 0.5^{C}	38.6 ± 0.4^{D}
3#	0.12^{B}	33 ± 1^{D}	39.3 ± 0.6^{D}

*All cultures harvested after reaching the stationary phase and LC was determined based on the Bligh and Dyer method [33]. Data are expressed as mean ± SD ($n = 3$). Means of BP, LC, and LP are compared using one-way ANOVA and ones with different letter are significantly different (at $P < 0.05$).
#1, 2, and 3 representing 50, 100, and 200 mg L^{-1} myoinositol implementation in Persian Gulf strain, respectively.

depicted in Figure 1. In this classification, Persian Gulf strain was under the family of Dunaliellaceae, close to Qum strain (Q1/1) and hypo-β-carotene producing strains. As observed in the figure, the Persian Gulf strain is situated close to *D. parva* and *D. viridis* which also confirmed the finding of the intron-sizing method, since these two strains have low β-carotene production capacity as well but can grow in hypersaline environments [40].

3.2. Studying the Algal Species Using Growth Parameters. Since the intracellular LC and FAs profile of microalgae are affected by both culture conditions and growth phase, all of the studied strains were cultivated under the same conditions (flasks containing Lake Media were kept at 20°C and a constant (24 : 0) 3klux photon flux of white and red LED lamps). Sole influence of myoinositol addition on lipid metabolism was also investigated under the same conditions as well. All cultures were harvested after reaching the stationary phase. The results of LC, BP, and LP have been presented in Table 1.

BP value slightly fluctuated for all the strains between 0.12 and 0.15 g L^{-1} day^{-1}, except in case of *D. salina* (Shariati) where significantly lower value of 0.05 g L^{-1} day^{-1} was recorded. Myoinositol addition into the *Dunaliella* sp. (Persian Gulf) culture caused a constant but nonmeaningful decrease in the BP value proportional to the increasing concentrations of myoinositol. The cells grown in the highest concentration of myoinositol (200 mgL^{-1}) had 20% less BP in comparison with those grown in myoinositol free culture (0.12 and 0.15 g L^{-1} day^{-1}, resp.).

The lowest amount of LC was obtained for *D. salina* (Shariati) followed by *Dunaliella* sp. (Persian Gulf), (18.9 and 22% dwt, resp.). In contrast, the highest LC values were also achieved for *Dunaliella* sp. (Persian Gulf) when myoinositol was added to the culture media. More specifically, the mean value of LC for cultures enriched by 200 mg L^{-1} myoinositol was around 33%. This record represents 50% increase in oil accumulation in comparison to the control. Similarly, the LP values were classified into four significantly different groups. The highest LP value belonged to the myoinositol treatment group. These findings revealed the efficiency of biochemical engineering strategies. This was also reported in another biochemical modulation study on the algae *C. sorokiniana* using 0.1% tryptophan supplementation. The authors recorded 57.28% enhancement in LP just 4 days after the treatment [41]. Their findings as well as those of the present study could in a way confirm the promising role of biochemical modulation when combined with selection of proper strains in enriching lipids quantity and consequently in biodiesel production.

Overall, LP, as an indicator of the produced oil in terms of both volume and time, showed a sharp increase after myoinositol addition. This parameter has been reported as a suitable variable to evaluate algal species potential for biodiesel production [42]. This would highlight the positive impact of myoinositol on increasing algal potential for producing biodiesel.

3.3. Integrated Growth and Lipid Production Using a Novel Algal Media. Generally, a two-stage cultivation is considered for algal lipid production: growth stage in which high N concentration is used to achieve the highest possible BP followed by the second stage where N-starvation is imposed to encourage lipid production [8]. James and coworkers [43] observed that when nitrogen was deprived for 4 days, LC increased for all the studied strains of *C. reinhardtii*. In their study, using such 2-stage cultivation strategy, the total FAs of the wild-type strains increased 1.3- and 1.4-fold. However, this would increase the cost and consequently deteriorates the economic aspect of the algal fuel production scenario in comparison with single-stage cultivation. On the other hand, it has been well documented that algal cultivation in a media with decreased nitrogen content results in a decline in biomass content [44]. This is ascribed to the fact that N-starvation leads to decreased duration of the exponential growth phase [45]. Therefore, providing high N content throughout the cultivation period while encouraging lipid production through other alternatives could play a significant role in achieving an economic algal biodiesel. In light of that

Table 2: Real-time PCR analysis of gene expression. Values were normalized against 18S rRNA as housekeeping gene and represent the relative mRNA expression (mean standard error) of three replicate cultures.

Treatment	$C_{T\,AccD}$	$C_{T\,18S}$	$\Delta C_{T.treat}$	$\Delta C_{T.control}$	$\Delta\Delta C_T$	$2^{-\Delta\Delta Ct}$
Control	26.7 ± 0.46	21.2 ± 1.1	−5.5	—	—	—
50 mg	27.19 ± 0.33	19.38 ± 0.5		−7.81	−2.31	0.2
100 mg	26.35 ± 0.41	18.87 ± 0.85	—	−7.48	−1.98	0.25
200 mg	30.27 ± 0.62	22.43 ± 0.72	—	−7.83	−2.33	0.2

in the present study, a new media named Lake Media, capable of encouraging high BP, was formulized using 2 g L^{-1} of NPK fertilizer, as a nitrogen source, and a considerable quantity of natural lake salt (60 g L^{-1}). By considering the different cost of by-product by *Dunaliella* sp. grown in various batch culture media, it is obviously clear that implementation of newly developed media in this research, Lake Media, provides a golden opportunity in large-scale cultivation of this microalgae and final production economically. In another study on this media, implementation of Lake Media declined the costs of carotenoid production to just 0.0029 USD mg^{-1} which is 200% lower than the standard media (Johnson and Olmos Media) and it compensates the lower cell density obtained by Lake Media (unpublished data).

At the same time and with simultaneity of BP increase, LC was also successfully encouraged in this media by myoinositol inclusion as lipid precursor. As a result, the normally used biphasic algal cultivation and lipid production were simplified into a single-phased process in which the combination of the Lake Media and myoinositol met all the requirements of the cells for growth and lipid synthesis simultaneously. This strategy could lead to decreasing the final cost of produced biodiesel.

3.4. Impact of Myoinositol on Acetyl-coA Carboxylase: A Key Gene in Lipid Synthesis. Quantification of the relative-fold change in mRNA levels of the AccD gene 28 days after myoinositol supplementation, in the treated sample in comparison with the control group, was conducted using the real-time PCR analysis. The $2^{-\Delta\Delta Ct}$ value decreased from 0.25 for the 100 mg L^{-1} myoinositol to 0.2 for 200 mg L^{-1}. As presented in Table 2, *AccD* gene exhibited decreasing responses to myoinositol supplementation. In fact, myoinositol resulted in a 75–80% decrease in *AccD* transcript abundance as compared to the control sample. This decrease could be explained as follows: supplementation of myoinositol as a lipid precursor caused an increase in lipid production and accumulation and this in turn resulted in a feedback inhibition, downregulation of the genes involved in lipid synthesis including *AccD*. This explanation is in line with the findings of Al-Feel who investigated the impact of inositol supplementation on lipid production while monitoring the response of another key gene involved in lipid production pathway, acetyl Co-A carboxylase (ACC_1) [25]. They reported that ACC_1 was repressed due to inositol supplementation but returned to near basal expression level by steady state.

Therefore, it could be concluded that inositol and its stereoisomer, myoinositol, exert their positive effect on lipid production through other genes involved in lipid production pathway and not the *AccD* and ACC_1 genes. In case of the *AccD* gene, this could also be confirmed by the fact that inositol stimulates transcription of a series genes which have a conserved domain in their promoter called UAS_{ino} (inositol-sensitive upstream activating sequence) element. This sequence is absent in the *AccD's* promoter. As for the ACC_1, despite the presence of this element, moderate variation in the expression of this gene by inositol supplementation was reported [24, 46].

On the other hand, based on the model presented by Thomas and Fell concerning regulation of enzymatic pathways, many enzymes are involved in controlling the rate of a reaction and alteration of one alone may have a small impact [47]. Therefore, one could point out that myoinositol could have influenced many metabolic processes, rather than targeting a single enzyme in a pathway, and as a result increased the total lipid accumulation. However, increased lipid production and accumulation and consequent feedback inhibition resulted in the downregulation of the key genes involved in lipid production pathway, that is, *AccD* and ACC_1.

Such hypothesis could be supported by the findings of a number of studies revealing that the extent of involved genes upregulation was not reflected in the fatty acid (FA) profile/content [48].

3.5. Proposed Molecular Mechanisms for Lipid Increase by Myoinositol Supplementation. In the present study, the total lipid accumulation was sharply increased by 50% in response to myoinositol implementation which could be attributed to myoinositol role in simultaneously increasing lipid storage and membrane lipids [49]. Previously, a survey on *Saccharomyces cerevisiae* showed a swift 5-6-fold increase in cellular membrane phosphatidylinositol (PI) content in response to inositol inclusion. This rise in PI content seems to be positively correlated with FA synthesis [50]. More specifically, inositol leads to higher production of negatively charged PI and consequently lower negative surface charge of the membrane. On the other hand, the distribution of long-chain acyl-CoA molecules in membrane and activity of *ACCase* are both controlled by negative surface charge, and therefore myoinositol supplementation would increase the capacity of the membrane for incorporation of long-chain acyl CoAs and consequently enhance the cellular FFA synthesis [51].

Although mechanisms describing the growth-promoting effect of myoinositol on algal cell have not been described precisely, their growth-promoting effects through plant growth regulators (phytohormones) have been previously pointed

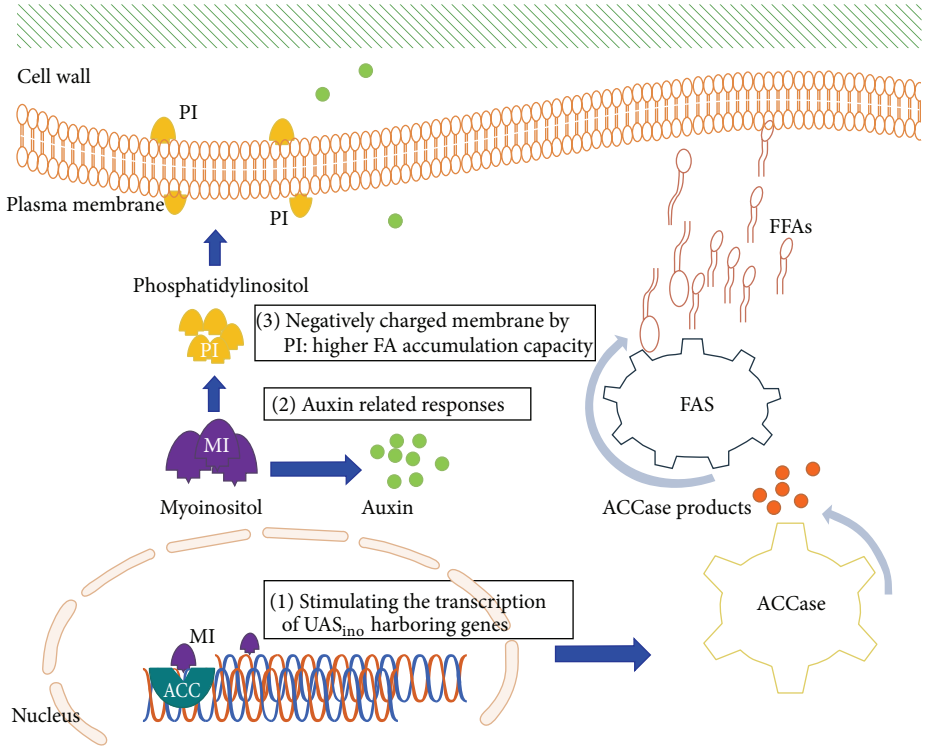

Figure 2: Proposed mechanisms for the lipid-promoting effects of myoinositol (MI) in algal cells, (1) through stimulating the transcription of the responsive genes (e.g., ACC) harboring inositol-sensitive upstream activating sequence (UAS$_{ino}$) element in their promoters which could in turn positively impact FA synthesis (FAS), (2) through auxin-related responses, and (3) by increasing membrane negative charge regulated by phosphatidylinositol (PI).

out [52, 53]. In fact, stimulation of signaling pathways by phytohormones plays a vital role in plant responses to environmental changes. Among phytohormones, auxin which is involved in plant growth and development [54] is regulated by the concentration of phosphoinositides, which are mainly synthesized from myoinositol [50]. In a study, Arroussi and coworkers managed to increase initial lipid content of *D. tertiolecta* (24%) to 38% and 43% after addition of auxin at 0.5 and 1 mg/L, respectively [55]. Therefore, one possible explanation for the lipid-promoting effect of myoinositol in *D. salina* could be attributed to the action of auxins. Moreover, myoinositol plays a key role in cell membrane charge alteration (by PI) which could consequently increase the membrane capacity for FFAs accumulation. Finally, myoinositol also stimulates the transcription of the responsive genes (e.g., ACC) harboring UAS$_{ino}$ element in their promoter which could in turn positively impact FA synthesis (FAS). The proposed mechanisms for the lipid-promoting effects of myoinositol are presented in Figure 2.

3.6. Fluorescence Microscopic Study of Neutral Lipids. Nile red has been widely used to screen wild and mutant variation to explore new candidates for biodiesel production from microalgae to dinoflagellate [56, 57]. In this study, the liposoluble fluorescence probe Nile red was used to visualize neutral lipids in the cells. As shown in Figure 3, the lipid bodies appear as yellow fluorescing circular organelles, while the red background fluorescence is attributed to chlorophyll autofluorescence. The highest LC, as determined by Nile red staining, was observed in cells treated by 200 mg L^{-1} myoinositol. In these cells, small drops of neutral lipids were seen dispersed throughout the cytoplasm (Figure 3), while cells with no myoinositol addition in the media were comparatively poor in terms of neutral LC during the lag stationary phase and showed limited number of small lipid bodies in the cells.

3.7. Quantitative Fluorescence Measurement of Neutral Lipids

3.7.1. Microplate Fluorometry. Result of total lipid measurement using microplate fluorometryin the same volume of the cell suspension was summarized in Figure 4. The fluorescence intensity dramatically increased in the samples treated by the increasing amount of myoinositol. More specifically, implementation of 100 mg L^{-1} myoinositol sharply increased the recorded fluorescence by 59% and further by 152% for 200 mg L^{-1} myoinositol in comparison with that of the control. All treatments were significantly different (at $P < 0.01$).

Effect of cell concentration on the fluorescence of neutral lipids was also taken into consideration by staining the same cell concentration (10^5 cells mL^{-1}) for all the investigated

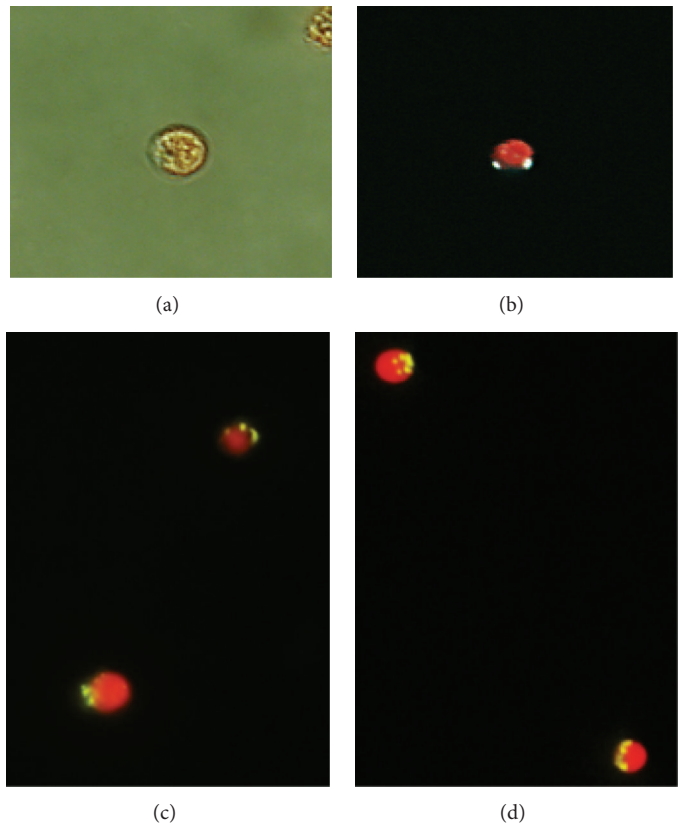

Figure 3: Epifluorescent microphotographs (magnification ×40) of microalgae stained with fluorochrome Nile red. Neutral lipids in cells are seen as lighter colored drops. (a) Bright field image and fluorescence image; (b) control; (c) 100 mg L^{-1} myoinositol supplementation; (d) 200 mg L^{-1} myoinositol supplementation. Microphotographs were taken using a Leica DMRXA compound light microscope with a Nikon (DXM 1200) digital camera, a band-pass filter with an excitation range of 450–490 nm, and a long-pass suppression filter with an edge wavelength of 515 nm.

samples to measure the relative amount of lipid stored in same number of cells. Similar to the results of total lipid measurement in cell suspensions, myoinositol was proven to stimulate single cells to accumulate more lipid in their cytoplasm. 200 mg L^{-1} myoinositol implementation led to 284% raise in the emitted fluorescence. A significant difference between the three studied levels of myoinositol (50, 100, and 200 mg L^{-1}) could be seen in the same cell number mode (120% increase in fluorescence emission for 100 and 200 mg L^{-1}). This was also confirmed by total extracted lipid data based on which 50, 100, and 200 mg L^{-1} myoinositol supplementation caused 13, 23, and 50% increase in LC, respectively.

3.7.2. Flow Cytometry. Flow cytometry, in conjunction with microplate fluorometry, represents an invaluable tool for screening and exploiting high lipid-producing microalgae strains. In this study, lipid accumulation was studied using flow cytometry 7 and 35 days after myoinositol supplementation. The results obtained revealed that on day 35 the mean fluorescence for the control was 199.6, whereas this value was at 225.65, 263.6, and 283.1 (13, 32, and 42% increase in comparison with the control), for the cells treated by 50, 100, and 200 mg L^{-1} myoinositol, respectively.

Moreover, the effect of exposure time to myoinositol and its relation with cell growth phase and lipid accumulation were also studied by comparing the mean fluorescence on days 7 and 35. The results clearly confirmed that the positive effect of myoinositol supplementation on lipid production is visible in the stationary phase when algal cells have already completed their growth or, in other words, the emitted fluorescence values recorded in the young algal cells (on the day 7) were not significantly different among the treatments (Figure 5).

Overall, there was a clear correlation between the fluorometry (microplate fluorescence and flow cytometry) results and those of LC gravimetrical determination (Figures 4 and 5 and Table 1). Therefore, fluorometry techniques could be suggested as powerful and high-throughput alternative analytical tools to monitor the effect of chemicals and biological molecules on lipid production and accumulation in algal cells.

3.8. The Role of Myoinositol Treatment on Algal FAs Profiles. Fatty acid methyl ester (FAME) profiles for different algal strains studied in this study are summarized in Table 3. It has been frequently reported that 16–18 carbon chain FAs are

Table 3: Types of fatty acids produced and properties of algal oil.

Strain	Fatty acid (%)							SFA	MUFA	PUFA	SFA/USFA
	16 : 0	16 : 1	18 : 0	18 : 1	18 : 2	18 : 3	20 : 1				
Dunaliella sp. (Persian Gulf)	9.19 ± 1.2	0.80 ± 0.8	4.27 ± 0.9	22.51 ± 0.7	3.84 ± 0.4	44.31 ± 2.1	1.42 ± 0.2	13.47	24.74	48.15	0.16
D. salina (Shariati)	12.02 ± 2.1	4.45 ± 0.2	1.91 ± 1.2	23.67 ± 1.6	2.28 ± 1.1	40.36 ± 2.2	1.40 ± 0.2	13.93	29.52	42.65	0.16
D. salina (UTEX200)	16.34 ± 1.4	1.04 ± 0.9	6.43 ± 1.2	19.58 ± 1.1	6.76 ± 1.2	27.71 ± 2.5	2.28 ± 0.3	22.77	22.89	34.47	0.28
D. salina (CCAP19/18)	15.87 ± 1.8	ND^{+}	6.14 ± 1.3	21.39 ± 2.1	15.92 ± 1.6	23.95 ± 1.9	ND	22.01	21.39	39.87	0.26
1*	7.05 ± 0.9	6.25 ± 0.3	1.55 ± 0.7	22.95 ± 0.8	12.15 ± 0.3	37.66 ± 0.4	1.12 ± 0.6	8.60	30.32	49.81	0.10
2*	7.75 ± 0.6	5.04 ± 0.8	1.42 ± 0.5	25.27 ± 1.9	18.58 ± 1.4	26.91 ± 1.9	ND	9.17	30.31	45.48	0.11
3*	8.41 ± 0.8	4.52 ± 1.1	2.14 ± 0.3	32.03 ± 2.2	13.58 ± 1.3	27.24 ± 1.4	ND^{-}	10.55	36.55	40.82	0.12

*1, 2, and 3 representing 50, 100, and 200 mg L^{-1} myoinositol implementation in Persian Gulf strain, respectively.
$^{+}$Not detected.
$^{-}$Non identified Fas which are around 10%.

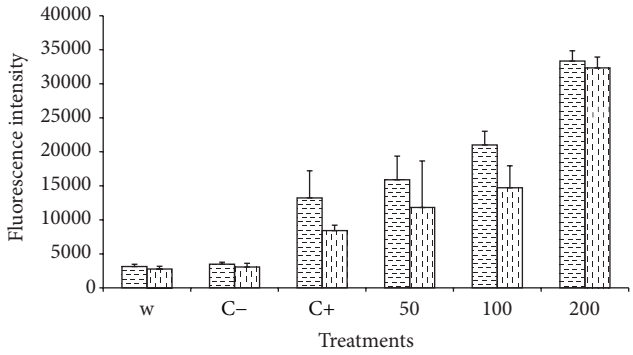

Figure 4: Fluorescence emission of Nile red-stained microalgae. The excitation and emission wavelengths for fluorescence measurement were at 522 and 628 nm, respectively. The cell density of the suspensions used for analysis was 10^5 cell mL^{-1}. Nile red staining was conducted based on the procedures described by Cooney et al. [28]. Data were the mean values of three replicates (vertical dashed lines: same volume; horizontal dashed lines: same cell number). C− and C+ represent nonstained and stained cell with no myoinositol inclusion, respectively.

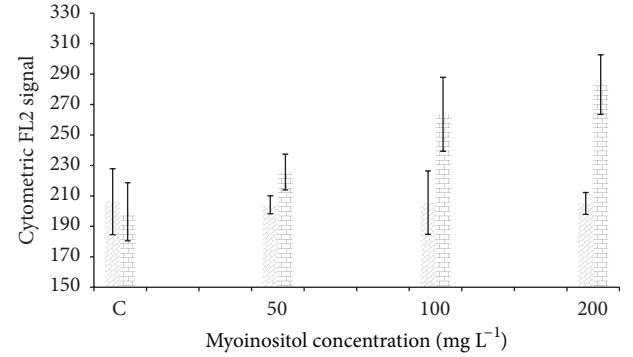

Figure 5: Variation of cytometric signal (FL2: yellow fluorescence, $\lambda = 575$ nm) in cells stained with Nile red (*Dunaliella* sp.). Horizontal and diagonal bricks represent the sample treated by myoinositol for 35 and 7 days, respectively.

Table 4: Comparison of the estimated properties of algal biodiesel from cells treated with myoinositol.

Strains	Biodiesel properties			
	CN	CP	BAPE	APE
Dunaliella sp. (Persian Gulf)	43.75	−0.16	92.47	118.82
D. salina (Shariati)	45.65	1.33	83.01	108.96
D. salina (UTEX200)	55.36	3.60	62.17	88.51
D. salina (CCAP19/18)	52.96	3.36	63.83	101.14
1*	42.27	−1.28	87.47	122.57
2*	47.61	−0.91	72.39	116.23
3*	47.16	−0.57	68.06	113.66

*1, 2, and 3 representing 100 and 200 mg L^{-1} myoinositol implementation in Persian Gulf strain, respectively.

dominant in algal cells [6, 28, 58]. The same observation was made in this study as well. In all the strains investigated, the omega-3 fatty acid, linolenic acid (18 : 3) made up the highest portion of the FAME profile. Persian Gulf strain grown in the Lake Media with no myoinositol enrichment was found to have the highest percentage for this FA (>44%) while the lowest record for 18 : 3 of around 26% was also observed in the same strain, but in presence of myoinositol. On the contrary, myoinositol inclusion (200 mg L^{-1}) led to increased percentages of monounsaturated FAs (MUFA) that is, palmitoleic acid (16 : 1) and oleic acid (18 : 1) by 4.6- and 0.4-folds, respectively. Moreover, in case of linoleic acid (18 : 2), low concentration of myoinositol (100 mg L^{-1}) considerably increased percentage of this FA, while 200 mg L^{-1} myoinositol implementation led to a significant decrease in 18 : 2 accumulation. Overall, MUFA were increased continuously by myoinositol addition in the media while PUFA were felt down vice versa.

These findings were similar to those of studies in which N-starvation was applied to enhance lipid accumulation in microalgae. Gurr and Harwood [59] reported relative accumulations in 18 : 1 and 18 : 2, accompanied by a decrease

Table 5: Sequences of primer pairs used in real-time PCR.

Primer name	Sequence
18S rRNA (forward)	5′-CAGACACGGGGAGGATTGACAGATTGAGAG-3′
18S rRNA (reverse)	5′-GCGCGTGCGGCCCAGAACATC-3′
AccD (forward)	5′-AAGACGCACAAGAACGAACAG-3′
AccD (reverse)	5′-AACTACAGAGCCCATACTTCCC-3′

in 18 : 0 acid when N-starvation was used. They explained that N-starvation promoted the desaturation pathways, beginning with delta-9 desaturase. In a similar study using N-starvation on *Botryococcus braunii*, an increase in the content of SFAs (up to 76.8%) and a substantial decrease in the PUFA content (up to 6.8%) were observed [19]. It could be concluded that myoinositol might also encourage the desaturation pathways.

3.9. Estimation of Biodiesel Properties. The impact of myoinositol on key biodiesel quality parameters such as allylic position equivalents (APE) and bisallylic position equivalents (BAPE), cetane number (CN), and cloud point (CP) was also investigated. The BAPE and APE values are effective means of predicting oxidative instability of biodiesel. The highest BAPE and APE values were measured for the control Persian Gulf (no myoinositol addition), while the lowest values were recorded for UTEX200 strain (Table 4). This could be explained by the highest and lowest levels of unsaturated FAs in particular 18 : 3 in the control Persian Gulf and UTEX200 strain, respectively. A decreasing trend for BAPE and APE values and consequently higher oxidative stability were observed when algal cells (Persian Gulf strain) were treated by myoinositol. For instance, BAPE decreased by 26% at myoinositol concentration of 200 mg L^{-1} (Table 4).

CN indicates the combustion quality of diesel fuels including biodiesel. In other words, the higher this value is, the easier it would be to start a standard diesel engine. An increase in this parameter was observed where algal cells were treated by myoinositol. Slight improvements in the estimated CP values were also recorded. Overall, it was shown that inclusion of myoinositol led to improved fuel properties.

In a different study Ngangkham et al. [41] also strived to improve *C. sorokiniana* oil quality for biodiesel production but different treatments from that of this study were applied. In particular, they reported reduced level of PUFA and consequent increased oxidative stability of the produced biodiesel. In conclusion and based on the findings of Ngangkham et al. [41] and those of the present investigation, biochemical engineering treatments could be regarded as efficient strategies for directed improvement of algal oil quality and resultant biodiesel based on a particular climate condition.

4. Conclusion

The present study was set to evaluate the effects of myoinositol on a locally isolated Persian microalgae strain, *Dunaliella* sp., with a specific focus on LP and biodiesel quality based on FA composition. Inclusion of myoinositol (200 mg L^{-1}) in the media improved the total lipid accumulation (up to 50%) and biodiesel quality parameters, that is, APE, BAPE, CN, and CP. Hypothetically, myoinositol treatment led to increased auxin and PI accumulation in the cells and consequently more negatively charged membranes. This in turn resulted in increased FFA synthesis and lipid accumulation. Biochemical modulation strategies should still be progressively considered in hope of finding more efficient and economically feasible strategies leading to more viable production systems.

Abbreviations

ACCase: Acetyl-CoA carboxylase
APE: Allylic position equivalents
BAPE: Bisallylic position equivalents
CN: Cetane number
CP: Cloud point
D.: *Dunaliella*
FA: Fatty acid
FAME: Fatty acid methyl ester
IV: Iodine value
LC: Lipid content
BP: Biomass productivity
LP: Lipid productivity
MSFA: Monosaturated FAs
MUFA: Monounsaturated FAs
PGR: Plant growth regulator
PI: Phosphatidylinositol
SFA: Total saturated fatty acids.

Conflict of Interests

The authors declare that there is no conflict of interests regarding the publication of this paper.

Acknowledgments

The authors' appreciation goes to Dr. Shariati for providing one of the algal strains used in this study. The authors would also like to thank Biofuel Research Team (BRTeam) and Agricultural Biotechnology Research Institute of Iran (ABRII) for financing this study. They also would like to thank Dr. S. Malekzadeh for his comments on the paper.

References

[1] M. Y. Menetrez, "Meeting the US renewable fuel standard: a comparison of biofuel pathways," *Biofuel Research Journal*, vol. 1, no. 4, pp. 110–122, 2014.

[2] F. Bux, "The potential of using wastewater for microalgal propagation," *Biofuel Research Journal*, vol. 1, no. 4, p. 106, 2014.

[3] E. Specht, S. Miyake-Stoner, and S. Mayfield, "Micro-algae come of age as a platform for recombinant protein production," *Biotechnology Letters*, vol. 32, no. 10, pp. 1373–1383, 2010.

[4] K. Beetul, S. Bibi Sadally, N. Taleb-Hossenkhan, R. Bhagooli, and D. Puchooa, "An investigation of biodiesel production from microalgae found in Mauritian waters," *Biofuel Research Journal*, vol. 1, pp. 58–64, 2014.

[5] D. R. Georgianna, M. J. Hannon, M. Marcuschi et al., "Production of recombinant enzymes in the marine alga *Dunaliella tertiolecta*," *Algal Research*, vol. 2, no. 1, pp. 2–9, 2013.

[6] A. F. Talebi, S. K. Mohtashami, M. Tabatabaei et al., "Fatty acids profiling: a selective criterion for screening microalgae strains for biodiesel production," *Algal Research*, vol. 2, no. 3, pp. 258–267, 2013.

[7] M. Tabatabaei, M. Tohidfar, G. S. Jouzani, M. Safarnejad, and M. Pazouki, "Biodiesel production from genetically engineered microalgae: future of bioenergy in Iran," *Renewable & Sustainable Energy Reviews*, vol. 15, no. 4, pp. 1918–1927, 2011.

[8] A. F. Talebi, M. Tohidfar, A. Bagheri, S. R. Lyon, K. Salehi-Ashtiani, and M. Tabatabaei, "Manipulation of carbon flux into fatty acid biosynthesis pathway in *Dunaliella salina* using AccD and ME genes to enhance lipid content and to improve produced biodiesel quality," *Biofuel Research Journal*, vol. 1, no. 3, pp. 91–97, 2014.

[9] S. Picataggio, T. Rohrer, K. Deanda et al., "Metabolic engineering of *Candida tropicalis* for the production of long-chain dicarboxylic acids," *Bio/Technology*, vol. 10, no. 8, pp. 894–898, 1992.

[10] A. F. Talebi, M. Tabatabaei, S. K. Mohtashami, M. Tohidfar, and F. Moradi, "Comparative salt stress study on intracellular ion concentration in marine and salt-adapted freshwater strains of microalgae," *Notulae Scientia Biologicae*, vol. 5, pp. 309–315, 2013.

[11] G. Olivieri, A. Marzocchella, R. Andreozzi, G. Pinto, and A. Pollio, "Biodiesel production from *Stichococcus* strains at laboratory scale," *Journal of Chemical Technology and Biotechnology*, vol. 86, no. 6, pp. 776–783, 2011.

[12] S. Elumalai and V. Prakasam, "Optimization of abiotic conditions suitable for the production of biodiesel from *Chlorella vulgaris*," *Indian Journal of Science and Technology*, vol. 4, pp. 91–97, 2011.

[13] D. Sasi, P. Mitra, A. Vigueras, and G. A. Hill, "Growth kinetics and lipid production using *Chlorella vulgaris* in a circulating loop photobioreactor," *Journal of Chemical Technology and Biotechnology*, vol. 86, no. 6, pp. 875–880, 2011.

[14] V. H. Work, R. Radakovits, R. E. Jinkerson et al., "Increased lipid accumulation in the *Chlamydomonas reinhardtii* sta7-10 starchless isoamylase mutant and increased carbohydrate synthesis in complemented strains," *Eukaryotic Cell*, vol. 9, no. 8, pp. 1251–1261, 2010.

[15] N. Mallick, S. Mandal, A. K. Singh, M. Bishai, and A. Dash, "Green microalga *Chlorella vulgaris* as a potential feedstock for biodiesel," *Journal of Chemical Technology and Biotechnology*, vol. 87, no. 1, pp. 137–145, 2012.

[16] M. Piorreck, K.-H. Baasch, and P. Pohl, "Biomass production, total protein, chlorophylls, lipids and fatty acids of freshwater green and blue-green algae under different nitrogen regimes," *Phytochemistry*, vol. 23, no. 2, pp. 207–216, 1984.

[17] W.-L. Chu, S.-M. Phang, and S.-H. Goh, "Environmental effects on growth and biochemical composition of *Nitzschia inconspicua* Grunow," *Journal of Applied Phycology*, vol. 8, no. 4-5, pp. 389–396, 1996.

[18] G. A. Thompson Jr., "Lipids and membrane function in green algae," *Biochimica et Biophysica Acta: Lipids and Lipid Metabolism*, vol. 1302, no. 1, pp. 17–45, 1996.

[19] N. O. Zhila, G. S. Kalacheva, and T. G. Volova, "Effect of nitrogen limitation on the growth and lipid composition of the green alga *Botryococcus braunii* Kütz IPPAS H-252," *Russian Journal of Plant Physiology*, vol. 52, no. 3, pp. 311–319, 2005.

[20] C. Jacquiot, "Action of meso-inositol and of adenine on bud formation in the cambium tissue of *Ulmus campestris* cultivated in vitro," *Comptes Rendus de l'Académie des Sciences*, vol. 233, pp. 815–817, 1951.

[21] D. S. Letham, "Regulators of cell division in plant tissues—II. A cytokinin in plant extracts: isolation and interaction with other growth regulators," *Phytochemistry*, vol. 5, no. 3, pp. 269–286, 1966.

[22] K. Watanabe, K. Tanaka, K. Asada, and Z. Kasai, "The growth promoting effect of phytic acid on callus tissues of rice seed," *Plant and Cell Physiology*, vol. 12, no. 1, pp. 161–164, 1971.

[23] T. C. Santiago and C. B. Mamoun, "Genome expression analysis in yeast reveals novel transcriptional regulation by inositol and choline and new regulatory functions for Opi1p, ino2p, and ino4p," *The Journal of Biological Chemistry*, vol. 278, no. 40, pp. 38723–38730, 2003.

[24] S. A. Jesch, X. Zhao, M. T. Wells, and S. A. Henry, "Genome-wide analysis reveals inositol, not choline, as the major effector of Ino2p-Ino4p and unfolded protein response target gene expression in yeast," *Journal of Biological Chemistry*, vol. 280, no. 10, pp. 9106–9118, 2005.

[25] W. Al-Feel, J. C. DeMar, and S. J. Wakil, "A *Saccharomyces cerevisiae* mutant strain defective in acetyl-CoA carboxylase arrests at the G2/M phase of the cell cycle," *Proceedings of the National Academy of Sciences of the United States of America*, vol. 100, no. 6, pp. 3095–3100, 2003.

[26] J. Olmos, J. Paniagua, and R. Contreras, "Molecular identification of *Dunaliella* sp. utilizing the 18S rDNA gene," *Letters in Applied Microbiology*, vol. 30, no. 1, pp. 80–84, 2000.

[27] M. R. Droop, "A note on the isolation of small marine algae and flagellates for pure cultures," *Journal of the Marine Biological Association of the United Kingdom*, vol. 33, no. 2, pp. 511–514, 1954.

[28] M. J. Cooney, D. Elsey, D. Jameson, and B. Raleigh, "Fluorescent measurement of microalgal neutral lipids," *Journal of Microbiological Methods*, vol. 68, no. 3, pp. 639–642, 2007.

[29] Y. Madoka, K.-I. Tomizawa, J. Mizoi, I. Nishida, Y. Nagano, and Y. Sasaki, "Chloroplast transformation with modified *accD* operon increases acetyl-CoA carboxylase and causes extension of leaf longevity and increase in seed yield in tobacco," *Plant and Cell Physiology*, vol. 43, no. 12, pp. 1518–1525, 2002.

[30] K. J. Livak and T. D. Schmittgen, "Analysis of relative gene expression data using real-time quantitative PCR and the $2^{-\Delta\Delta C_T}$ method," *Methods*, vol. 25, no. 4, pp. 402–408, 2001.

[31] W. Chen, C. H. Zhang, L. Song, M. Sommerfeld, and H. Qiang, "A high throughput Nile red method for quantitative measurement of neutral lipids in microalgae," *Journal of Microbiological Methods*, vol. 77, no. 1, pp. 41–47, 2009.

[32] Y.-H. Lee, S.-Y. Chen, R. J. Wiesner, and Y.-F. Huang, "Simple flow cytometric method used to assess lipid accumulation in fat cells," *Journal of Lipid Research*, vol. 45, no. 6, pp. 1162–1167, 2004.

[33] E. G. Bligh and W. J. Dyer, "A rapid method of total lipid extraction and purification," *Canadian Journal of Biochemistry and Physiology*, vol. 37, no. 8, pp. 911–917, 1959.

[34] G. Lepage and C. C. Roy, "Direct transesterification of all classes of lipids in a one-step reaction," *The Journal of Lipid Research*, vol. 27, no. 1, pp. 114–120, 1986.

[35] A. Sarin, R. Arora, N. P. Singh, R. Sarin, R. K. Malhotra, and K. Kundu, "Effect of blends of Palm-Jatropha-Pongamia biodiesels on cloud point and pour point," *Energy*, vol. 34, no. 11, pp. 2016–2021, 2009.

[36] A. F. Talebi, M. Tabatabaei, and Y. Chisti, "BiodieselAnalyzer: a user-friendly software for predicting the properties of prospective biodiesel," *Biofuel Research Journal*, vol. 1, pp. 55–57, 2014.

[37] J. Olmos-Soto, J. Paniagua-Michel, R. Contreras, and L. Trujillo, "Molecular identification of β-carotene hyper-producing strains of dunaliella from saline environments using species-specific oligonucleotides," *Biotechnology Letters*, vol. 24, no. 5, pp. 365–369, 2002.

[38] R. Raja, S. Hema, D. Balasubramanyam, and R. Rengasamy, "PCR-identification of *Dunaliella salina* (Volvocales, Chlorophyta) and its growth characteristics," *Microbiological Research*, vol. 162, no. 2, pp. 168–176, 2007.

[39] M. A. Hejazi, A. Barzegari, N. H. Gharajeh, and M. S. Hejazi, "Introduction of a novel 18S rDNA gene arrangement along with distinct ITS region in the saline water microalga Dunaliella," *Saline Systems*, vol. 6, article 4, 2010.

[40] J. Olmos, L. Ochoa, J. Paniagua-Michel, and R. Contreras, "DNA fingerprinting differentiation between-carotene hyper-producer strains of Dunaliella from around the world," *Saline Systems*, vol. 5, no. 1, article 5, 2009.

[41] M. Ngangkham, S. K. Ratha, R. Prasanna et al., "Biochemical modulation of growth, lipid quality and productivity in mixotrophic cultures of *Chlorella sorokiniana*," *SpringerPlus*, vol. 1, no. 1, pp. 1–13, 2012.

[42] L. Rodolfi, G. C. Zittelli, N. Bassi et al., "Microalgae for oil: strain selection, induction of lipid synthesis and outdoor mass cultivation in a low-cost photobioreactor," *Biotechnology and Bioengineering*, vol. 102, no. 1, pp. 100–112, 2009.

[43] G. O. James, C. H. Hocart, W. Hillier et al., "Fatty acid profiling of *Chlamydomonas reinhardtii* under nitrogen deprivation," *Bioresource Technology*, vol. 102, no. 3, pp. 3343–3351, 2011.

[44] J.-Y. An, S.-J. Sim, J. S. Lee, and B. W. Kim, "Hydrocarbon production from secondarily treated piggery wastewater by the green alga *Botryococcus braunii*," *Journal of Applied Phycology*, vol. 15, no. 2-3, pp. 185–191, 2003.

[45] F. Brenckmann, C. Largeau, E. Casadevall, and C. Berkaloff, "Influence de la nutrition azotéesur la croissance et la production des hydrocarbures de l'algue unicellulaire *Botryococcus braunii*," *Energy from Biomass*, pp. 717–721, 1985.

[46] H. J. Schuller, A. Hahn, F. Troster, A. Schutz, and E. Schweizer, "Coordinate genetic control of yeast fatty acid synthase genes *FAS1* and *FAS2* by an upstream activation site common to genes involved in membrane lipid biosynthesis," *EMBO Journal*, vol. 11, no. 1, pp. 107–114, 1992.

[47] S. Thomas and D. A. Fell, "The role of multiple enzyme activation in metabolic flux control," *Advances in Enzyme Regulation*, vol. 38, no. 1, pp. 65–85, 1998.

[48] A. Lei, H. Chen, G. Shen, Z. H. Hu, L. Chen, and J. Wang, "Expression of fatty acid synthesis genes and fatty acid accumulation in *Haematococcus pluvialis* under different stressors," *Biotechnology for Biofuels*, vol. 5, article 18, 2012.

[49] M. L. Gaspar, H. F. Hofbauer, S. D. Kohlwein, and S. A. Henry, "Coordination of storage lipid synthesis and membrane biogenesis," *Journal of Biological Chemistry*, vol. 286, no. 3, pp. 1696–1708, 2011.

[50] M. L. Gaspar, M. A. Aregullin, S. A. Jesch, and S. A. Henry, "Inositol induces a profound alteration in the pattern and rate of synthesis and turnover of membrane lipids in *Saccharomyces cerevisiae*," *The Journal of Biological Chemistry*, vol. 281, pp. 22773–22785, 2006.

[51] M. Sumper, "Control of fatty acid biosynthesis by long chain acyl CoAs and by lipid membranes," *European Journal of Biochemistry*, vol. 49, no. 2, pp. 469–475, 1974.

[52] J. M. Stevenson, I. Y. Perera, I. Heilmann, S. Persson, and W. F. Boss, "Inositol signaling and plant growth," *Trends in Plant Science*, vol. 5, no. 6, pp. 252–258, 2000.

[53] Y. Luo, G. Qin, J. Zhang et al., "D-myo-inositol-3-phosphate affects phosphatidylinositol-mediated endomembrane function in Arabidopsis and is essential for auxin-regulated embryogenesis," *Plant Cell*, vol. 23, no. 4, pp. 1352–1372, 2011.

[54] S. Zhang and B. van Duijn, "Cellular auxin transport in algae," *Plants*, vol. 3, no. 1, pp. 58–69, 2014.

[55] H. El Arroussi, R. Benhima, I. Bennis, N. El Mernissi, and I. Wahby, "Improvement of the potential of *Dunaliella tertiolecta* as a source of biodiesel by auxin treatment coupled to salt stress," *Renewable Energy*, vol. 77, pp. 15–19, 2015.

[56] C. Fuentes-Grünewald, E. Garcés, S. Rossi, and J. Camp, "Use of the dinoflagellate *Karlodinium veneficum* as a sustainable source of biodiesel production," *Journal of Industrial Microbiology & Biotechnology*, vol. 36, no. 9, pp. 1215–1224, 2009.

[57] T. T. Y. Doan, B. Sivaloganathan, and J. P. Obbard, "Screening of marine microalgae for biodiesel feedstock," *Biomass and Bioenergy*, vol. 35, no. 7, pp. 2534–2544, 2011.

[58] I. Lang, L. Hodac, T. Friedl, and I. Feussner, "Fatty acid profiles and their distribution patterns in microalgae: a comprehensive analysis of more than 2000 strains from the SAG culture collection," *BMC Plant Biology*, vol. 11, article 124, 2011.

[59] M. I. Gurr and J. L. Harwood, *Lipid Biochemistry: An Introduction*, Chapman & Hall, London, UK, 4th edition, 1991.

Hindawi Publishing Corporation
BioMed Research International
Volume 2015, Article ID 125241, 8 pages
http://dx.doi.org/10.1155/2015/125241

Research Article

Improving Biomethane Production and Mass Bioconversion of Corn Stover Anaerobic Digestion by Adding NaOH Pretreatment and Trace Elements

ChunMei Liu, HaiRong Yuan, DeXun Zou, YanPing Liu, BaoNing Zhu, and XiuJin Li

College of Chemical Technology, Centre for Resource and Environmental Research, Beijing University of Chemical Technology, 15 Beisanhuan East Road, Chaoyang District, Beijing 100029, China

Correspondence should be addressed to XiuJin Li; xjli@mail.buct.edu.cn

Received 2 December 2014; Revised 17 January 2015; Accepted 3 February 2015

Academic Editor: Alberto Reis

This research applied sodium hydroxide (NaOH) pretreatment and trace elements to improve biomethane production when using corn stover for anaerobic digestion. Full-factor experimental tests identified the best combination of trace elements with the NaOH pretreatment, indicating that the best combination was with 1.0, 0.4, and 0.4 $mg \cdot L^{-1} \cdot d^{-1}$ of elements Fe, Co, and Ni, respectively. The cumulative biomethane production adding NaOH pretreatment and trace elements was 11,367 mL; total solid bioconversion rate was 55.7%, which was 41.8%–62.2% higher than with NaOH-pretreatment alone and 22.2%–56.3% higher than with untreated corn stover. The best combination was obtained 5–9 days shorter than T_{90} and maintained good system operation stability. Only a fraction of the trace elements in the best combination was present in the resulting solution; more than 85% of the total amounts added were transferred into the solid fraction. Adding 0.897 g of Fe, 0.389 g of Co, and 0.349 g of Ni satisfied anaerobic digestion needs and enhanced biological activity at the beginning of the operation. The results showed that NaOH pretreatment and adding trace elements improve corn stover biodegradability and enhance biomethane production.

1. Introduction

Corn is one of the three major crops in China and is widely planted in the northern part of China. Corn stover is one of the most abundant lignocellulosic crop residues, with an annual production of 0.1 billion tons. Most of this residue remains unused [1]. It is quite common to see the open-field burning of corn stover across corn planting areas during the harvest season; these fires lead to serious air pollution and fire disaster and threaten traffic safety.

Biomethane production through anaerobic digestion is an energy-efficient and environmentally friendly way to treat and reuse agricultural organic materials. These wastes can be used as alternative feedstock to produce renewable energy, biomethane, valuable digested residues, liquid fertilizers, and soil conditioners [2]. However, anaerobic digestion is not currently popular, because of its poor biodegradability and digestibility. This is particularly true with treating crop residues.

Corn stover is mainly composed of polysaccharide (cellulose and hemicellulose) and lignin, forming complex three-dimensional structures. The native cellulose fraction of corn stover resists enzymatic breakdown due to the complex structure of lignin and hemicellulose with the cellulose, making enzymatic disassembly difficult [3]. To obtain fast enzymatic hydrolysis of feedstock with a high sugar yield, the cell structures must be broken and porosity increased. Therefore, pretreatment is required to prepare the native cellulose fraction for enzymatic hydrolysis to monosaccharides.

Generally, pretreatment methods are classified into physical pretreatments (i.e., milling, liquid hot water, and steam), chemical pretreatments (alkaline, acidic, and oxidative), and biological pretreatments (i.e., commercial enzymes or fungi). Previous studies have found that alkali pretreatment is

the best known method for enhancing complex material biodegradation and providing the most significant benefits [4].

In addition to pretreatment challenges, existing trace elements and nitrogen are insufficient for anaerobic microorganisms when corn stover is used alone as a feedstock for anaerobic digestion. This results in a decrease in biogas production after a certain treatment period and a process failure if no external nutrients and buffering agents are added [5]. Misunderstanding or underestimating trace nutrient requirements of methanogens can also be a serious problem in applying anaerobic biotechnology, and trace element availability as micronutrients plays a significant role in the performance and stability of substrates ranging from organic household waste to more defined lignocellulosic substrates [6].

Trace elements such as cobalt, nickel, iron, tungsten, or molybdenum serve as enzyme cofactors and are involved in the biomethane formation biochemistry [7]. Li and Dong (2001) reported that the most required trace elements were Fe, Co, and Ni [8]. For example, methyl-coenzyme M and cofactor F_{430} contain nickel; the acetate converting enzyme complex carbon monoxide dehydrogenase (CODH) contains a nickel-iron-sulfur component; and the methyl-H_4SPT contains cobalt [9]. However, no information was found on the influence of trace elements on biomethane production and mass bioconversion of corn stover sole substrate.

Elemental deficiencies may negatively influence biological processes and biomethane formation; on the contrary, higher concentration of trace elements may be toxic to methanogens [10]. Consequently, adequate trace element concentrations (Fe, Co, and Ni) must be quantified accurately when added to an experimental reactor. However, essential trace element availability for the bacterial community is still a concern when studying single substrates rather than complex material mixtures, as different forms of trace elements have not been studied.

This study's objective was to determine the optimal combination of the trace elements Fe, Co, and Ni and to investigate the performance and synergistic effect of combining NaOH pretreatment with additional trace elements during corn stover anaerobic digestion. Factors evaluated included biogas production, mass bioconversion, and trace element bioavailability.

2. Materials and Methods

2.1. Feedstock and Inoculum. The corn stover used in this study was collected from Beichen County of Tianjin City, China. The corn stover was chopped using a paper chopper (PC500, Staida Co., Tianjin, China) and then ground through a 20 mesh screen using a universal pulverizer (YSW-180, Yanshan Zhengde Co., Beijing, China). Previous study revealed that a NaOH dose of 2%, 88% moisture content, and a 3-day treatment time were appropriate for wet state NaOH pretreatment of corn stover [1]. This method was selected because of the improvement in corn stover's biodegradability and environmental friendliness. The wet state NaOH pretreatment was conducted in a laboratory at ambient temperature (20 ± 2°C) for three days.

Table 1: Characteristics of corn stover and activated sludge used in this study.

Indexes (dry matter)	Corn stover	Activated sludge
Total solid (%)	94.93 ± 0.36	14.33 ± 0.13
Volatile solid (%)	85.14 ± 0.24	5.95 ± 0.19
Total carbon (%)	42.65 ± 0.14	30.12 ± 0.39
Total nitrogen (%)	1.22 ± 0.17	3.28 ± 0.32
Cellulose (%)	38.82 ± 0.43	—
Hemicellulose (%)	29.02 ± 0.37	—
Lignin (%)	7.16 ± 0.14	—
Fe (mg/Kg)	624.59 ± 12.85	8559.60 ± 78.43
Co (mg/Kg)	0.39 ± 0.01	3.55 ± 0.01
Ni (mg/Kg)	7.45 ± 0.12	14.81 ± 0.39

Table 2: Factors and levels of coding table.

Factor	Level			Compounds
	1 $mg \cdot L^{-1} \cdot d^{-1}$	2 $mg \cdot L^{-1} \cdot d^{-1}$	3 $mg \cdot L^{-1} \cdot d^{-1}$	
A (Fe)	1.00	5.00	10.00	$FeCl_2 \cdot 4H_2O$
B (Co)	0.05	0.20	0.40	$CoCl_2 \cdot 6H_2O$
C (Ni)	0.20	0.40	0.60	$NiCl_2 \cdot 6H_2O$

The sludge (Inoculum) was collected from Shunyi County of Beijing City, China. Table 1 provides corn stover and sludge characteristics.

2.2. Experimental Set-Up. NaOH-pretreated corn stover was added with the three trace elements in batch anaerobic digesters, to investigate the combined effect of the trace elements and NaOH pretreatment on digestion performance.

Different concentrations of a well-defined trace element solution were added to anaerobic batch experiments according to our research and other authors' research [11]. To study the interaction of elements Fe ($FeCl_2 \cdot 4H_2O$), Co ($CoCl_2 \cdot 6H_2O$), and Ni ($NiCl_2 \cdot 6H_2O$), a full-factor test was designed to find the best element combinations; Table 2 shows the coding factors and levels. Higher trace element concentrations had inhibitory and toxic effects on anaerobic digestion [12]. As such, it was necessary to determine the trace metal amounts required to supplement levels already present in the substrate and measure levels in the digester's solid and liquid residue streams to assess potential toxicity issues in their use and disposal.

Digestion experiments were performed in batch anaerobic digesters, and each experiment was repeated three times. Each digester was 1 L in volume, with a working volume of 0.8 L. A loading rate of 65 g·TS/L was applied for the NaOH-pretreated corn stover. Each digester was seeded to maintain the sludge MLSS (mixed liquid suspended solids) in the digester at 15 g/L [13]. Urea was added to each digester to adjust the carbon-to-nitrogen ratio (C/N) to 25, believed to be optimal for anaerobic bacteria growth. The pH was adjusted to 7.5 ± 0.1 using calcium hydroxide ($Ca(OH)_2$) solution at the beginning of the anaerobic digestion process. Prepared

digesters were then placed in a water bath for anaerobic digestion tests. The water bath was operated at mesophilic temperature (35 ± 1°C) for a time period of 50 days.

Batch experiments were conducted for the best combination. Untreated (raw) and NaOH-pretreated corn stover were used as separate control samples, with the same operating conditions described above.

2.3. Analytical Methods

2.3.1. Biogas Analyses. Each anaerobic digester's biogas production was recorded daily using the water displacement method, and the corresponding cumulative biogas volume was calculated. The measured volume was then converted to a biogas volume at a standard temperature and pressure using the ideal gas law; this volume was used to calculate biomethane volume based on the BVF (biomethane volume fraction). The biogas BVF was analyzed daily using a gas chromatograph (GC) (SP-2100, BeiFenRuiLi Co., Beijing, China) equipped with a molecular sieve (TDX-01) packed 2 m × 3 mm stainless-steel column and a thermal conductivity detector (TCD). The temperatures of the oven, injector port, and TCD were 140, 150, and 150°C, respectively. Argon was used as the carrier gas at a 30 mL min^{-1} flow rate. A standard gas (BeiFenRuiLi Co., Beijing), composed of 10.02% H_2, 4.98% N_2, 50.1% CH_4, and 34.9% CO_2, was used to calibrate the system.

2.3.2. Chemical Composition Analyses. Total solids (TS), volatile solids (VS), and mixed liquor suspended solids (MLSS) of the corn stover, sludge, and their mixture were measured using APHA standard methods. Total carbon (TC) and total nitrogen (TN) were determined using a Vario EL/microcube elemental analyzer (Elementar, Germany). Lignin, cellulose, and hemicellulose content were determined using an automatic fiber analyzer (ANKOM A2000i, ANKOM, USA) using procedures proposed by Van Soest [14]. The pH was measured with a pH meter (3-Star, Thermo Orion, USA). Trace elements were quantified using an inductively coupled plasma optical emission spectrometer (iCAP 7500, Thermo Scientific, USA).

2.4. Data Analyses. Each analytical datum was the mean of at least three measurements. Full-factor test results, the standard deviations, and analysis of variance were analyzed using the statistical software SPSS 17.0 for Windows; analysis of variance was tested using a least-significant difference (LSD) method.

3. Results and Discussion

3.1. Determination of Optimal Trace Element Level. Serial batch experiments were conducted to investigate the effect of adding trace elements on biomethane production and to determine optimal trace element levels. All corn stover samples used for trace element tests were pretreated with NaOH. Table 3 presents biomethane productions with different concentrations of Fe, Co, and Ni. Batch trials with the combination A1B3C2 achieved the highest biomethane production, with concentrations of Fe, Co, and Ni at 1.0 $mg{\cdot}L^{-1}{\cdot}d^{-1}$, 0.4 $mg{\cdot}L^{-1}{\cdot}d^{-1}$, and 0.4 $mg{\cdot}L^{-1}{\cdot}d^{-1}$, respectively. The result is similar to findings from Li and Dong (2001), who reported an increase of biogas production after adding the combination of Fe (0.3 $mg{\cdot}L^{-1}{\cdot}d^{-1}$), Co (0.05 $mg{\cdot}L^{-1}{\cdot}d^{-1}$), and Ni (0.20 $mg{\cdot}L^{-1}{\cdot}d^{-1}$) during anaerobic digestion [8].

Table 4 shows between-subject effects. Factor B and the interaction of A∗B∗C, B∗C, A∗C were highly significant. Factors A and C and the interaction of A∗B had no effect on the test results. In terms of their respective influence, A∗B∗C was greater than B, which was greater than B∗C, which was greater than A∗C. The three trace elements Fe, Co, and Ni interacted with one another; the interaction of all three trace elements was higher than the interaction of a single element and two elements. Speece noted that the interaction among Fe, Co, Ni, Mo, and Se plays an important role in anaerobic digestion processes [6]. As such, group A1B3C2 was considered to be the optimal trace element combination and was used for subsequent tests.

3.2. Biomethane Production

3.2.1. Daily Biogas and Biomethane Production. The daily biogas production and the biomethane volume fraction for each group were recorded throughout the digestion test period. Figure 1(a) shows the daily biogas productions for different groups, demonstrating that the overall change trends were very similar. All daily biogas productions experienced fluctuation; biogas generation started after seeding and experienced several small peaks before finally ceasing. The start-up time, the biogas production peak value, and the time of the peak value which was reached differed for different groups. The digesters with A1B3C2 and NaOH-pretreated corn stover experienced rapid start-up after seeding. The highest daily biogas production reached 1,525 mL on Day 11 for the A1B3C2 group. For the NaOH-pretreated group, production reached 965 mL on Day 13; for the untreated group, production reached 880 mL on Day 24. Compared to the untreated corn stover and NaOH-pretreated corn stover, results indicate that the A1B3C2 group reached higher daily biogas production within a shorter digestion time.

Figure 1(b) shows the biomethane volume fraction (BVF) of the three groups. All showed similar general trends, with the BVF first increasing and then levelling off at a relatively constant level. However, the BVFs of the A1B3C2 and NaOH-pretreated groups increased quickly at start-up and reached constant levels earlier. The BVF of the untreated group increased slowly and took a longer time to reach a constant level. The average BVF of the A1B3C2 group was 61.8%; this is higher than the BVF of 55.7% for the NaOH-pretreated group and the BVF of 50.8% for the untreated group.

This finding indicates that combining NaOH pretreatment with supplemental trace elements could increase BVF. The result agrees with a study by Chen et al., who reported that the biogas volume increased by 43.4% and that BVF increased by 5.1% when Fe, Co, and Ni were applied at concentrations of 1.0, 0.1, and 0.2 $mg{\cdot}L^{-1}{\cdot}d^{-1}$, respectively [15]. A higher BVF may bring significant economic benefit, as

Table 3: Analysis of full-factor test.

Experimental group	Codes of factor and level (actual levels)			Cumulative biomethane production (mL)
	A (Fe) $mg \cdot L^{-1} \cdot d^{-1}$	B (Co) $mg \cdot L^{-1} \cdot d^{-1}$	C (Ni) $mg \cdot L^{-1} \cdot d^{-1}$	
1	1 (1.00)	1 (0.05)	1 (0.20)	10386 ± 94
2	1 (1.00)	1 (0.05)	2 (0.40)	10001 ± 56
3	1 (1.00)	1 (0.05)	3 (0.60)	10666 ± 396
4	1 (1.00)	2 (0.20)	1 (0.20)	10730 ± 62
5	1 (1.00)	2 (0.20)	2 (0.40)	10323 ± 491
6	1 (1.00)	2 (0.20)	3 (0.60)	9638 ± 365
7	1 (1.00)	3 (0.40)	1 (0.20)	10320 ± 118
8	1 (1.00)	3 (0.40)	2 (0.40)	11367 ± 361
9	1 (1.00)	3 (0.40)	3 (0.60)	11132 ± 163
10	2 (5.00)	1 (0.05)	1 (0.20)	9593 ± 274
11	2 (5.00)	1 (0.05)	2 (0.40)	10517 ± 141
12	2 (5.00)	1 (0.05)	3 (0.60)	10839 ± 239
13	2 (5.00)	2 (0.20)	1 (0.20)	10322 ± 456
14	2 (5.00)	2 (0.20)	2 (0.40)	9868 ± 259
15	2 (5.00)	2 (0.20)	3 (0.60)	10076 ± 388
16	2 (5.00)	3 (0.40)	1 (0.20)	10307 ± 101
17	2 (5.00)	3 (0.40)	2 (0.40)	10158 ± 560
18	2 (5.00)	3 (0.40)	3 (0.60)	10861 ± 76
19	3 (10.00)	1 (0.05)	1 (0.05)	10274 ± 367
20	3 (10.00)	1 (0.05)	2 (0.40)	10504 ± 649
21	3 (10.00)	1 (0.05)	3 (0.20)	10340 ± 103
22	3 (10.00)	2 (0.20)	1 (0.05)	10127 ± 441
23	3 (10.00)	2 (0.20)	2 (0.40)	10678 ± 582
24	3 (10.00)	2 (0.20)	3 (0.20)	10116 ± 33
25	3 (10.00)	3 (0.40)	1 (0.05)	10872 ± 156
26	3 (10.00)	3 (0.40)	2 (0.40)	10767 ± 372
27	3 (10.00)	3 (0.40)	3 (0.20)	9837 ± 105

Table 4: The result of between-subjects effects (dependent variables: X).

Source	III model 0	df	Mean square	F	Sig.
Correcting model	42544349.6[a]	26	1636321.137	2.635	0.001
Intercept	22460617248	1	22460617248	36165.606	0.000
A	933550.222	2	466775.111	0.752	0.476
B	6618446.889	2	3309223.444	5.328	0.008
C	644693.556	2	322346.778	0.519	0.598
A ∗ B	2944740.444	4	736185.111	1.185	0.328
A ∗ C	6475833.778	4	1618958.444	2.607	0.046
B ∗ C	8525127.111	4	2131281.778	3.432	0.014
A ∗ B ∗ C	16401957.556	8	2050244.694	3.301	0.004
Error	33536652.000	54	621049.111		
Total	22536698250.000	81			
Total correction	76081001.556	80			

[a] $R^2 = 0.559$ (regulate $R^2 = 0.347$).

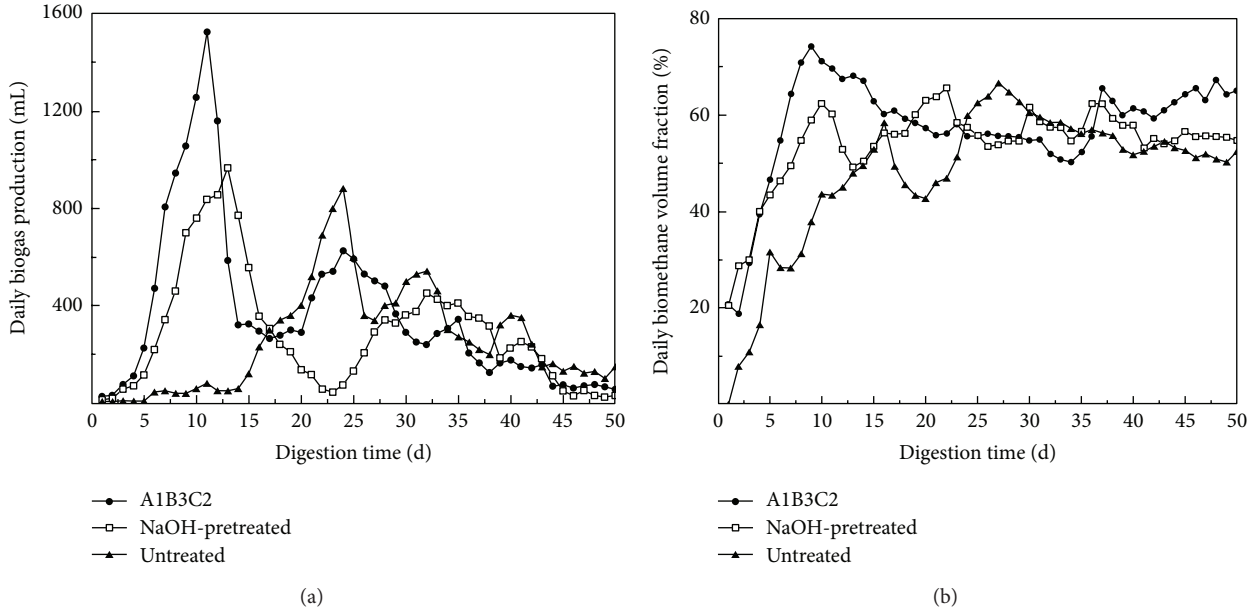

Figure 1: The daily biogas production (a) and biomethane volume fraction (b) for different groups.

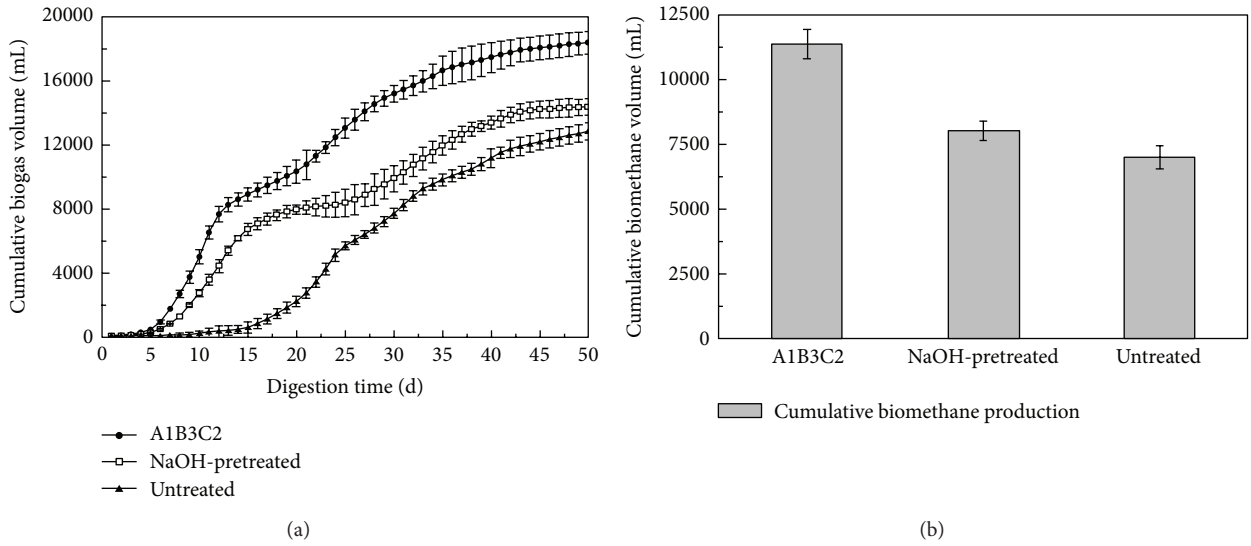

Figure 2: Cumulative biogas production (a) and biomethane production (b) for different groups.

it increases the biomethane yield for a given amount of corn stover.

3.2.2. Cumulative Biogas and Biomethane Production. Cumulative biogas production was calculated based on the daily biogas production during anaerobic fermentation. Figure 2(a) shows the changes in cumulative biogas productions for the three groups studied. After 50 days of digestion, the A1B3C2 group reached the highest cumulative biogas production of 18,400 mL. This was 27.9% higher than tests with NaOH-pretreatment and 43.1% higher than tests with untreated corn stover. This increase was attributed to the synergistic effect from NaOH pretreatment and trace elements addition. The synergistic effect was mainly due to the complementary characteristics of digested corn stover, more balanced nutrients, and improved biodegradability.

Multiple comparisons using the LSD method were performed on the cumulative biogas productions for the three groups. Test results showed that the cumulative biogas production with the A1B3C2 group was significantly higher than those of the others ($a = 0.05$). It further confirmed that combining NaOH pretreatment with trace elements could significantly improve biogas production when corn stover was used as a sole feedstock.

The energy contained in biogas is determined using both biogas volume and BVF. Cumulative biomethane volume,

Table 5: Biogas and biomethane yields and bioconversion rates for different groups.

Groups	Biogas yields		Biomethane yields		Bioconversion rates (%)	
	mL/g TS	mL/g VS	mL/g TS	mL/g VS	TS	VS
A1B3C2	354 ± 17	393 ± 31	219 ± 12	243 ± 24	55.7 ± 0.5%	65.9 ± 0.6%
NaOH-pretreated	277 ± 23	307 ± 26	154 ± 16	171 ± 20	45.6 ± 0.2%	57.8 ± 0.5%
Untreated	247 ± 15	275 ± 18	135 ± 14	150 ± 19	35.6 ± 0.9%	53.0 ± 0.3%

representing total energy gain, was calculated by timing daily biogas production with the corresponding BVF. Figure 2(b) shows the results. When anaerobic fermentation processes were completed, the cumulative biomethane volume reached 11,367 mL, 8,018 mL, and 7,009 mL for the A1B3C2, NaOH-pretreated, and untreated corn stover groups, respectively. The A1B3C2 group's cumulative biomethane volume was 41.8% higher than the NaOH-pretreated group and 62.2% higher than the untreated corn stover group, respectively. This confirms the significant influence of trace elements and NaOH pretreatment on biomethane production. Multiple comparisons using the LSD method also showed a significant difference ($a = 0.05$) in cumulative biomethane volume among three groups. Speece also demonstrated that adding trace elements of Fe, Co, and Ni could significantly increase biomethane production [16].

3.2.3. Digestion Time T_{90}. Digestion time is another indicator of substrate biodegradability and digestion efficiency. Digestion time T_{90} was defined as the number of days required to achieve 90% of potential biogas generation.

This study's anaerobic digestion process was extended for up to 50 days past the time when biogas production was near zero. The T_{90} for the A1B3C2 group was 33 days, 5–9 days shorter than NaOH-pretreated and untreated groups. The significant reduction in digestion time further indicated that the A1B3C2 group not only initiated digestion quickly, but also accelerated the biogas production process. Gonzalez-Gil et al. [17] studies indicated that adding Ni and Co can shorten the reaction's lag phase and facilitate the methanogen process [17]. This could bring significant economic benefits, by increasing the production efficiency or treatment capacity of a digester by using a shortened digestion time.

3.3. Mass Bioconversion

3.3.1. Bioconversion of TS and VS. Biogas is generated from a substrate's biological conversion during anaerobic digestion. Organic matter conversion into biogas reduces the amount of organic dry matter, resulting in a decrease in TS and VS.

Based on mass balance, the TS and VS bioconversion rates were calculated; Table 5 shows the results. Both TS and VS were reduced significantly through anaerobic microorganism bioconversion. However, the TS and VS bioconversion rates differed from each other and also differed between the three groups. The TS bioconversion rate was lower than VS for all three groups. TS and VS bioconversion rates for the A1B3C2 group were 55.7% (TS) and 65.9% (VS). These rates were 22.2%–56.3% higher than with the NaOH-pretreated group and 14.0%–53.1% higher than with the untreated corn stover. The A1B3C2 group achieved a higher bioconversion rate, representing significant biodegradability improvement. This is attributed to the combined role of NaOH pretreatment and trace elements, which improved corn stover biodegradability and also provided more balanced nutrients for anaerobic bacteria.

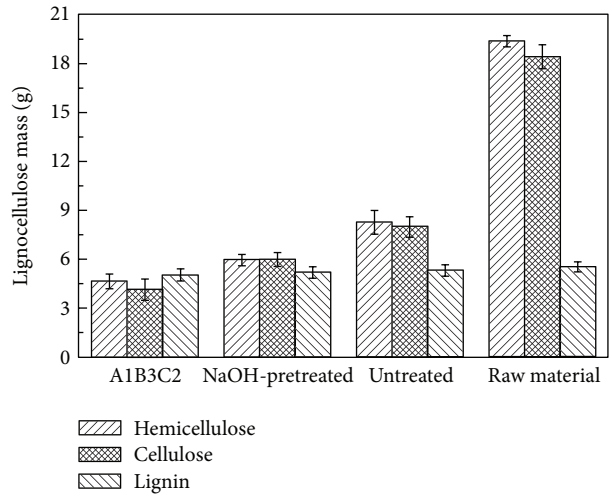

Figure 3: The changes of chemical compositions.

3.3.2. Bioconversion of Chemical Compositions. LCH (lignin, cellulose, and hemicellulose) are the main components of corn stover, accounting for 75.0% of the total dry matter and providing the main carbon sources for anaerobic microorganisms. Biogas production is greatly affected by the availability and digestibility of cellulose and hemicellulose and the association of lignin with the carbohydrates. The more biogas produced, the more the components are reduced. In this part of the study, cellulose, hemicellulose, and lignin bioconversion rates were analyzed to investigate main component bioconversion characteristics.

Figure 3 shows the changes in chemical compositions for the three studied groups at the end of anaerobic digestion. Bioconversion rates of the cellulose, hemicellulose, and lignin differed across the three groups. Hemicellulose and cellulose were clearly converted for all three groups. The total LCH bioconversion rates were 72.8%, 65.1%, and 54.9% for the A1B3C2, NaOH-pretreated, and untreated groups, respectively, when compared to raw material. The bioconversion rates of hemicellulose significantly increased by 76.1%, 69.3%, and 57.5% for the A1B3C2, NaOH-pretreated, and untreated

Table 6: The amount of trace elements in feedstock and effluent.

Element	Feedstock (mg)			Effluent (mg)	
	Activated sludge	Corn stover	Element addition	Liquid	Solid
Fe	122.16 ± 0.23	32.47 ± 0.85	48.00	12.66 ± 0.21	192.18 ± 1.42
Co	0.19 ± 0.01	0.07 ± 0.01	19.47	0.78 ± 0.01	19.20 ± 0.12
Ni	0.21 ± 0.01	0.39 ± 0.02	19.20	1.70 ± 0.13	17.38 ± 0.16

Table 7: System stability of anaerobic digestion.

Different groups	pH	Ammonia nitrogen (mg/L)	Alkalinity (mg/L)	Volatile fatty acids (mg/L)
A1B3C2	7.44 ± 0.02	490 ± 30	8550 ± 850	269 ± 50
NaOH-pretreated	7.45 ± 0.02	518 ± 56	10700 ± 300	511 ± 10
Untreated	7.47 ± 0.02	490 ± 42	9255 ± 225	785 ± 21

groups, respectively. The bioconversion rates of cellulose significantly increased by 77.5%, 67.5%, and 56.7% for the A1B3C2, NaOH-pretreated, and untreated groups, respectively. Lignin amounts had almost no change. The A1B3C2 group achieved the maximum LCH bioconversion rate.

Pretreatment before anaerobic digestion is a simple and effective method to improve lignocellulosic material biodegradability. Pretreatment can decompose cellulose and hemicellulose into relatively biodegradable components and break the link between polysaccharide and lignin to make cellulose and hemicellulose more accessible to bacteria [18]. Additionally, adding trace elements for corn stover anaerobic digestion can enhance microorganism activity. This result further verified NaOH pretreatment effectiveness and the ability of trace elements to improve biodegradability and enhance bioenergy production.

3.3.3. Trace Element Bioavailability. Methanogens absorbed and fixed trace elements through extracellular complexion, extracellular precipitation, and intracellular accumulation [19]. Fe, Co, and Ni concentrations in effluent were measured to assess trace element availability at the end of anaerobic digestion. Table 6 lists the trace elements present in the feedstock and effluent from the A1B3C2 group. The table shows that effluent trace elements mainly existed as solids in the A1B3C2 group; the amounts of trace elements in the solids accounted for 93.8%, 96.1%, and 91.1% of total Fe, Co, and Ni amounts added, respectively. Karlsson et al. (2012) also noted that only a fraction of trace elements is present in solution; in most cases, trace element bioavailability for anaerobic bacteria metabolic pathways is not related to the total amount in the medium [11]. The calculated result shows that approximately 89.6% Fe, 97.2% Co, and 87.4% Ni of the total amount added were converted to solid form. As such, adding Fe 0.897 g, Co 0.389 g, and Ni 0.349 g at the beginning of operation can both satisfy anaerobic digestion needs and enhance biological activity.

3.4. System Stability. It is important that a digester operate in a stable state, while maintaining good performance. When using corn stover as a sole substrate, the digestion system has an increased potential for instability, due to possible lower buffering capability. Digestion system stability depends on a number of factors, including pH, volatile fatty acids (VFAs), ammonia nitrogen, and alkalinity. This study assessed these parameters to evaluate the stability of corn stover anaerobic digestion when combining NaOH pretreatment and trace element supplements.

Table 7 shows that each group's pH value was maintained at 7.30–7.45 at the end of methanogenesis throughout the digestion period. Ammonia nitrogen and alkalinity were important parameters in maintaining anaerobic system stability. Free ammonia was produced from organic nitrogen degradation, causing alkalinity variation in the anaerobic system. Adequate ammonia content can effectively improve the efficiency of anaerobic digestion, while ammonia nitrogen may inhibit methanogen activity when levels exceed 2,000 mg/L. Table 7 shows that the ammonia nitrogen for the three groups ranged from 490 to 518 mg/L, within an acceptable range. The anaerobic digestion system alkalinity was 8,550–10,700 mg/L. This higher alkalinity supports strong system stability. These findings indicate that the corn stover with NaOH pretreatment and trace element supplements did not inhibit ammonia nitrogen, while maintaining high alkalinity, thereby ensuring stable system operation.

VFAs were important intermediate products during anaerobic digestion. VFAs in the A1B3C2 group were significantly lower than those with NaOH pretreatment and untreated group (Table 6). The A1B3C2 group benefited methanogenic bacterial growth and biomethane production.

4. Conclusions

Combining NaOH pretreatment and trace element addition is an effective method to improve corn stover biodegradability and enhance biomethane production. The best combination was adding 1.0, 0.4, and 0.4 $mg \cdot L^{-1} \cdot d^{-1}$ of trace elements Fe, Co, and Ni (A1B3C2), respectively. When compared to NaOH-pretreated and untreated corn stover, A1B3C2 group experienced 41.8% and 62.2% more cumulative biomethane

volumes, 22.2%–56.3% and 14.0%–53.1% more TS and VS bioconversion rates, and 5–9 days shorter T_{90}, while also maintaining good operational stability.

Conflict of Interests

The authors declare that there is no conflict of interests regarding the publication of this paper.

Acknowledgments

The authors are grateful to the fund supports from the University Doctorial Foundation (20120010110004) and the Twelfth Five-Year National Key Technologies R&D Program (no. 2010BAC67B03).

References

[1] M. Zheng, X. Li, L. Li, X. Yang, and Y. He, "Enhancing anaerobic biogasification of corn stover through wet state NaOH pretreatment," *Bioresource Technology*, vol. 100, no. 21, pp. 5140–5145, 2009.

[2] H. Pobeheim, B. Munk, J. Johansson, and G. M. Guebitz, "Influence of trace elements on methane formation from a synthetic model substrate for maize silage," *Bioresource Technology*, vol. 101, no. 2, pp. 836–839, 2010.

[3] K.-L. Chang, J. Thitikorn-Amorn, J.-F. Hsieh et al., "Enhanced enzymatic conversion with freeze pretreatment of rice straw," *Biomass & Bioenergy*, vol. 35, no. 1, pp. 90–95, 2011.

[4] P. Salehian, K. Karimi, H. Zilouei, and A. Jeihanipour, "Improvement of biogas production from pine wood by alkali pretreatment," *Fuel*, vol. 106, pp. 484–489, 2013.

[5] L. Hinken, I. Urban, E. Haun, I. Urban, D. Weichgrebe, and K.-H. Rosenwinkel, "The valuation of malnutrition in the monodigestion of maize silage by anaerobic batch tests," *Water Science and Technology*, vol. 58, no. 7, pp. 1453–1459, 2008.

[6] R. E. Speece, *Nutrient Requirements in Anaerobic Digestion of Biogas*, USA Elsevier Applied Sciences Publication, London, UK, 1987.

[7] K. Mori, M. Hatsu, R. Kimura, and K. Takamizawa, "Effect of heavy metals on the growth of a methanogen in pure culture and coculture with a sulfate-reducing bacterium," *Journal of Bioscience and Bioengineering*, vol. 90, no. 3, pp. 260–265, 2000.

[8] Y. X. Li and C. J. Dong, "Determining trace metals stimulating methanogens and their supplement dosage," *Environmental Pollution & Control*, vol. 23, no. 3, pp. 116–118, 2001.

[9] H. C. Friedmann, A. Klein, and R. K. Thauer, "Structure and function of the nickel porphinoid, coenzyme F_{430}, and of its enzyme, methyl coenzyme M reductase," *FEMS Microbiology Reviews*, vol. 87, no. 3-4, pp. 339–348, 1990.

[10] S. Jansen, G. Gonzalez-Gil, and H. P. van Leeuwen, "The impact of Co and Ni speciation on methanogenesis in sulfidic media-Biouptake versus metal dissolution," *Enzyme and Microbial Technology*, vol. 40, no. 4, pp. 823–830, 2007.

[11] A. Karlsson, P. Einarsson, A. Schnürer, C. Sundberg, J. Ejlertsson, and B. H. Svensson, "Impact of trace element addition on degradation efficiency of volatile fatty acids, oleic acid and phenyl acetate and on microbial populations in a biogas digester," *Journal of Bioscience and Bioengineering*, vol. 114, no. 4, pp. 446–452, 2012.

[12] Y. Y. Li and B. Li, "The anaerobic digestion of and the requirements for trace elements of coal gasification wastewater," *Journal of Wuyi University*, vol. 4, no. 22, pp. 1–5, 2008.

[13] R. H. Zhang and Z. Q. Zhang, "Biogasification of rice straw with an anaerobic-phased solids digester system," *Bioresource Technology*, vol. 68, no. 3, pp. 235–245, 1999.

[14] P. J. van Soest, J. B. Robertson, and B. A. Lewis, "Methods for dietary fiber, neutral detergent fiber, and nonstarch polysaccharides in relation to animal nutrition," *Journal of Dairy Science*, vol. 74, no. 10, pp. 3583–3597, 1991.

[15] C. M. Chen, G. M. Zeng, B. B. Zhang et al., "Study on improvement of trace activators and energy production in Anaerobic digestion of municipal organic refuse," *Journal of Nanhua University*, vol. 18, no. 1, pp. 12–16, 2004.

[16] R. E. Speece, "Anaerobic biotechnology for industrial wastewater treatment," *Environmental Science & Technology*, vol. 17, no. 9, pp. 416–427, 1983.

[17] G. Gonzalez-Gil, R. Kleerebezem, and G. Lettinga, "Effects of nickel and cobalt on kinetics of methanol conversion by methanogenic sludge as assessed by on-line CH_4 monitoring," *Applied and Environmental Microbiology*, vol. 65, no. 4, pp. 1789–1793, 1999.

[18] H. Chen, L. Liu, X. Yang, and Z. Li, "New process of maize stalk amination treatment by steam explosion," *Biomass & Bioenergy*, vol. 28, no. 4, pp. 411–417, 2005.

[19] D. Q. Zhou, *Microbiology Tutorials*, Beijing Higher Education Press, Beijing, China, 2002.

Hindawi Publishing Corporation
BioMed Research International
Volume 2015, Article ID 456834, 8 pages
http://dx.doi.org/10.1155/2015/456834

Research Article

Nanofibrillated Cellulose and Copper Nanoparticles Embedded in Polyvinyl Alcohol Films for Antimicrobial Applications

Tuhua Zhong,[1] Gloria S. Oporto,[1] Jacek Jaczynski,[2] and Changle Jiang[1]

[1]*Division of Forestry and Natural Resources, West Virginia University, Morgantown, WV 26506, USA*
[2]*Division of Animal and Nutritional Sciences, West Virginia University, Morgantown, WV 26506, USA*

Correspondence should be addressed to Gloria S. Oporto; gloria.oporto@mail.wvu.edu

Received 26 December 2014; Revised 30 March 2015; Accepted 15 April 2015

Academic Editor: Lei Zhao

Our long-term goal is to develop a hybrid cellulose-copper nanoparticle material as a functional nanofiller to be incorporated in thermoplastic resins for efficiently improving their antimicrobial properties. In this study, copper nanoparticles were first synthesized through chemical reduction of cupric ions on TEMPO nanofibrillated cellulose (TNFC) template using borohydride as a copper reducing agent. The resulting hybrid material was embedded into a polyvinyl alcohol (PVA) matrix using a solvent casting method. The morphology of TNFC-copper nanoparticles was analyzed by transmission electron microscopy (TEM); spherical copper nanoparticles with average size of 9.2 ± 2.0 nm were determined. Thermogravimetric analysis and antimicrobial performance of the films were evaluated. Slight variations in thermal properties between the nanocomposite films and PVA resin were observed. Antimicrobial analysis demonstrated that one-week exposure of nonpathogenic *Escherichia coli* DH5α to the nanocomposite films results in up to 5-log microbial reduction.

1. Introduction

Currently in the Appalachian region there is a vast amount of low-value, low-quality hardwood that can potentially be used as feedstock for novel bioproducts. Only West Virginia generates 2.41 million dry tones of underutilized wood per year that might be a great source for nanocellulose production. Today the technology to separate and obtain wood polymers at nanoscale exists and it has been demonstrated with success; however, specific applications for these novel raw materials are still a challenge. Based on our preliminary results [1], one interesting application is the utilization of micro- and nanostructures of cellulose as templates and stabilizers for biocide nanoparticles with emphasis of application as antimicrobial nanocomposites in the packaging and/or medical industry.

Metals, such as copper and silver, are relatively common antimicrobial materials that can be incorporated as nanomaterials in thermoplastic films for packaging and/or medical industry [2–4]; however, to avoid leaching, to improve metal dispersion, and to improve the contact between the metal and the bacterial wall a supportive material might be required. In addition, it is expected that the metal ions can be released from the film in a controlled way to effectively prevent microbial growth. To date, the development of nanocomposite films fabricated from thermoplastic resins with cellulose nanofibers has emerged as a potentially effective approach for improving mechanical properties of these films [5, 6]. Our own preliminary findings provide evidence that these cellulose nanofibers could be used as support materials for copper nanoparticles improving also the antimicrobial properties of the films.

In general, the prevailing concept of grafting metal on the surface of cellulose derivatives involves trapping the metallic cations via electrostatic interactions with negatively charged groups (e.g., carboxylate and hydroxyl) present in the correspondent template. The presence of carboxyl groups on the cellulose backbone will help to stabilize and reduce copper ions on the cellulosic structure. In this research our focus was centered in the utilization of TEMPO-oxidized cellulose nanofibers as nanosized cellulose for the synthesis of copper nanoparticles. The hybrid material was embedded in a biodegradable polymer, polyvinyl alcohol, and the performance of the final film was evaluated.

Table 1: Preparation of the hybrid TNFC-copper nanoparticles.

Sample	TNFC gel (g)	TNFC (g)	$CuSO_4$ (0.1 mol/L) (mL)	$NaBH_4$ (0.5 mol/L) (mL)	Total liquid amount (mL)
TNFC-copper nanoparticles (1)	12	0.1152	6.4	2.56	30
TNFC-copper nanoparticles (2)	12	0.1152	8.0	3.2	30
TNFC-copper nanoparticles (3)	12	0.1152	9.6	3.84	30
TNFC-copper nanoparticles (4)	12	0.1152	11.2	4.42	30

TEMPO or 2,2,6,6-tetramethylpiperidine-1-oxyl molecule is a highly stable nitroxyl radical which is used extensively in the selective oxidation of primary alcohols to corresponding aldehydes and carboxylic acids [7]. In aqueous environments, TEMPO catalyzes the conversion of carbohydrate primary alcohols to carboxylate (COO-) functionalities in the presence of a primary oxidizing agent, for example, sodium hypochlorite (NaOCl). Various TEMPO-mediated oxidation reactions of mono-, oligo-, and polysaccharides for regioselective conversion of primary hydroxyls to carboxylate groups have been published elsewhere [8, 9]. In particular, wood celluloses can be converted to individual nanofibers 3-4 nm wide with several microns length by TEMPO-mediated oxidation and successive mild disintegration in water [7, 10, 11]. During this reaction significant amounts of C6 carboxylate groups are selectively formed on each cellulose microfibril surface without any changes to the original crystallinity or crystal width of wood celluloses.

Polyvinyl alcohol (PVA) is a commercial important water-soluble, semicrystalline, transparent, biocompatible, and biodegradable polymer. It has been successfully blended with several natural materials such as fibers and fillers for PVA mechanical properties improvements. With increasing interest in the use of biodegradable and sustainable plastics, PVA has been used in several applications such as tissue scaffolding, filtration materials, and membranes and drug delivery [6, 12, 13].

As mentioned previously, in this preliminary work a simple method was developed to produce hybrids of TEMPO nanofibrillated cellulose (TNFC) and copper nanoparticles. The hybrid material was subsequently embedded in polyvinyl alcohol thermoplastic resin and the final films were produced using a solvent casting method. The films were evaluated in terms of its morphology and thermal and antimicrobial properties.

2. Materials and Methods

2.1. Materials. TEMPO nanofibrillated cellulose (TNFC) (0.96 wt.%) from the Forest Product Laboratory, Madison, WI; technical-crystal cupric sulfate pentahydrate ($CuSO_4{\cdot}5H_2O$) from Fisher Scientific, USA; sodium borohydride ($NaBH_4$) (0.5 M) from Acros Organics, USA; poly(vinyl alcohol) (99-100% hydrolyzed, approx. M.W. 86000) was from Acros Organics, USA; Nonpathogenic *E. coli* DH5α (α substrain of DH5 described by Hanahan in 1985, "DH" stands for Douglas Hanahan) is a very sensitive microorganism. This *E. coli* contains mutations of the *recA* and *gyrA* (gyrase subunit A) genes that are necessary for DNA repair and replication. Therefore, *recA* and *gyrA* mutants have impaired ability to repair and recombine their DNA strands making the mutants sensitive to any stress including chemicals. This is why this sensitive and nonpathogenic *E. coli* was selected as a model microbial target in this study. Sterile trypticase soy broth (TSB) from Becton Dickinson, USA; Petrifilm *E. coli*/Coliform Count Plate from 3M, USA; Butterfield phosphate buffer from Hardy Diagnostics, USA.

2.2. Preparation of the Hybrid TNFC-Copper Nanoparticles. Hybrid TNFC-copper nanoparticles were prepared by introducing copper nanoparticles on TNFC substrate by the chemical reduction of cupric ions. Twelve grams of TNFC gel containing 0.96 wt.% cellulose nanofibers was dissolved in the deionized water under vigorous magnetic stirring. A predefined amount of $CuSO_4$ solution (0.1 mol/L) as shown in Table 1 was added by drops into the TEMPO-oxidized cellulose nanofibers solution. The mixture of TNFC and cupric sulfate was subjected to high-speed mixing while the cupric sulfate solution was added. Then the mixture was allowed to react at room temperature for 3 h. After that, cupric ions were reduced to metallic copper or copper oxide nanoparticles by adding the predefined amount of reducing agent sodium borohydride (0.5 mol/L).

2.3. Preparation of PVA/TNFC and PVA/TNFC-Copper Nanoparticles Nanocomposite Films. Polyvinyl alcohol/TNFC-copper nanoparticle nanocomposite films were prepared by solvent casting method described elsewhere [14]. Ninety milliliters of deionized water was heated to 90°C using a hot plate. Upon the desired temperature, 10 g of PVA was sprinkled into the hot water under vigorous magnetic stirring, after all PVA was added; the beaker will be covered; the mixture was heated at 90°C for 2 h. Subsequently, hybrid TNFC-copper nanoparticles solution was added by drops into clear PVA solution under vigorous magnetic stirring for 2 h. The resulting solution was transferred to glass dish and put in the desiccator to degas for 24 h under vacuum and then put in the oven at 50°C for 24 h. PVA films with different copper concentration were formed and the compositions of the film were shown in Table 2. According to the weight ratio of copper in the composites, that is, 0.4, 0.5, and 0.6 wt.%, the nanocomposite films were coded as PVA/TNFC-Cu0.4, PVA/TNFC-Cu0.5, and PVA/TNFC-Cu0.6. Pure PVA

Table 2: Preparation of the PVA/TNFC-copper nanoparticles nanocomposite films.

Composition	Sample code			
	PVA/TNFC-Cu0.4	PVA/TNFC-Cu0.5	PVA/TNFC-Cu0.6	PVA/TNFC-Cu0.7
PVA (g)	10	10	10	10
TNFC-copper nanoparticles (1) (mL)	30	—	—	—
TNFC-copper nanoparticles (2) (mL)	—	30	—	—
TNFC-copper nanoparticles (3) (mL)	—	—	30	—
TNFC-copper nanoparticles (4) (mL)	—	—	—	30
Copper content within final films (wt. %)	0.4	0.5	0.6	0.7

and PVA/TNFC films were also prepared as control for antimicrobial testing.

2.4. Transmission Electron Microscopy (TEM). The morphology and particle size of copper nanoparticles on TNFC substrate were observed by JEOL TEM-2100 instrument (Tokyo, Japan) operating at 120 kV. TEM samples were typically prepared by dropping the hybrid TNFC-copper nanoparticles solution on a 200-mesh Nickel grid coated with a carbon film.

2.5. Thermogravimetric Analyzer (TGA) Characterization. The thermal behaviors of pure PVA and its nanocomposite films were determined by TA Q50 thermogravimetric analyzer (Delaware, USA), with temperature ramp-up rate of 10°C/min while being purged with nitrogen at a flow rate of 20 mL/min. The sample weight was chosen between 3 mg and 4 mg for all of the samples tested.

2.6. Determination of Antimicrobial Activity of PVA/TNFC-Copper Nanoparticles Nanocomposite Films. *E. coli* lyfo-disks were reconstituted by crushing one pellet using a sterile spatula in 0.5 mL of sterile TSB. The content was aseptically transferred to 99.5 mL of sterile TSB and allowed to grow aerobically at 37°C for 24 h in an incubator/shaker set at 150 rpm (C24, New Brunswick Scientific, New Jersey, USA). This procedure yielded 100 mL of *E. coli* stock culture. For experiments, a loopful of the stock culture was transferred to 100 mL of sterile TSB followed by incubation at 37°C for 24 h in the C24 incubator/shaker set at 150 rpm. This procedure yielded a culture with appropriately 10^8 colony-forming units per milliliter (CFU/mL). A 2 mL aliquot of such culture was transferred to a surface of pure PVA, PVA/TNFC, and PVA/TNFC-copper nanoparticles films and incubated at room temperature for 1 week. To prevent excessive evaporation of the *E. coli* culture from the surface of films, the films were kept in an aerobic environment with saturated humidity. After 1-week exposure, 1 mL of *E. coli* culture was removed from the surface of films to enumerate *E. coli* survivors. Prior to removal, the *E. coli* culture on films was carefully mixed to obtain equal cell distribution. Enumeration was performed by a standard serial 10-fold dilution procedure and spread plating in a biosafety cabinet under aseptic procedures [15, 16]. A 1 mL aliquot of the *E. coli* culture removed from the surface of films was aseptically mixed with 9 mL of diluent (Butterfield phosphate buffer, Hardy Diagnostics, Santa Maria, CA, USA) followed by shaking the diluent bottle to uniformly distribute bacterial cells. Subsequent serial 10-fold dilutions were aseptically made by taking 10 mL of diluted sample and transferring it to a 90 mL diluent bottle. Survivors were enumerated on selective medium (Petrifilm *E. coli*/Coliform Count Plate, 3M, St. Paul, MN, USA) using a standard spread-plating technique. A 1.0 mL aliquot of each serial 10-fold dilution was pipetted and spread on 3M Petrifilm plates. The 3M Petrifilm plates were incubated at 35°C for 48 h [17]. Only plates with 15–150 colonies were counted.

Experiments were independently triplicated ($n = 3$). Enumeration of *E. coli* survivors in each equipment was performed in duplicate. Mean values for *E. coli* survivors were used to calculate log reductions of *E. coli* on the tested films (Figure 5). Differences between treatments (i.e., different films) were tested using the Least Significant Difference (LSD) test. All statistical analyses of data were performed using JMP version 12 Statistical Software (Statistical Discovery, from SAS).

3. Results and Discussion

3.1. Morphology of Copper Nanoparticles on TNFC Template. Figure 1 displays the TEM image of hybrid TNFC-copper nanoparticles (a), particle size histogram (b), and its corresponding EDX spectrum (c). Spherical copper nanoparticles with the particle size ranging from 5 nm to 14 nm and with average particles size 9.2 ± 2.0 nm are observed. EDX confirms the formation of copper nanoparticles by exhibiting peaks at approximately 8 keV (Figure 1(c)).

3.2. TGA Analysis. Figure 2 shows typical TGA and DTG curves of the PVA composite films. All the PVA/TNFC-Cu composite films exhibited four distinct weight loss stages at 30–210°C (loss of weakly physic-sorbed water), 210–230°C (decomposition of TNFC-copper nanoparticles nanocomposites, the thermal behavior of TNFC-copper nanoparticles is similar to that of carboxymethyl cellulose-copper nanoparticles reported by Nadagouda and Varma [18]), 230–380°C (decomposition of side chain of PVA), and 380–550°C (decomposition of main chain of PVA). Major weight losses were observed in the range of 210–550°C, which corresponded to the structural decomposition of PVA and

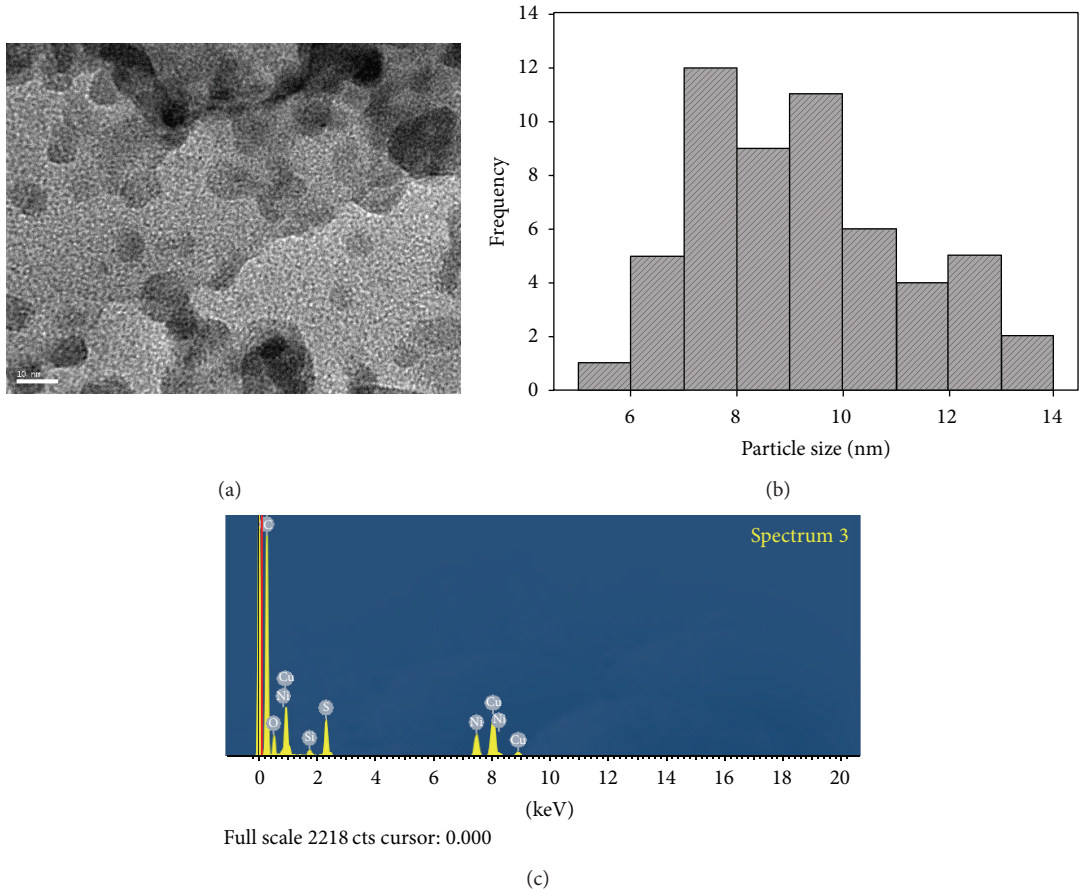

Figure 1: (a) TEM images of hybrid TNFC-copper nanoparticles (scale bar = 10 nm); (b) histogram of particle size distribution (n = 55 particles); (c) EDX spectrum of the hybrid TNFC-copper nanoparticles.

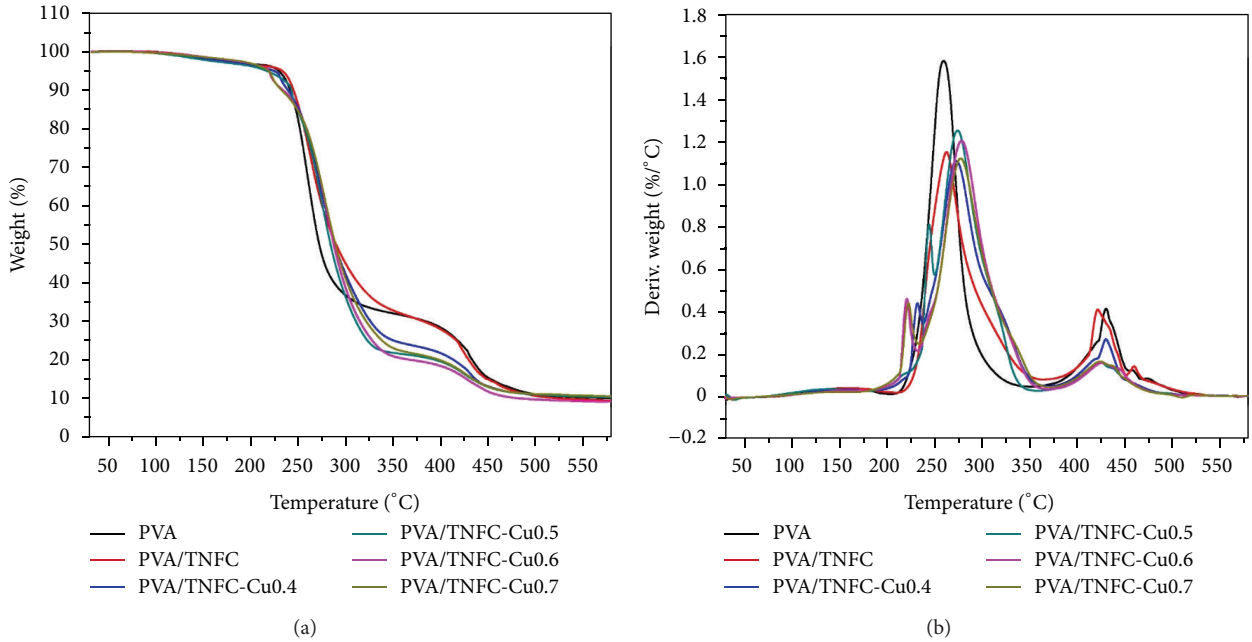

Figure 2: (a) TGA curves for the pure PVA, PVA/TNFC film, and PVA/TNFC-Cu composite films; (b) the corresponding DTG curves. Peak temperatures (T_{max}) of PVA, PVA/TNFC, PVA/TNFC-Cu0.4, PVA/TNFC-Cu0.5, PVA/TNFC-Cu0.6, and PVA/TNFC-Cu0.7 were 260, 263, 274, 275, 278, and 278°C, resp.).

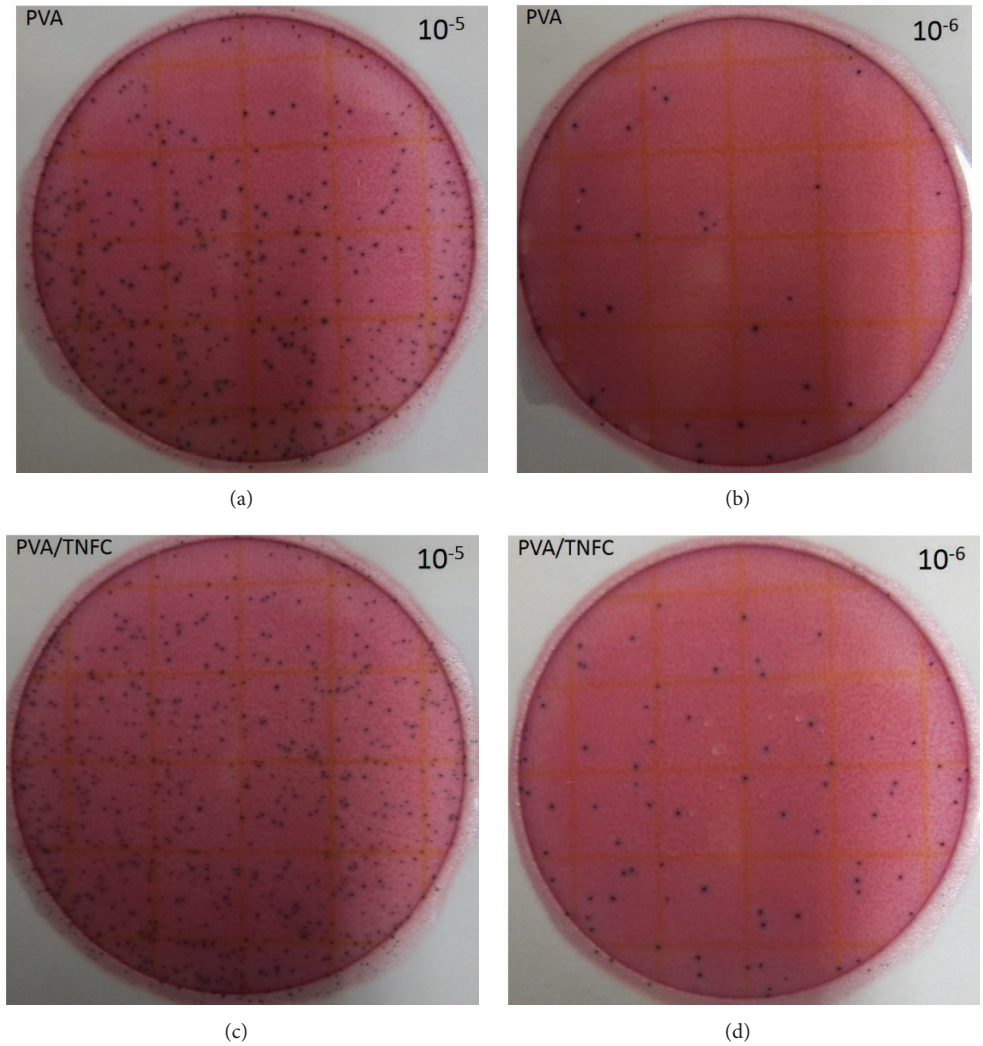

Figure 3: Bacterial enumeration of the 24 h *Escherichia coli* culture exposed to control materials: (a, b) PVA film and (c, d) PVA/TNFC film for 1 week at room temperature. (a, c) Representative Petrifilm plates for 10^{-5} dilution; (b, d) representative Petrifilm count plates for 10^{-6} dilution.

thermal degradation of TNFC. T_{max} is the decomposition temperature corresponding to the maximum weight loss and relates to the maximum decomposition rate. In Figure 2(b), we can see that T_{max} of PVA/TNFC-Cu composite films shifted to higher temperature compared to that of pure PVA and PVA/TNFC; an increase of T_{max} was observed from 260 to 278°C for PVA and PVA/TNFC-Cu0.7 composite film, respectively. The thermal decomposition of PVA/TNFC-Cu films shifted slightly toward high temperature, suggesting that the composite films had higher thermal stability, which can be attributed to the presence of copper nanoparticles embedded in the PVA matrix.

3.3. Antimicrobial Activity of PVA/TNFC-Copper Nanoparticles Films. The antimicrobial properties of pure PVA, PVA/TNFC films, and PVA/TNFC-copper nanoparticle films with different copper concentration were tested against *E. coli*. Figures 3 and 4 show representative images of visual examples of different serial 10-fold dilutions for *E. coli* survivors following their exposure to pure PVA and PVA/TNFC films (Figure 3) and PVA/TNFC-copper nanoparticle films with different copper concentration (Figure 4). The initial concentration of *E. coli* (i.e., prior to exposure to films) was approximately 10^8 CFU/mL. Figure 3 shows relatively minimal reduction of the initial *E. coli* concentration following exposure to pure PVA and PVA/TNFC films, while Figure 4 shows a trend of increasing microbial reduction as a function of greater copper nanoparticles concentration in films.

The counts from enumeration of *E. coli* survivors (representative images shown in Figures 3 and 4) were log-converted and used to determine *E. coli* reductions as a function of exposure to different films (Figure 5). Figure 5 shows that PVA and PVA/TNFC films resulted in similarly ($P > 0.05$) minimal reduction of *E. coli*. However, increasing

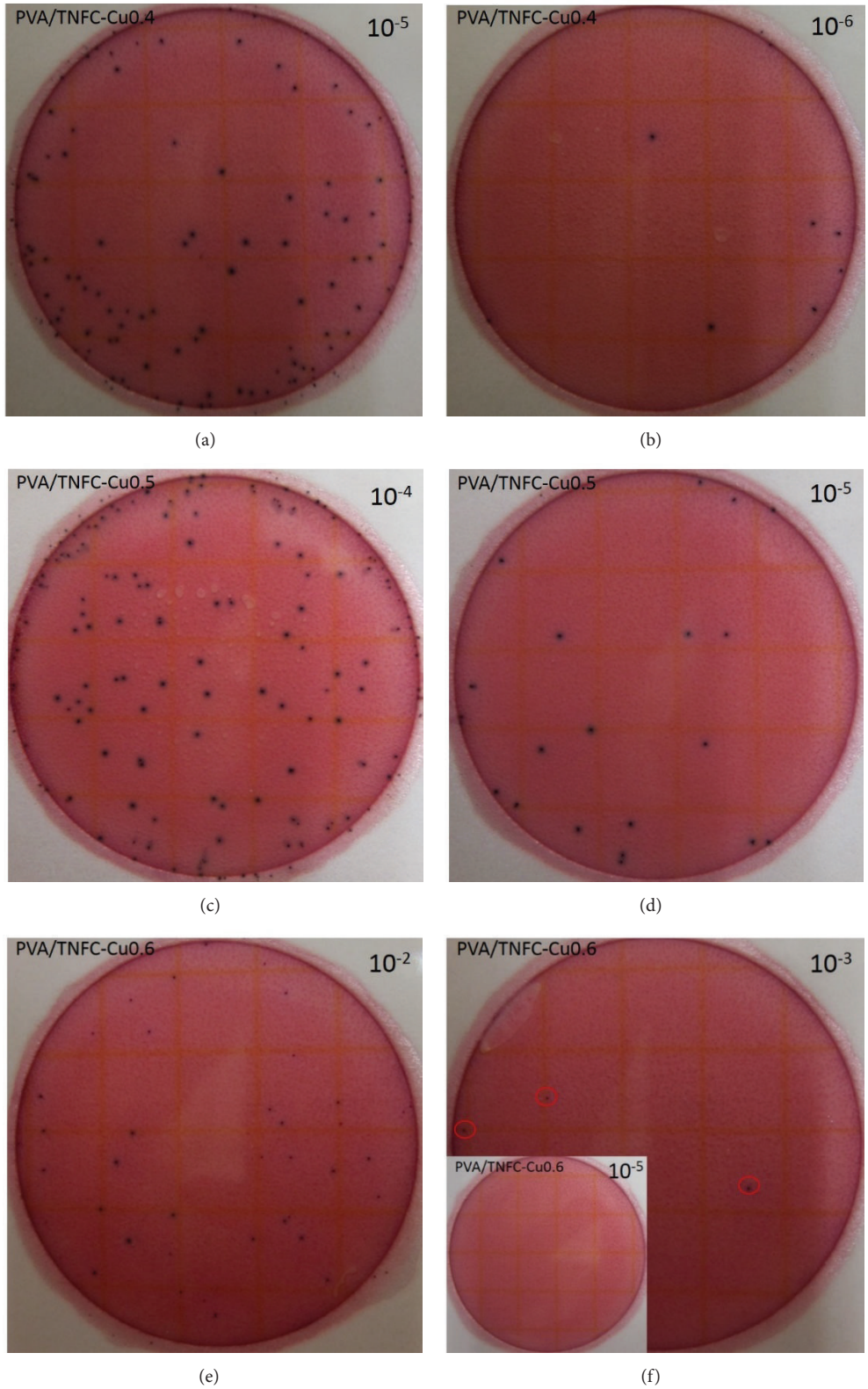

Figure 4: Bacterial enumeration of the 24 h *Escherichia coli* culture exposed to PVA nanocomposite film containing various copper content: (a, b) PVA/TNFC-Cu0.4, (c, d) PVA/TNFC-Cu0.5, and (e, f) PVA/TNFC-Cu0.6 films for 1 week at room temperature. (a–f) Representative Petrifilm count plates for various dilutions.

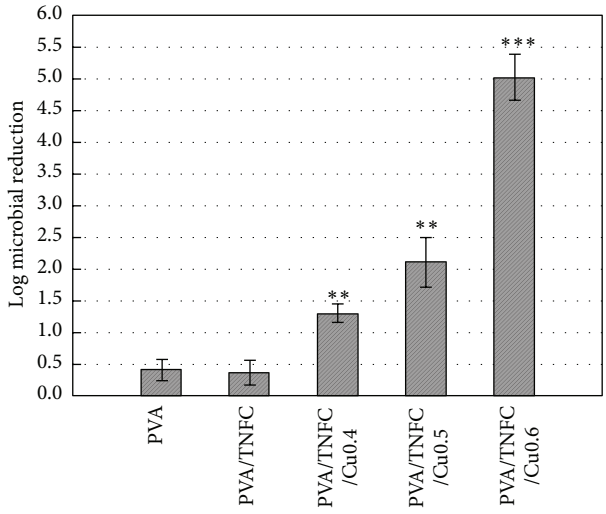

Figure 5: Microbial reduction induced by PVA/TNFC-copper nanoparticles after 1-week exposure. The asterisks refer to significant levels compared to one of the controls: PVA/TNFC, $P < 0.05$ (∗), $P < 0.01$ (∗∗), and $P < 0.001$ (∗ ∗ ∗).

concentration of copper nanoparticles in PVA/TNFC films resulted in greater ($P < 0.05$) reduction of *E. coli*. After 1-week exposure of *E. coli* to films containing 0.4%, 0.5%, and 0.6% of copper nanoparticles, reduction of *E. coli* has gradually increased ($P < 0.05$) and reached about 5-log reduction for the highest inclusion of copper nanoparticles in the film. Based on Figure 5, embedding copper nanoparticles in the PVA/TNFC film results in inactivation of *E. coli* that shows greater efficacy with higher concentration of copper nanoparticles. However, it needs to be emphasized that *E. coli* used in this study as a microbial target was a very sensitive strain; and, therefore, the antimicrobial efficacy of copper nanoparticles would likely be less profound for a typical foodborne pathogen such as *E. coli* O157:H7. Further research using more resistant foodborne pathogens is recommended.

Even though the antimicrobial mechanism of copper nanoparticles against microorganisms has not been fully understood, three hypothetical mechanisms are the most widely accepted and reported in the literature: (1) copper nanoparticles accumulate in the bacterial membrane and cause changes in membrane permeability [19]; (2) reactive oxygen species (ROS) produced through Fenton-type reactions lead to free-radical-mediated cellular damage [20, 21]; (3) the release of copper ions from nanoparticles causes inactivation of enzymes and depletion of intracellular ATP as well as disruption of DNA replication [22].

In this study we propose that the antimicrobial effect of PVA/TNFC-copper nanoparticles films is directly related to the transfer of copper ions leaching in a controlled manner from the PVA matrix to bacterial cells. This is consistent with the traditional hypothesis that metal ions attach to the negatively charged bacterial cell wall, resulting in disruption of cell wall permeability and thus inducing protein denaturation and finally cell death. PVA is a hydrophilic polymer; and, therefore, it is hygroscopic. Water sorption may induce the release of copper ions trapped in nanoparticles within the PVA matrix because of surface oxidation that occurs when copper nanoparticles are exposed to oxygen [4].

4. Conclusions

Copper nanoparticles with average diameter of 9.2 ± 2.0 nm were successfully synthesized on the TEMPO nanofibrillated cellulose. The decomposition temperature, corresponding to the maximum weight loss, increased from 260°C for pure PVA, to 278°C for the PVA composite. The incorporation of hybrid TNFC-copper nanoparticles within PAV matrix endows the resulting composite films with antimicrobial properties. The PVA film containing copper content up to 0.6 wt.% exhibited a strong antimicrobial activity against *E. coli* DH5α, resulting in up to 5-log microbial reduction. The results suggest that TNFC-copper nanoparticles nanocomposites as antimicrobial nanofillers are valuable for PVA applications.

Conflict of Interests

The authors declare that there is no conflict of interests regarding the publication of this paper.

Acknowledgments

Funding for this work was provided by NIFA McStennis WVA00098 "Efficient utilization of biomass for biopolymers in central Appalachia" and USDA NIFA Grant no. 2013-34638-21481 "Development of novel hybrid cellulose nanocomposite film with potent biocide properties utilizing low-quality Appalachian hardwoods."

References

[1] T. Zhong, G. S. Oporto, J. Jaczynski, A. T. Tesfai, and J. Armstrong, "Antimicrobial properties of the hybrid copper nanoparticles-carboxymethyl cellulose," *Wood and Fiber Science*, vol. 45, no. 2, pp. 215–222, 2013.

[2] M. A. Del Nobile, M. Cannarsi, C. Altieri et al., "Effect of Ag-containing nano-composite active packaging system on survival of *Alicyclobacillus acidoterrestris*," *Journal of Food Science*, vol. 69, no. 8, pp. E379–E383, 2004.

[3] J. An, M. Zhang, S. Wang, and J. Tang, "Physical, chemical and microbiological changes in stored green asparagus spears as affected by coating of silver nanoparticles-PVP," *LWT—Food Science and Technology*, vol. 41, no. 6, pp. 1100–1107, 2008.

[4] A. Llorens, E. Lloret, P. A. Picouet, R. Trbojevich, and A. Fernandez, "Metallic-based micro and nanocomposites in food contact materials and active food packaging," *Trends in Food Science & Technology*, vol. 24, no. 1, pp. 19–29, 2012.

[5] H. Liu, J. Song, S. Shang, Z. Song, and D. Wang, "Cellulose nanocrystal/silver nanoparticle composites as bifunctional nanofillers within waterborne polyurethane," *Applied Materials and Interfaces*, vol. 4, no. 5, pp. 2413–2419, 2012.

[6] D. Liu, X. Sun, H. Tian, S. Maiti, and Z. Ma, "Effects of cellulose nanofibrils on the structure and properties on PVA nanocomposites," *Cellulose*, vol. 20, no. 6, pp. 2981–2989, 2013.

[7] A. Isogai, T. Saito, and H. Fukuzumi, "TEMPO-oxidized cellulose nanofibers," *Nanoscale*, vol. 3, no. 1, pp. 71–85, 2011.

[8] A. E. J. de Nooy, A. C. Besemer, and H. van Bekkum, "Selective oxidation of primary alcohols mediated by nitroxyl radical in aqueous solution. Kinetics and mechanism," *Tetrahedron*, vol. 51, no. 29, pp. 8023–8032, 1995.

[9] P. L. Bragd, H. van Bekkum, and A. C. Besemer, "TEMPO-mediated oxidation of polysaccharides: survey of methods and applications," *Topics in Catalysis*, vol. 27, no. 1–4, pp. 49–66, 2004.

[10] H. Fukuzumi, T. Saito, T. Iwata, Y. Kumamoto, and A. Isogai, "Transparent and high gas barrier films of cellulose nanofibers prepared by TEMPO-mediated oxidation," *Biomacromolecules*, vol. 10, no. 1, pp. 162–165, 2009.

[11] G. Rodionova, Ø. Eriksen, and Ø. Gregersen, "TEMPO-oxidized cellulose nanofiber films: effect of surface morphology on water resistance," *Cellulose*, vol. 19, no. 4, pp. 1115–1123, 2012.

[12] E. Ogur, "Polyvinyl alcohol: materials, processing and application," *Rapra Review Reports*, vol. 16, no. 12, pp. 1–130, 2005.

[13] M. S. Peresin, Y. Habibi, J. O. Zoppe, J. J. Pawlak, and O. J. Rojas, "Nanofiber composites of polyvinyl alcohol and cellulose nanocrystals: manufacture and characterization," *Biomacromolecules*, vol. 11, no. 3, pp. 674–681, 2010.

[14] Q. Cheng, S. Wang, T. G. Rials, and S.-H. Lee, "Physical and mechanical properties of polyvinyl alcohol and polypropylene composite materials reinforced with fibril aggregates isolated from regenerated cellulose fibers," *Cellulose*, vol. 14, no. 6, pp. 593–602, 2007.

[15] J. L. Black and J. Jaczynski, "Temperature effect on inactivation kinetics of *Escherichia coli* O157:H7 by electron beam in ground beef, chicken breast meat, and trout fillets," *Journal of Food Science*, vol. 71, no. 6, pp. M221–M227, 2006.

[16] L. Levanduski and J. Jaczynski, "Increased resistance of *Escherichia coli* O157:H7 to electron beam following repetitive irradiation at sub-lethal doses," *International Journal of Food Microbiology*, vol. 121, no. 3, pp. 328–334, 2008.

[17] Association of Official Analytical Chemists International, *AOAC Official Methods of Analysis*, Association of Official Analytical Chemists International, Gaithersburg, Md, USA, 16th edition, 1995.

[18] M. N. Nadagouda and R. S. Varma, "Synthesis of thermally stable carboxymethyl cellulose/metal biodegradable nanocomposites for potential biological applications," *Biomacromolecules*, vol. 8, no. 9, pp. 2762–2767, 2007.

[19] N. A. Amro, L. P. Kotra, K. Wadu-Mesthrige, A. Bulychev, S. Mobashery, and G.-Y. Liu, "High-resolution atomic force microscopy studies of the *Escherichia coli* outer membrane: structural basis for permeability," *Langmuir*, vol. 16, no. 6, pp. 2789–2796, 2000.

[20] A. K. Chatterjee, R. Chakraborty, and T. Basu, "Mechanism of antibacterial activity of copper nanoparticles," *Nanotechnology*, vol. 25, no. 13, Article ID 135101, 12 pages, 2014.

[21] C. E. Santo, P. V. Morais, and G. Grass, "Isolation and characterization of bacteria resistant to metallic copper surfaces," *Applied and Environmental Microbiology*, vol. 76, no. 5, pp. 1341–1348, 2010.

[22] L. Macomber and J. A. Imlay, "The iron-sulfur clusters of dehydratases are primary intracellular targets of copper toxicity," *Proceedings of the National Academy of Sciences of the United States of America*, vol. 106, no. 20, pp. 8344–8349, 2009.

Hindawi Publishing Corporation
BioMed Research International
Volume 2015, Article ID 289759, 10 pages
http://dx.doi.org/10.1155/2015/289759

Research Article

Production by Tobacco Transplastomic Plants of Recombinant Fungal and Bacterial Cell-Wall Degrading Enzymes to Be Used for Cellulosic Biomass Saccharification

Paolo Longoni,[1,2] Sadhu Leelavathi,[3] Enrico Doria,[1,4] Vanga Siva Reddy,[3] and Rino Cella[1]

[1]*Dipartimento di Biologia e Biotecnologie, Università di Pavia, Via Ferrata 9, 27100 Pavia, Italy*
[2]*Dipartimento de Biologie Végétale, Université de Geneva, 30 Quai Ernest Ansermet, Sciences III, 1211 Genève, Switzerland*
[3]*Plant Transformation Group, International Center for Genetic Engineering and Biotechnology, Aruna Asaf Ali Marg, New Delhi 110067, India*
[4]*Centre of Sustainable Livelihood (CSL), Vaal University of Technology, Vanderbijlpark 1900, South Africa*

Correspondence should be addressed to Vanga Siva Reddy; vsreddy@icgeb.res.in and Rino Cella; rino.cella@unipv.it

Received 26 December 2014; Revised 6 April 2015; Accepted 9 April 2015

Academic Editor: Lei Zhao

Biofuels from renewable plant biomass are gaining momentum due to climate change related to atmospheric CO_2 increase. However, the production cost of enzymes required for cellulosic biomass saccharification is a major limiting step in this process. Low-cost production of large amounts of recombinant enzymes by transgenic plants was proposed as an alternative to the conventional microbial based fermentation. A number of studies have shown that chloroplast-based gene expression offers several advantages over nuclear transformation due to efficient transcription and translation systems and high copy number of the transgene. In this study, we expressed in tobacco chloroplasts microbial genes encoding five cellulases and a polygalacturonase. Leaf extracts containing the recombinant enzymes showed the ability to degrade various cell-wall components under different conditions, singly and in combinations. In addition, our group also tested a previously described thermostable xylanase in combination with a cellulase and a polygalacturonase to study the cumulative effect on the depolymerization of a complex plant substrate. Our results demonstrate the feasibility of using transplastomic tobacco leaf extracts to convert cell-wall polysaccharides into reducing sugars, fulfilling a major prerequisite of large scale availability of a variety of cell-wall degrading enzymes for biofuel industry.

1. Introduction

Biofuels are currently obtained from edible vegetable products (sucrose, starch, and triglycerides), but ethical considerations as well as problems of economic sustainability have stimulated the development of second and third generation biofuels derived from nonedible cellulosic biomass and lipogenic unicellular algae [1, 2]. The conversion of plant biomass and cultivation waste (Agri-Waste) into bioethanol is considered a sustainable process as it (1) reduces the dependency on fossil fuels like coal- and petroleum-based products, (2) reduces the negative impact on the environment being a carbon-neutral cycle, (3) allows us to obtain secondary byproducts with application in pharmaceutical and biotechnological industries from the residual biomass. The plant cell wall is a complex structure consisting of a mixture of cellulose, hemicelluloses, and lignin, varying from plant to plant. Cellulose is the most diffuse source of reduced carbon in the world, ranking second only to fossil carbon [3]. In order to convert plant biomass into biofuels, cell-wall macromolecules must be depolymerized to sugar monomers that can be fermented to ethanol or other alcohols with a higher number of carbons through the action of yeast or bacterial strains. Alternatively they can be used as growth substrate for lipogenic microorganisms to obtain lipid to be later transformed in biofuel by different treatments. The current technology adopted to degrade cellulose uses high energy-consuming approaches in order to destroy its stable paracrystalline portion. Several fungi and bacteria synthesize all the enzymes required to degrade cell-wall polysaccharides

to simple sugars or oligosaccharides from which they obtain the energy to support their growth. Some of these microorganisms are thermotolerant and possess enzymes active at medium-high temperatures (60°C), reviewed in [4, 5]. A particularly important need is the availability of large amounts of suitable enzyme cocktails for the saccharification of huge amounts of cellulosic residues and wastes. Current estimates suggest that about 225 M tons of cellulosic biomass/year are available in EU alone [6]. The cost of enzymes used for saccharification is one of the three crucial parameters for the economical sustainability of biofuel production [7, 8].

A number of bacterial and fungal strains able to depolymerize plant cell walls have been described and characterized [9, 10]. However, the expression level of these enzymes by wild-type strains is generally low. The recombinant DNA technology in combination with improved bioreactors has been shown to increase significantly the production of microbial enzymes. Prokaryotic and eukaryotic expression systems based on recombinant DNA approaches have been employed for the production of proteins/enzymes of commercial interest and their advantages and disadvantages evaluated [5, 11–14]. Enzymes used for industrial applications, among which biofuel production is found, are currently produced *via* microbial fermentation even if the process requires high investment, production, and maintenance costs. Several studies show that protein/enzyme production by plant molecular farming might offer some advantages over microorganisms, as plants have both eukaryotic (nuclear) and prokaryotic (chloroplast) expression systems [15–18] that can be used singly or in combination. Transgenic plants were shown to be a valuable system for the production of a variety of antibodies, proteins/enzymes, and vaccines [19]. A large number of genetically modified crops expressing genes encoding insecticidal proteins and enzymes conferring resistance to herbicides are grown all over the world [20]. However, the production of recombinant proteins/enzymes based on nuclear transformation remained a major limitation as the level of recombinant proteins accumulation is generally low. Conversely, a chloroplast-based expression system offers several advantages with respect to the molecular farming notion. Plastid genome (plastome), being prokaryotic in origin, uses operons for the expression of multiple foreign genes under a single promoter. As the integration of transgene constructs takes place through homologous recombination, there is a unique transformation event without any positional effects, contrary to what is observed in the case of nuclear transformation due to random integration of foreign genes into the nuclear genome. Due to independent plastidial transcription, translation, and protein folding machineries, recombinant genes were generally shown to be expressed in chloroplasts at levels higher than that achieved with nuclear-based expression systems [21]. In most plant species, among which *Nicotiana tabacum*, the plastome is inherited maternally thus avoiding transgene dispersion by pollen. Moreover, tobacco, being a nonfood and nonfeed plant, is ideal as a recombinant protein expression system since it does not mix with the food chain, a major issue for regulatory clearances for commercial activities [22]. The low cultivation cost and ease of up-scale production of transplastomic plants (plants with transformed plastid genome) by simply increasing the cultivation area provide additional advantages. More than a decade ago, Leelavathi et al. [15] were the first to demonstrate the feasibility of accumulating a bacterial thermostable xylanase, which has several industrial applications including the biofuel industry, using a chloroplast genetic engineering approach. Later, this approach has been used to express a large number of cellulolytic enzymes [16, 23–26]. Besides pointing to chloroplast transformation as a promising technology for the large scale production of recombinant enzymes, the study of Leelavathi et al. [15] also showed that the plant produced recombinant xylanase retained all biochemical functions, similarly to the native bacterial one. It is also noteworthy that thermostability of recombinant enzymes is a crucial feature since it allows us to partially overlap the cellulose pretreatment process with its digestion.

In the present work we expressed in tobacco chloroplasts five cellulase genes isolated from different microbial organisms and a polygalacturonase gene from *Aspergillus niger*. Leaf extracts containing the recombinant enzymes were tested for their ability to degrade various cell-wall components under different conditions, singly and in combinations. Also the previously described thermostable xylanase [15] was used in combination with cellulases and a polygalacturonase to study the cumulative effect on the depolymerization of complex plant biomass. Our results demonstrate the feasibility of converting cell-wall polysaccharides into reducing sugars using a combination of tobacco cell extracts containing enzymes with compatible temperature and pH optima.

2. Materials and Methods

2.1. Chemicals. All the reagents and chemicals were purchased from Sigma-Aldrich (St. Louis, MO, USA).

2.2. Construction of Chloroplast Plastid Transformation Vectors for the Over Production of Cellulolytic Enzymes in Tobacco. The plastid transformation vector pVSR326 (Figure 1, GenBank acc. number AF527485) was used to clone all genes used in the study. pVSR326 vector contains the *aadA* coding sequence, which confers resistance to both spectinomycin and streptomycin, under the constitutive 16S rRNA promoter and with the terminator of *rbcL* [15, 21].

The DNA sequences of genes encoding the enzymes used in the present study stored in the GenBank are GH6 CHGG_10762 (*Cel6*, exoglucanse) and *gh7* CHGG_08475 (*Cel7*, endoglucanase), GH45 (*EndoV*, endoglucanase) CHGG_08509 of *Chaetomium globosum* [27], GH 5 (*CelK1*, endoglucanase) (GenBank acc. number AAL83749) from *Paenibacillus* sp. KCTC8848P; GH7_CBH-EG *Cel3*, exocellobiohydrolase from *Phanerochaete chrysosporium* (AAB46373); *TF6A* (GenBank acc. number M73321); *Pga2* (GenBank acc. number XM_001397030); *Vlp2* peroxidase (GenBank acc. number XM_001220787). For cloning into transformation vector, gene sequences were either amplified by polymerase chain reaction (PCR) using the primers indicated in Table 1 or got synthesized based on protein sequence.

Table 1

Gene	Forward primer (sequence from 5′-3′)	Reverse primer (sequence from 5′-3′)
Cel7	TGCTACATCACCCCCTTCAT	GTACTTGCGGTGGATGGACT
Cel6	GATGTGGGCCAACGACTACT	GTGGATGGTCAGCTCCTTGT
Cel3	ATGGCACAGCAGGCAGGTACAC	ATAACACTGGCTGTAATACGGATTC
CelK1	ATGGCCAGCGTTAAAGGTTATTACC	TTCTGCTGCTGCTTTTGCCTGTTCTGC
EndoV	TACGCCATGGCTCGCTCTACTCCCATTCTTCG	AGCTGAGCTCTTAAAGGCATTGCGAGTACCAGTCG
Pga2	ATGGACAGCTGCACGTTCACC	CTAACAAGAGGCCACCGAAGG
Vlp2	ATGTCGACCGCAACTCGCACTTTC	TTAGGCGTTGACGGTCTTGAACAC
TF6A	ATGTCCCCCAGACCTCTTCGC	TCAGCTGGCGGCGCAGGTAAG

Alternatively, on the basis of the amino acid sequence available for *celK1* (GenBank acc. number AAL83749) we designed synthetic cDNA according to tobacco chloroplast "codon usage" (http://www.kazusa.or.jp/codon/) to optimize synthesis and accumulation of the relevant enzyme. All sequences were cloned at *Nco*I and *Sac*I sites of pVSR326 (Genbank acc. No. AF527485) by replacing the *uidA* (GUS) reporter gene. Sequences containing an internal *Nco*I restriction site (i.e., *Pga2*) were cloned in two steps. In the first step the C-terminal end of the *Pga2* was cloned as *Nco*I-*Sac*I fragment and then the N-terminal end of the genes was cloned as *Nco*I-*Nco*I fragment. The orientation of the ATG in relation to the C-terminal part was confirmed by PCR and sequencing. All the genes are placed under the *psbA* gene regulatory elements.

2.3. Plant Transformation and Molecular Analysis. Transplastomic tobacco (*Nicotiana tabacum* cv. Petit Havana) plants were obtained using the particle delivery method described earlier [15]. Bombarded leaf explants (T0) were regenerated on selective RMOP medium containing spectinomycin (500 mg/L). Regenerated green shoots obtained 30 days after bombardment were grown to maturity to collect seeds (T1) that were germinated on agar plates containing spectinomycin and streptomycin (500 mg/L, each). In order to obtain homotransplastomic lines, T1 leaf explants were cultured on RMOP medium containing spectinomycin and streptomycin (500 mg/L, each). This process was repeated up to three times (T3).

Southern blot analysis was used to confirm site-specific integration of transgenes and homoplasticity of transplastomic plants. Total genomic DNA was isolated using the Trizol method (Sigma-Aldrich, USA), digested with *Cla*I, separated on 0.8% agarose gel and blotted onto Nylon membranes that after UV irradiation were probed with ^{32}P labeled DNA corresponding to *rbcL-accD* DNA flanking region and to the coding region of the genes of interest. Northern blot analysis was carried out to confirm efficient transcription of all tested genes. In both cases standard procedures were followed for hybridization and washing [28].

2.4. Protein Extraction and Enzyme Activity. Following a preliminary screening of activity with leaves of different age, fully expanded leaves were used to extract the enzymes of interest. Crude leaf homogenates were used in all cases, in view of developing a simple and cost-effective industrial saccharification process. A 1 g leaf sample from each transplastomic plant was cut into small pieces and ground in a mortar with liquid nitrogen and 3 mL of extraction buffer added to the resulting powder. Acetate or phosphate buffer was used in the 4.0–8.0 pH range as indicated. The plant homogenate was then mixed and centrifuged for 10 min at 16,873 ×g and collected the supernatant in a new Eppendorf tube. In order to eliminate the presence of the endogenous sugars that may subsequently interfere with the reducing sugar assay and to concentrate it, the leaf extract was filtered using Vivaspin 500 (28-9322-18) columns with a cut-off of 3 kDa. The concentration of total soluble protein (tsp) was determined using the Bradford reagent (Sigma-Aldrich, USA) according to the manufacturer's instructions. For all enzyme assays a concentration of 0.1 mg/mL of total soluble protein (tsp) content was used.

2.5. Preparation of the Poplar Wood Powder. The poplar wood samples used for laboratory analysis are represented from branches and stem of a poplar clone supplied by the "Franco Alasia Vivai" company, Savigliano (Cuneo), Italy. Before conducting the experiments, the wood samples were dried overnight at 40°C and then cut into small pieces (length 0.5–1 cm; width 2-3 mm; height 1-2 mm) using vineyard scissors. Wood chips were then ground to fine powder using the mill MM301 from Retch at the frequency of 30 vibrations/sec for 20 seconds, repeating each cycle for three times.

2.6. Enzymatic Activity Assays. Cellulase activity was assayed, incubating for 60 min at different temperatures, in 1 mL of the plant extract (0.1 mg/mL, tsp) containing 0.02 g of carboxymethylcellulose (CMC) or microcrystalline cellulose (MCC); xylanase activity was determined incubating the same extract with 0.02 g of xylan in the same experimental conditions used for the previous assay; the same procedure was adopted to test the polygalacturonase activity using polygalacturonic acid or apple pectin as substrates. In order to assess the total hydrolytic activity of the leaf extract, 0.02 g of the wood powder was incubated with 1 mL of plant extract; the amount of released reducing sugars was determined by dinitrosalicylic acid (DNS) method [29]. A fraction of the incubated extract (250 μL) was added to 250 μL of water and to 1.5 mL of DNS reagent in a 2 mL test-tube, boiled for 10 minutes, and then cooled down at room temperature. Sample

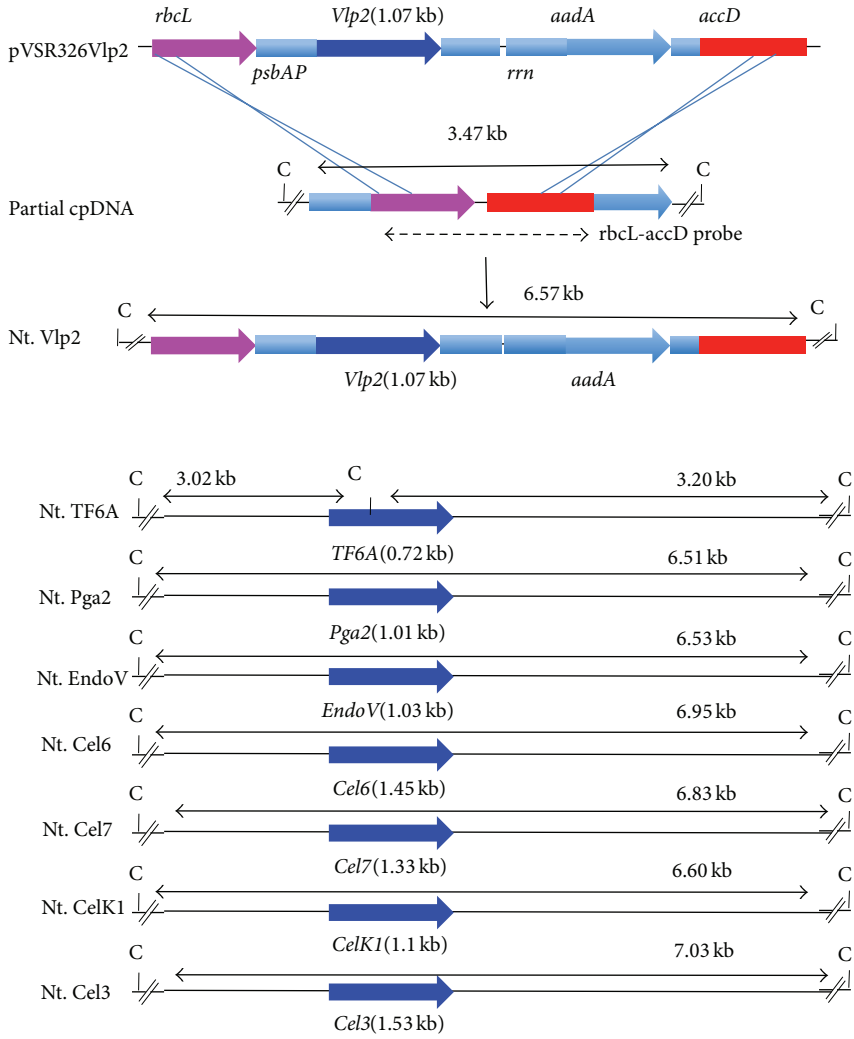

FIGURE 1: Portion of the chloroplast transformation vector map containing the gene coding for Vlp2 (pVSR326Vlp2), integration site of tobacco chloroplast DNA (cpDNA), and the same region in transplastomic tobacco plants are shown. Also restriction map of vectors containing genes coding for other cellulolytic enzymes is shown. All the genes coding for cellulolytic enzymes were put under the expression signals of rice *psbA*. Lines with double arrow indicate the size of DNA fragments after the restriction digestion with *Cla*I restriction enzyme. Dashed arrow indicates the FLK probe (*rbcL-aacD* flanking region) used to confirm site specific integration of transgenes. A possible mechanism for site-specific integration of *aadA* and *Vlp2* through two homologous recombination events (crossed lines) is also shown. Size of the coding region of each gene is shown in brackets.

absorbance at 540 nm was recorded against a water-DNS mixture blank. A glucose calibration curve (0.2–0.5 mg/mL) was used to determine the amount of reducing sugars (mg/g of substrate) after the reaction. Celk1 cellulase activity was tested also using a filter paper as a substrate: disks of filter paper (5 mm of diameter) were incubated at the indicated temperature with 3 mL of the plant extract (pH 5) containing 0.1 mg/mL of protein content. The amount of sugars released was determined by DNS assay after 1.5, 6, and 20 hours of incubation. A control sample was prepared incubating the paper sheet with the same volume of acetate buffer (pH 5). Peroxidase activity of VPL2 was determined spectrophotometrically at 610 nm monitoring the oxidation of phenol red [30].

3. Results

3.1. Vector Construction for the Transformation of Tobacco. Sequences encoding cell-wall degrading enzymes derived from different sources were cloned into pVSR326 vector by replacing the coding region of reporter *uidA* gene with the sequence of interest (Figure 1). pVSR326 vector integrates the transgene cassette into the Single Large Copy region between *rbcL* and *accD* noncoding region in a site specific manner [21]. The recombinant gene encoding the enzyme of interest was placed under the regulation of chloroplast-specific *psbA* gene promoter and terminator (Figure 1). The native *rbc*L-*acc*D region was used as flanking regions for a site-specific integration of transgenes through two possible homologous

Table 2: Activity of various tobacco chloroplast expressed enzymes on carboxymethylcellulose (CMC) and on microcrystalline cellulose (MCC) substrates.

Enzyme	Activity U/mg protein		Type	Generation of plants used in the study
	CMC	MCC		
Cel63	0.3 ± 0.02	0.5 ± 0.03	Exoglucanase	T3
Cel3	0.36 ± 0.02	0.12 ± 0.005	Endoglucanase	T3
CelK1	3.6 ± 0.15	0.2 ± 0.03	Endoglucanase	T3
Cel6	0.16 ± 0.03	0.4 ± 0.05	Exoglucanase	T1
Cel7	0.25 ± 0.009	0.21 ± 0.03	Endoglucanase	T1

recombination events (Figure 1). The pVSR326 contained a selectable *aadA* gene conferring resistance to spectinomycin/streptomycin. The direction and the size of the expected transcripts for all the genes are shown in Figure 1.

3.2. Production of Stable Tobacco Transplastomic Plants. The Bio-Rad Biolistic PDS-1000/He Particle Delivery System was used to transform tobacco chloroplasts [21]. Transplastomic plants were selected under spectinomycin containin medium [15]. Out of 20 leaves bombarded with each construct, about 30–45 green shoots were obtained, 30 days after bombardment on RMOP selection medium. In order to obtain homotransplastomic lines, leaf explants from the regenerated plants were subcultured again on selective RMOP medium. This process was repeated up to three times and the degree of homoplasticity was assessed by southern hybridization. One of cellulase-producing lines T3 lines, *cel3*, turned white and lost its ability to grow autotrophically. Interestingly, these plants could be maintained in the greenhouse in a heteroplasmic state (see Figure S1 in Supplementary Material available online at http://dx.doi.org/10.1155/2015/289759). Severe pleiotropic effects were also observed with plants expressing *Bgl1C*, *Cel6B*, *Cel9A*, and *Xeg74* genes from *Thermobifida fusca* [25] and therefore these lines were not further considered. Southern blot hybridization was used to prove stable and site specific integration of transgenes and the selectable *aadA* gene into the tobacco plastid genome. Hybridization with the flanking region (*rbcL-accD* probe) has confirmed site-specific integration of transgenes into the intergenic region between *rbcL* and *acc*D genes (Figure 2). Absence of any band corresponding to the low molecular weight band observed in the wild type plants is a clear indication for the homotransplastomic nature of their plastome. The stable integration of transgenes into plastid genome was further confirmed by reprobing the blots with gene specific coding sequences as probes. An expected size band was observed in all the transformed plants (Figure 2). The *aadA* gene that confers resistance against spectinomycin and streptomycin was used again to test the progeny for stable inheritance of the transgenes in the T1 generation. All seedlings derived from seeds produced after self-pollinatination are expected to remain green when germinated on plates containing both spectinomycin and streptomycin, if the progeny inherit the selectable *aadA* gene [21]. When the seeds obtained after self-pollination of T0 generation plants were germinated on the agar plates containing both spectinomycin and streptomycin, all seedlings remained green while the seedlings from the wild type untransformed plants turned white, providing evidence for the stable integration and inheritance of the transgenes by the progeny plants (data not shown). Furthermore, northern blot analysis confirmed efficient transcription of transgenes since transcripts of the expected size were found in all the transplastomic plants analyzed (Figure 3). The intensity of the transcript bands suggests efficient transcription of transgenes under *psbA* gene regulatory elements in tobacco chloroplasts. In some cases, in addition to the expected size of transcripts, additional minor bands of higher molecular weight were observed. These might represent transcripts of the same transgenes arising from the *rbcL gene* promoter present upstream to the site of transgene integration.

3.3. Expression of Cell-Wall Degrading Enzymes in Chloroplasts and Their Biochemical Properties. In order to assess the activity of the chloroplast-accumulated enzymes, crude extracts obtained from healthy tobacco plants were tested using commercially available substrates or raw wood.

Among T3 generation plants, those producing CelK1 showed the highest cellulase activity at 60°C in a pH range of 5.0–6.0 and using CMC cellulose as a substrate (Table 2). However, as shown in Figure 4, the amount of reducing sugars released dropped considerably when the temperature was raised to 70°C. Optimal CelK1 enzyme activity was observed at pH 6.0 and 60°C (Figure 4). As for the NT. Vlp2 transplastomic plants, we failed to detect peroxidase activity in leaf homogenates and therefore this transformant was not further considered.

The transplastomic Nt. Pga2 plant expressing *Pga2* showed significant pectinase activity when its leaf extract was tested on apple pectin substrate. The most efficient Pga2 activity was observed in the 6.0–8.0 pH range and at a temperature ranging between 60°C and 70°C; in particular the polygalacturonidase activity was higher at highest temperature and basic conditions (Figure 5(a)). The amount of reducing molecules (galacturonic acid monomers or oligogalacturonides) released at 70°C and pH 8.0 was more than four times the amount of those released at 50°C and pH 7.0, suggesting that the Pga2 is a thermostable enzyme that retained its activity when produced in tobacco chloroplasts (Figure 5(a)). Even when Pga2 was tested using raw popular wood as a substrate, a very high activity was observed at 60°C and pH 8.0 (Figure 5(b)). On the other hand, despite the efficient transcription, no detectable cellulase activity was

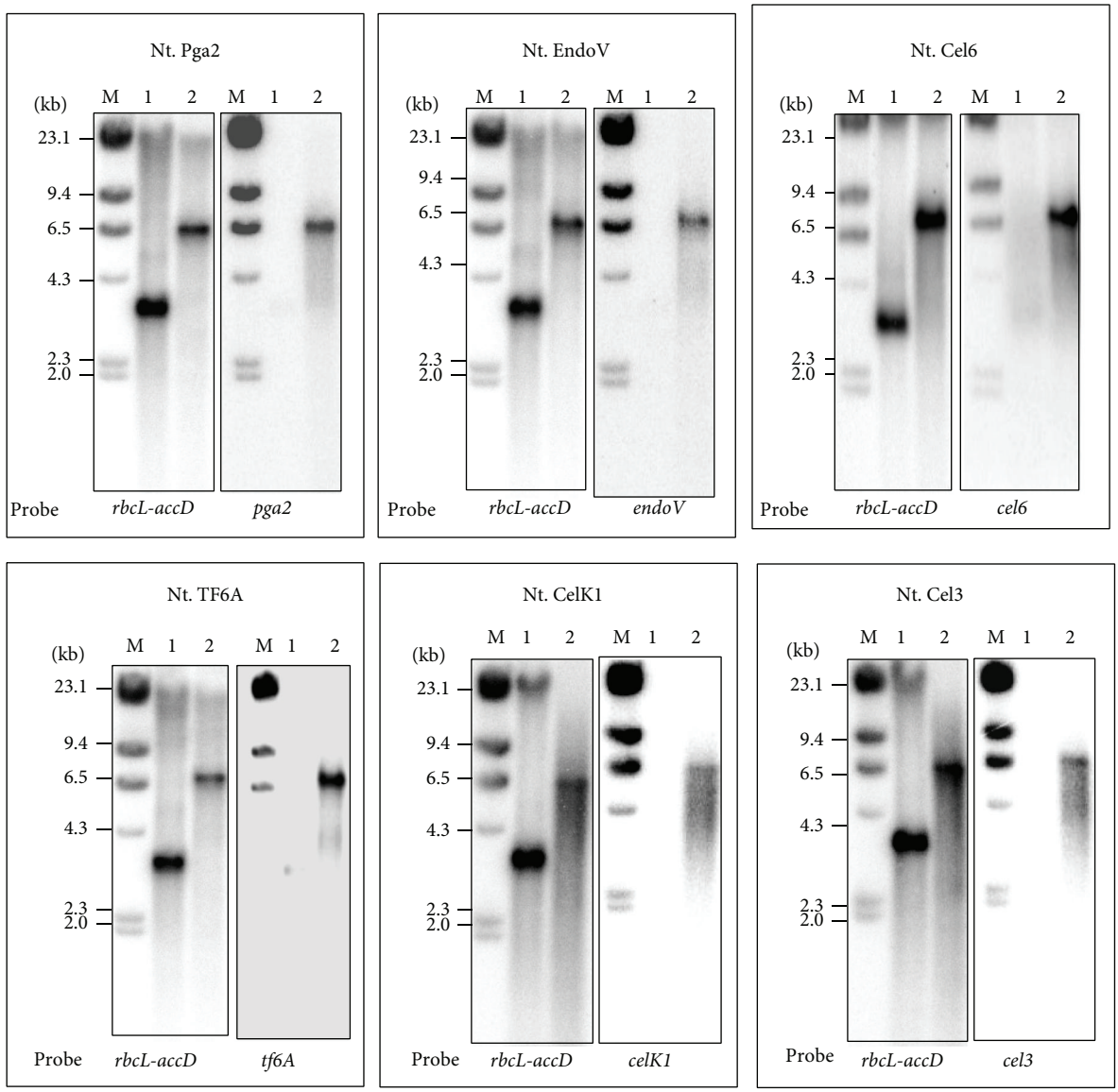

Figure 2: Southern blot hybridization to show site-specific integration of introduced transgenes into tobacco plastid genome for the representative transplastomic plant. The partial coding region of *rbcL* and *accD* was used to show the stable and site specific integration of transgenes. Gene specific DNA probe was also used to confirm the stable integration of the transgene. Note the lack of any untransformed plastid DNA in the transplastomic lines. Molecular marker (M), wild type (1), and transformed (2) plants.

observed in the plants transformed with *Cel6*, *Cel7*, *TF6A*, and *EndoV* genes.

3.4. A Combination of CelK1 and Xylanase (BSX) or Pga2 with Similar Thermostable Properties Improves the Depolymerization of a Complex Cellulosic Biomass. To study the depolymerization of a complex substrate such as poplar wood powder we tested a combination of enzymes in different temperature and pH conditions. CelK1 leaf extract was used in combination with a homogenate obtained from either a previously described line overexpressing a thermostable xylanase (BSX) [15, 18] or a *Pga2* transformed line. Since the final protein concentration in each assay was 0.1 mg/mL, the amount of reducing sugars released from poplar wood when assayed at pH 7 with a mixture of CelK1 and BSX was synergistic as compared to the action of each enzyme alone (Figure 6(a)). The same synergistic effect was also observed when raw wood powder was exposed to the action of a combination of CelK1 and Pga2 (Figure 6(b)). As compared to CelK1 alone, the amount of reducing sugars released increased by more than twofold when Pga2 was present in the reaction mixture. These results cannot be explained only by the fact that the two enzymes use different substrates but rather suggest that the removal of pectin or xylan makes cellulose more accessible to Celk1. On the basis of these encouraging results we tested a mixture of the three enzymes (BSX, Pga2, and CelK1) for the ability to release reducing

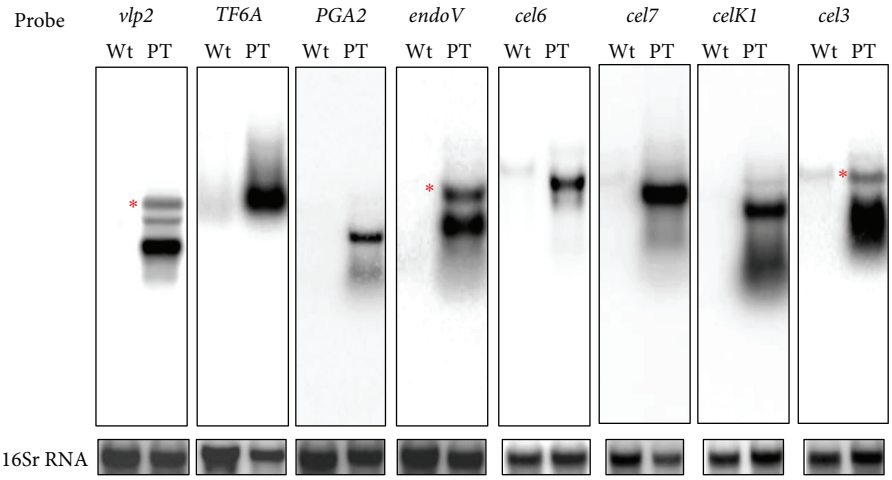

Figure 3: Northern blot analysis showing the expression of transgenes in tobacco chloroplasts. RNA isolated from untransformed control (Wt) and plastid transformed (PT) was separated on formaldehyde-agarose gels, blotted on to the Hybond-N+ membrane, and hybridized with gene specific probes. For the loading control, the same blots were hybridized again with 16S rRNA probe (lower panel): (1) Nt. Vlp2, (2) Nt. TF6A, (3) Nt. Pga2, (4) Nt. EndoV, (5) Nt. Cel6, (6) Nt. Cel7, (7) Nt. CelK1, and (8) Nt. Cel3. The red asterisks indicate the putative longer transcript initiated by the upstream *rbcL* promoter element.

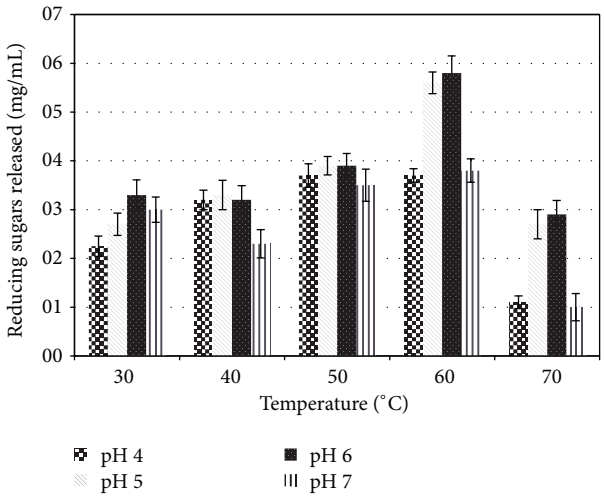

Figure 4: Reducing sugar released by the recombinant endoglucanase Nt CelK1 in different temperature and pH conditions using CMC as a substrate. The final protein concentration in each assay was 0.1 mg/mL. The activity values are expressed as mg/mL of reducing sugars assayed by the DNS method.

sugars. As shown in Figure 7, the best results were obtained at 70°C and pH 8. However, since the temperature optimum of CelK1 is 60°C, it might be advisable to perform the digestion of the biomass in two steps: treat the raw wood powder first with BSX and/or Pga2 at 70°C, and then add Celk1 and continue the incubation at 60°C. As far as the temperature is concerned, this is a particular interesting result since at the industrial process for the production of bioethanol, the woody biomass is subjected to a heat treatment of over 100°C (steam explosion) before the enzyme addition and thus the possibility of adding cell-wall degrading enzymes at 70°C might effectively contribute to reduce the saccharification time and contribute to speed up the industrial process.

4. Discussion

Expression of cell-wall degrading enzymes in plants using a nuclear-based transformation approach is a major challenge as the cellulolytic enzyme(s) can interact with the plant cell wall and thereby interfere with cell growth and plant development [31]. To prevent potentially harmful consequences caused by recombinant cell-wall degrading enzymes, a number of strategies were evaluated among which targeting to subcellular compartments [32], rhizosecretion into hydroponic culture medium [33], and accumulation of a fusion storage proteins in seed oil bodies [34]. However, all these approaches are characterized by a low expression of recombinant enzymes generally associated with nuclear transformation and expression system. Thus, chloroplast transformation was deemed more suitable to obtain a high level of accumulation of recombinant proteins. Although chloroplast transformation offers the possibility of polycistronic transcription, we chose to express a single enzyme per transplastomic plant for two main reasons. First, single cell-wall degrading enzymes find large industrial application. For instance, cellulases are used in the textile industry (stonewashing), [35], while xylanases are used for pulp whitening and animal feed processing [36]. Moreover, the availability of a repertoire of single enzymes allows a better formulation of the most suitable cocktail optimal for each lignocellulosic biomass available (woody biomass, grasses, wastepaper, etc.).

Secondly, whenever an enzyme cocktail is required, the availability of single enzymes offers the possibility to plan the timely addition of different enzymes. For instance, the efficiency at which cell-wall cellulose can be digested will

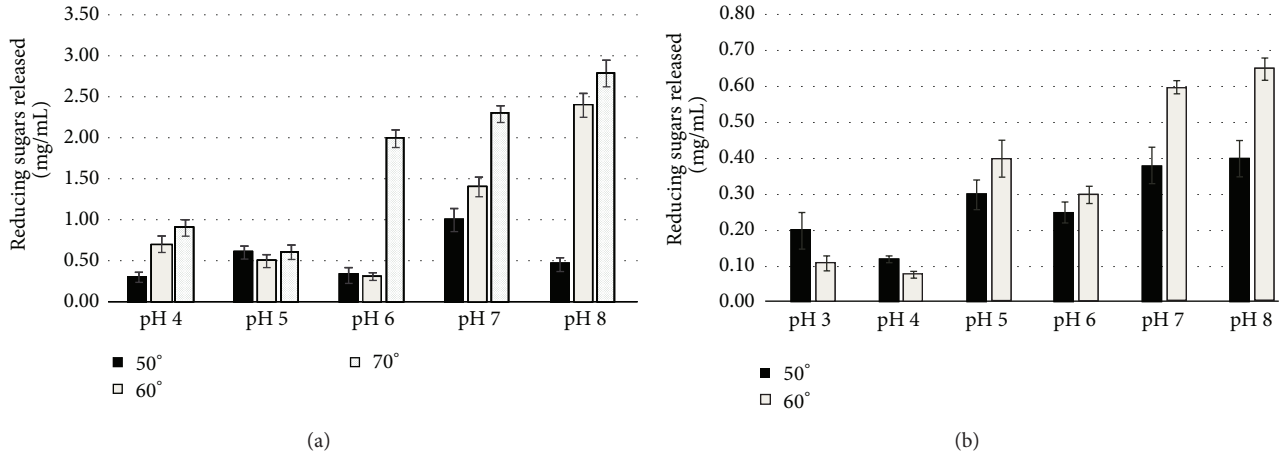

Figure 5: Activity of the recombinant polygalacturonase Nt Pga2 in different pH and temperature conditions using different substrates: (a) apple pectin (Sigma-Aldrich), (b) raw poplar wood. The final protein concentration in each assay was 0.1 mg/mL. The activity values are expressed as mg/mL of reducing sugars.

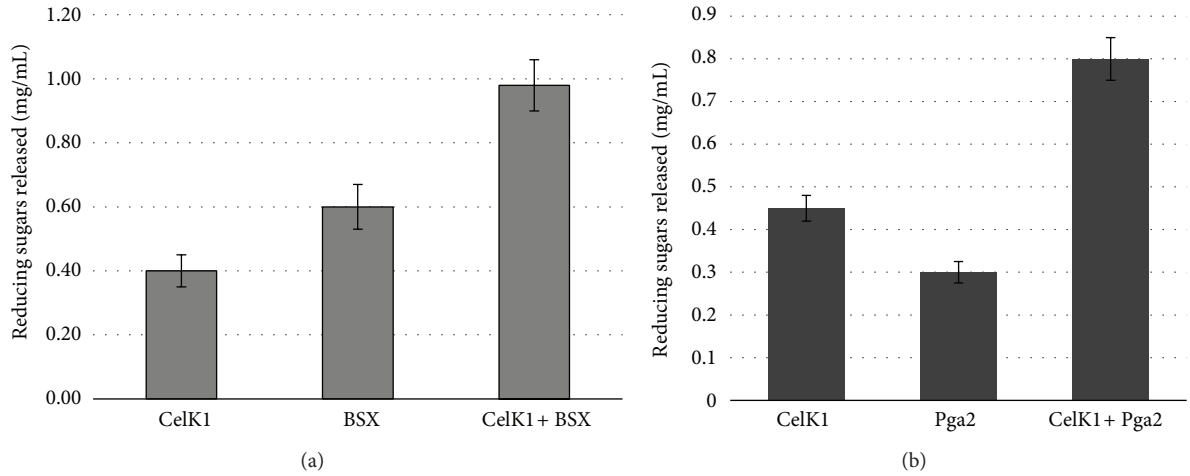

Figure 6: Activity of recombinant Nt CelK1 in combination with recombinant Nt BSX (a) or recombinant Nt Pga2 (b) on raw poplar wood as substrate. The final protein concentration in each assay was 0.1 mg/mL. The activity is expressed as mg/mL of reducing sugars released.

be improved if the biomass is pretreated with a polygalacturonidase before the addition of cellulases. In fact, a combination of CelK1 and PGA2 enzymes showed an additive effect on the release of reducing sugars from poplar wood (Figure 6(b)). Interestingly, when both CelK1 and PGA2 were used together the amount of reducing sugars released increased by more than twofold those suggesting that the removal of pectin by PGA2 is making cellulose more accessible to CelK1.

A third important reason to avoid a simultaneous multiple expression of several genes refers to a possible incompatibility of accumulation of a given protein with chloroplast physiology. In fact, it was observed that plants singly expressing *bgl1C*, *cel6B*, *cel9A*, and *xeg74* genes from *T. fusca* showed severe pleiotropic effects [25]. Therefore, the interference of a single protein with chloroplast biogenesis and/or stability of the photosynthetic apparatus might hamper the expression of the remaining ones.

In the biorefinery process for the production of bioethanol, a pretreatment of plant biomass is required to make cell-wall polymers more accessible to the enzymes required for their deconstruction [37]. Although energy-consuming, such pretreatment, is necessary to reduce the amount of enzymes, which represent the most relevant cost of the entire process [38]. It is tempting to speculate that plant molecular farming, due to the ease of large scale production of recombinant enzymes, might effectively contribute to reduce the saccharification cost.

In conclusion, this study proves that a combination of three enzymes targeting different components of the plant cell wall but having compatible temperature and pH optima not only improves the saccharification of cellulose present in a complex plant biomass but also reduces the number of steps involved in the downstream processing. Our future endeavor would include identification of factors involved in the low or lack of expression/accumulation of beta-glycosidase (*Bgl*)

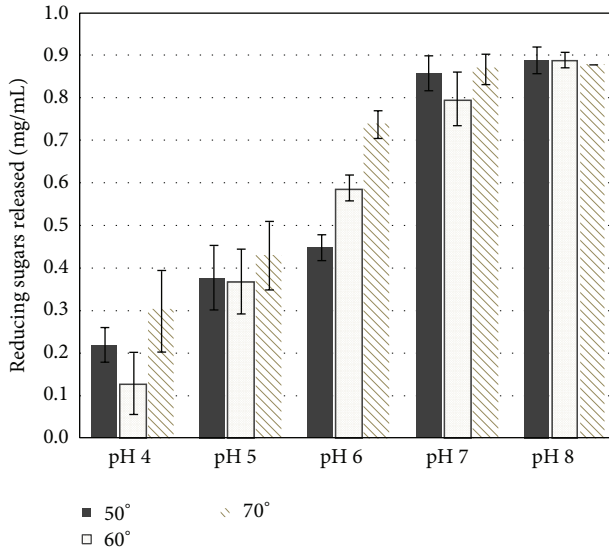

Figure 7: Activity assays of the enzymatic cocktail composed by recombinant Nt BSX, Nt CelK1, and Nt Pga2 in different pH and temperature conditions. Raw popular wood was used as substrate. The activity is expressed as the concentration of reducing sugar released.

and also identify *Bgl* genes from other sources having suitable biochemical properties, in order to improve further the cellulosic biomass saccharification.

Conflict of Interests

The authors declare that there is no conflict of interests regarding the publication of this paper.

Authors' Contribution

Paolo Longoni and Sadhu Leelavathi contributed equally.

Acknowledgments

The authors thank Ranjana Pathak and Abhishek Das for their help in southern and northern analyses. The authors thank Professor Felice Cervone for providing the *Pga2* coding sequence. The authors gratefully acknowledge Fondazione Bussolera-Branca for generous financial support. Also, the authors are thankful to ICGEB and DBT, Government of India. The authors are indebted to Dr. Fabio Pierotti Cei and Professor Roberto Schmid for their continuous support and interest in the work.

References

[1] A. Carroll and C. Somerville, "Cellulosic biofuels," *Annual Review of Plant Biology*, vol. 60, pp. 165–182, 2009.

[2] S. A. Scott, M. P. Davey, J. S. Dennis et al., "Biodiesel from algae: challenges and prospects," *Current Opinion in Biotechnology*, vol. 21, no. 3, pp. 277–286, 2010.

[3] L. R. Lynd, M. S. Laser, D. Bransby et al., "How biotech can transform biofuels," *Nature Biotechnology*, vol. 26, no. 2, pp. 169–172, 2008.

[4] L. E. Taylor, Z. Dai, S. R. Decker et al., "Heterologous expression of glycosyl hydrolases in planta: a new departure for biofuels," *Trends in Biotechnology*, vol. 26, no. 8, pp. 413–424, 2008.

[5] A. L. Demain and P. Vaishnav, "Production of recombinant proteins by microbes and higher organisms," *Biotechnology Advances*, vol. 27, no. 3, pp. 297–306, 2009.

[6] S. Searle and C. Malins, *White Paper—Availability of Cellulosic Residues and Wastes in the EU*, The International Council on Clean Transportation (ICCT), Washington, DC, USA, 2013, http://www.theicct.org/.

[7] R. Wooley, M. Ruth, J. Sheehan, K. Ibsen, H. Majdeski, and A. Galvez, "Lignocellulosic biomass to ethanol process design and economics utilizing co-current dilute acid prehydrolysis and enzymatic hydrolysis current and futuristic scenarios," Tech. Rep. NREL/TP-580-26157, 1999.

[8] V. Lunin, "New cellulase identification method holds promise for lower-cost biofuels," Tech. Rep. NREL/FS-2700-58228, National Renewable Energy Laboratory, 2013.

[9] D. E. Koeck, A. Pechtl, V. V. Zverlov, and W. H. Schwarz, "Genomics of cellulolytic bacteria," *Current Opinion in Biotechnology*, vol. 29, pp. 171–183, 2014.

[10] Z. Zhao, H. Liu, C. Wang, and J.-R. Xu, "Comparative analysis of fungal genomes reveals different plant cell wall degrading capacity in fungi," *BMC Genomics*, vol. 14, no. 1, article 274, 2013.

[11] J. A. Fernández-Robledo and G. R. Vasta, "Production of recombinant proteins from protozoan parasites," *Trends in Parasitology*, vol. 26, no. 5, pp. 244–254, 2010.

[12] D. L. Hacker, M. de Jesus, and F. M. Wurm, "25 years of recombinant proteins from reactor-grown cells—where do we go from here?" *Biotechnology Advances*, vol. 27, no. 6, pp. 1023–1027, 2009.

[13] G. Potvin and Z. Zhang, "Strategies for high-level recombinant protein expression in transgenic microalgae: a review," *Biotechnology Advances*, vol. 28, no. 6, pp. 910–918, 2010.

[14] R. Surzycki, K. Greenham, K. Kitayama et al., "Factors effecting expression of vaccines in microalgae," *Biologicals*, vol. 37, no. 3, pp. 133–138, 2009.

[15] S. Leelavathi, N. Gupta, S. Maiti, A. Ghosh, and V. S. Reddy, "Overproduction of an alkali- and thermo-stable xylanase in tobacco chloroplasts and efficient recovery of the enzyme," *Molecular Breeding*, vol. 11, no. 1, pp. 59–67, 2003.

[16] D. Verma, A. Kanagaraj, S. Jin, N. D. Singh, P. E. Kolattukudy, and H. Daniell, "Chloroplast-derived enzyme cocktails hydrolyse lignocellulosic biomass and release fermentable sugars," *Plant Biotechnology Journal*, vol. 8, no. 3, pp. 332–350, 2010.

[17] N. Scotti, M. M. Rigano, and T. Cardi, "Production of foreign proteins using plastid transformation," *Biotechnology Advances*, vol. 30, no. 2, pp. 387–397, 2012.

[18] L. Pantaleoni, P. Longoni, L. Ferroni et al., "Chloroplast molecular farming: efficient production of a thermostablexylanase by *Nicotiana tabacum* plants and long-term conservation of the recombinant enzyme," *Protoplasma*, vol. 251, pp. 639–648, 2014.

[19] H. Daniell, N. D. Singh, H. Mason, and S. J. Streatfield, "Plant-made vaccine antigens and biopharmaceuticals," *Trends in Plant Science*, vol. 14, no. 12, pp. 669–679, 2009.

[20] J. Clive, "Global status of commercialized biotech/GM crops: 2013," ISAAA Brief no. 46, International Service for the Acquisition of Agri-biotech Applications (ISAAA), Ithaca, NY, USA, 2013.

[21] V. S. Reddy, S. Leelavathi, A. Selvapandiyan et al., "Analysis of chloroplast transformed tobacco plants with cry1Ia5 under rice psbA transcriptional elements reveal high level expression of Bt toxin without imposing yield penalty and stable inheritance of transplastome," *Molecular Breeding*, vol. 9, no. 4, pp. 259–269, 2002.

[22] J. Watson, V. Koya, S. H. Leppla, and H. Daniell, "Expression of *Bacillus anthracis* protective antigen in transgenic chloroplasts of tobacco, a non-food/feed crop," *Vaccine*, vol. 22, no. 31-32, pp. 4374–4384, 2004.

[23] L.-X. Yu, B. N. Gray, C. J. Rutzke, L. P. Walker, D. B. Wilson, and M. R. Hanson, "Expression of thermostable microbial cellulases in the chloroplasts of nicotine-free tobacco," *Journal of Biotechnology*, vol. 131, no. 3, pp. 362–369, 2007.

[24] S. Jung, S. Kim, H. Bae, H.-S. Lim, and H.-J. Bae, "Expression of thermostable bacterial beta-glucosidase (BglB) in transgenic tobacco plants," *Bioresource technology*, vol. 101, no. 18, pp. 7155–7161, 2010.

[25] K. Petersen and R. Bock, "High-level expression of a suite of thermostable cell wall-degrading enzymes from the chloroplast genome," *Plant Molecular Biology*, vol. 76, no. 3–5, pp. 311–321, 2011.

[26] P. Agrawal, D. Verma, and H. Daniell, "Expression of *Trichoderma reesei* β-mannanase in tobacco chloroplasts and its utilization in lignocellulosic woody biomass hydrolysis," *PLoS ONE*, vol. 6, no. 12, Article ID e29302, 2011.

[27] P. Longoni, M. Rodolfi, L. Pantaleoni et al., "Functional analysis of the degradation of cellulosic substrates by a *Chaetomium globosum* endophytic isolate," *Applied and Environmental Microbiology*, vol. 78, no. 10, pp. 3693–3705, 2012.

[28] J. Sambrook, E. F. Fritsch, and T. Maniatis, *Molecular Cloning. A Laboratory Manual*, Cold Spring Harbor Laboratory Press, Cold Spring Harbor, NY, USA, 1989.

[29] T. K. Ghose, "Measurement of cellulase activities," *Pure and Applied Chemistry*, vol. 59, no. 2, 1987.

[30] A. B. Orth, D. J. Royse, and M. Tien, "Ubiquity of lignin-degrading peroxidases among various wood-degrading fungi," *Applied and Environmental Microbiology*, vol. 59, no. 12, pp. 4017–4023, 1993.

[31] K. Herbers, I. Wilke, and U. A. Sonnewald, "A thermostable xylanase from *Clostridium thermocellum* expressed at high levels in the apoplast of transgenic tobacco has no detrimental effects and is easily purified," *Nature Biotechnology*, vol. 13, no. 1, pp. 63–66, 1995.

[32] K. Herbers, H. J. Flint, and U. Sonnewald, "Apoplastic expression of the xylanase and β(1-3,1-4) glucanase domains of the *xyn* D gene from *Ruminococcus flavefaciens* leads to functional polypeptides in transgenic tobacco plants," *Molecular Breeding*, vol. 2, no. 1, pp. 81–87, 1996.

[33] N. V. Borisjuk, L. G. Borisjuk, S. Logendra, F. Petersen, Y. Gleba, and I. Raskin, "Production of recombinant proteins in plant root exudates," *Nature Biotechnology*, vol. 17, no. 5, pp. 466–469, 1999.

[34] J.-H. Liu, L. B. Selinger, K.-J. Cheng, K. A. Beauchemin, and M. M. Moloney, "Plant seed oil-bodies as an immobilization matrix for a recombinant xylanase from the rumen fungus *Neocallimastix patriciarum*," *Molecular Breeding*, vol. 3, no. 6, pp. 463–470, 1997.

[35] A. Miettinen-Oinonen and P. Suominen, "Enhanced production of *Trichoderma reesei* endoglucanases and use of the new cellulase preparations in producing the stonewashed effect on denim fabric," *Applied and Environmental Microbiology*, vol. 68, no. 8, pp. 3956–3964, 2002.

[36] A. D. Harris and C. Ramalingam, "Xylanases and its application in food industry. A review," *Journal of Experimental Sciences*, vol. 1, pp. 1–11, 2010.

[37] M. Sticklen, "Plant genetic engineering to improve biomass characteristics for biofuels," *Current Opinion in Biotechnology*, vol. 17, no. 3, pp. 315–319, 2006.

[38] C. C. Geddes, I. U. Nieves, and L. O. Ingram, "Advances in ethanol production," *Current Opinion in Biotechnology*, vol. 22, no. 3, pp. 312–319, 2011.

Hindawi Publishing Corporation
BioMed Research International
Volume 2015, Article ID 342716, 9 pages
http://dx.doi.org/10.1155/2015/342716

Research Article

Enzymatic Saccharification of Lignocellulosic Residues by Cellulases Obtained from Solid State Fermentation Using *Trichoderma viride*

Tanara Sartori,[1,2] Heloisa Tibolla,[1,2] Elenizi Prigol,[1] Luciane Maria Colla,[1] Jorge Alberto Vieira Costa,[3] and Telma Elita Bertolin[1]

[1]*Laboratory of Fermentations, Course of Food Engineering, School of Engineering and Architecture, University of Passo Fundo, Campus I, 99052900 Passo Fundo, RS, Brazil*
[2]*Department of Food Engineering, School of Food Engineering, University of Campinas, Campinas, SP, Brazil*
[3]*Laboratory of Biochemical Engineering, School of Chemistry and Food, Federal University Foundation of Rio Grande, Rio Grande, RS, Brazil*

Correspondence should be addressed to Telma Elita Bertolin; telma@upf.br

Received 12 November 2014; Revised 26 February 2015; Accepted 3 March 2015

Academic Editor: Lei Zhao

The aim of this study was to verify the viability of lignocellulosic substrates to obtain renewable energy source, through characterization of the cellulolytic complex, which was obtained by solid state fermentation using *Trichoderma viride*. Enzymatic activity of the cellulosic complex was measured during saccharification of substrates filter paper, eucalyptus sawdust, and corncob, and compared with the activity of commercial cellulase. The characterization of the enzymes was performed by a 2^2 Full Factorial Design, where the pH and temperature were the variables of study. Enzymatic saccharification of different substrates appearedviable until 12 to be viable until 12 h; after this period the activity decreased for both enzymatic forms (cellulolytic complex and commercial cellulase). The enzymatic activity of the commercial cellulase was favored with the use of corncob as substrate, while the cellulolytic complex does not show any difference in its specificity by the substrates studied. The largest activities of both enzymes were obtained in the temperature and pH range between 40°C and 50°C and 4.8 and 5.2, respectively. The cellulolytic complex obtained appeared to be viable for the saccharification of lignocellulosic residues compared with the commercial cellulase.

1. Introduction

The growing demand for energy for transportation and industrial processes stimulates the search for new energetic renewable matrixes to replace fossil fuels that have limited reserves, turning feasible the use of agroindustrial residues that besides being abundant reduce the environmental impact [1, 2].

The lignocellulosic biomass is the largest source of carbohydrate, since it is the main plant cellular wall. It consists of lignins chains, cellulose, and hemicellulose, which are intertwined and chemically linked by noncovalent forces and by covalent crossed connections, becoming a substrate of difficult hydrolysis [3, 4].

The cellulolytic enzymes are synthesized by microorganisms like bacteria and fungi. *Cellulomonas fimi*, *Clostridium thermocellum* [5], and *Bacillus subtilis* [6] stand out among the cellulose-producing bacteria. The most studied species of filamentous fungi are *Trichoderma viride* [7], *Aspergillus niger* [8], *Penicillium funiculosum* [9], and *Rhizopus oligosporus* [10]. These enzymes act in synergism breaking glucosidic bonds type β-1.4 from the cellulose chain, resulting in the release of oligosaccharides, cellobiose, and glucose [11].

The greatest difficulty for the use of the lignocellulosic residues is represented by the physical barrier formed by the lignin, which prevents the use of the native cellulose; thus the enzymes cannot penetrate this barrier easily. The separation of the lignin may be achieved through physical, chemical,

or biological treatments or their combination. The chemical treatment is usually used through acid or alkaline hydrolysis [11].

The most used techniques in the cellulose biomass hydrolysis are the chemical and enzymatic methods. The chemical hydrolysis presents advantages because of its high rate and unnecessary pretreatment, but the enzymatic hydrolysis is superior to it, in several aspects, as, for instance, before the possibility to be performed at low temperatures (45°C–50°C) and atmospheric pressure, there is no subproducts formation, increasing the yield of fermentable sugar production. The enzymatic reactions may occur under mild conditions of pH (4.8) not causing corrosion problems in equipment. Thus, to reach high conversion of cellulose it is necessary to have high concentrations of enzymes, increasing the cost of production. Therefore, the study of microorganisms, which produce high productivity cellulases, is very important, as well as the development of economic production techniques [8].

Fermentation in solid state consists in the process of microbial growing in solid substrate, with enough moisture to guarantee the cells growing and metabolism, and does not exceed the maximum retention capacity of water of the solid matrix, that is, exempt of free water [12]. The materials used in the fermentation are resulting from raw materials, products, and/or agroindustrial residues, where these later show low or none commercial value [13].

The filamentous fungi present better capacity of growing under conditions of low levels of water. *Trichoderma* sp. is an important microorganism in the production of cellulases, demonstrating capacity to produce the enzyme from several substrates, like corncob [14, 15], rice straw [16], wheat straw [17], and sugarcane straw [18].

According to Leu and Zhu [19], the efficiency of the enzymatic saccharification depends on factors such as the type of pretreatment of the substrate and the catalytic action of the enzymes (inhibiting effect by the final product formed, deactivation or denaturation due to reaction time, temperature, stirring and pH, synergic actuation of cellulolytic complex enzymes, and enzymes and substrate concentrations). The control of these parameters, aiming at great conditions for the enzymatic hydrolysis, is important so that greater reaction yield is obtained.

In this context, the objective was to study the saccharification of lignocellulosic residues by the cellulases obtained by fermentation in solid state using *Trichoderma viride*, evaluating the enzymatic behavior during the process of saccharification of different substrates (filter paper, eucalyptus sawdust, and corncob) through a 2^2 Full Factorial Design with three center points.

2. Material and Methods

2.1. Microorganism, Maintenance, and Inoculum Preparation. The microorganism used was *Trichoderma viride*, which was obtained from the Tropical Foundation of Researches and Technology André Tosello, Campinas, SP. It was kept in agar filter paper, containing ($g \cdot L^{-1}$) the following: KH_2PO_4, 1.0; $(NH_4)_2SO_4$, 0.5; KCl, 0.5; $MgSO_4 \cdot 7H_2O$, 0.2; $CaCl_2$, 0.1; yeast extract, 0.5; filter paper Whatman number 1, 10.0; agar, 20.0. The maintenance of the cultures was performed in test tubes, which were kept under refrigeration at 4°C.

The inoculum was prepared in Erlenmeyer flasks of 1000 mL with 50 mL of medium agar filter paper, to which 1 mL of spores suspension was added, resulting from the growth in test tubes. The Erlenmeyer flasks were kept in an oven at 30°C for 7 d, for later suspension with the addition of Tween 80 0.1% sterilized, which were filtered in cotton, for later use as inoculum.

2.2. Delignification of the Substrate. The corncob was the substrate used in the fermentation processes, which was delignified according to the method adapted from Sukumaran et al. [8]. The treatment was performed from a substrate concentration (lignified raw material) of 10% (w/v) with alkaline solution (NaOH 0.25 $mol \cdot L^{-1}$). This mixture was placed in stainless steel flasks covered with aluminum foils for later autoclaving, remaining at 121°C for 1 h at 110 kPa. After cooling, the substrate was neutralized with H_2SO_4 1 $mol \cdot L^{-1}$ in the proportion of 0.125 mL_{acid}/mL_{base} until the pH is close to neutralization. The mixture was washed in flowing water in order to remove the excess of reagents by using sieves with opening of 40 mesh so that there is no loss of raw material.

The delignified substrate was submitted to drying in an oven at 35°C during 24 h for total removal of moisture, obtaining a 50% delignified substrate.

2.3. Medium Culture and Fermentation to Obtain the Cellulolytic Complex. The corncob was used as the source of carbon, which was passed through sieve whose opening was 1.18 mm (14 mesh). To this substrate was added 30% (v/w) of macro- and micronutrients solution, adapted from the method described by Aguiar et al. [20], containing ($g \cdot L^{-1}$) KH_2PO_4, 2.0; $(NH_4)_2SO_4$, 1.4; $CO(NH_2)_2$, 0.3; $MgSO_4 \cdot 7H_2O$, 0.3; $CaCl_2$, 0.3; $FeSO_4 \cdot 7H_2O$, 0.005; $MnSO_4$, 0.00156; $ZnSO_4 \cdot 7H_2O$, 0.0014; $CoCl_2 \cdot 6H_2O$, 0.0020. The substrate moisture was adjusted in 63% with distilled water and the pH of the medium was adjusted in 4.8 with acid solution (H_2SO_4 0.5 $mol \cdot L^{-1}$).

Solid state fermentation for the production of cellulolytic enzymes (cellulolytic complex) was carried out in Erlenmeyer flasks of 250 mL with 10 g of medium culture, 0.5 g filter paper, and 1.0 mL of spores suspension (inoculum), containing 10^9 $spores \cdot mL^{-1}$. The concentration of spores in suspension was estimated by counting in microscope, using a Neubauer chamber. The experiments were incubated at 30°C for 192 h.

2.4. Saccharification of Different Substrates by Using the Cellulolytic Complex. The lignocellulosic substrates corncob (C), eucalyptus sawdust (ES), or filter paper (FP) delignified were used in the saccharification assays. The enzymes of the cellulolytic complex (CC) were obtained from the bran of solid state fermentation with *Trichoderma viride*. The commercial cellulase (CE) was used to compare yield of saccharification.

Table 1: Enzymatic activity (U/g) of the cellulolytic complex, obtained from the fermented bran, under pH and temperature conditions tested in the Full Factorial Design with three central points.

Experiment	T (°C)	pH	Substrate		
			Filter paper	Eucalyptus sawdust	Corncob
1	40	4.4	10.634[d]	8.241[c]	9.200[b]
2	40	5.2	9.629[cd]	10.146[d]	10.785[c]
3	60	4.4	8.421[bc]	7.256[b]	8.271[a]
4	60	5.2	7.762[ab]	6.631[a]	8.992[b]
5	50	4.8	6.649[a]	9.391[d]	9.543[b]
6	50	4.8	6.984[a]	10.118[d]	9.359[b]
7	50	4.8	6.880[a]	10.044[d]	9.086[b]

In the same column, different letters mean statistical difference at 5% significance.

The saccharification of the substrates was performed by using a 2^2 Full Factorial Design (FFD) with three central points. The studied variables were temperature and pH, according to the matrix of experiments showed in Table 1.

The experiments were made in Erlenmeyer flasks of 300 mL, containing 5 g of substrate and 75 mL of citrate buffer 0.05 mol·L^{-1}, with pH variable according to the experimental planning. The mixture was submitted to a thermostatic bath (temperature variable according to the factorial design) for 10 min for medium adaptation, after 5 g of fermented bran containing the cellulolytic complex or 5 mL of commercial enzyme with dilution of 1 : 100 (v/v) was added. The saccharification was made during 24 h, without agitation. The experiments were performed in triplicate. The control experiments were performed by using citrate buffer to replace the source of enzymes.

The enzymatic activity of the cellulolytic complex and of the commercial enzyme was evaluated according to the filter paper assay (FPU) adapted from Ghose [21]. Enzyme cellulase is defined as a cellulolytic complex, which is formed by three different enzymes (endoglucanases, exoglucanases, and β-glicosidases). These enzymes act in synergism, in a cooperative association, producing substrates to one another [22, 23].

The efficiency of saccharification was evaluated through the reducing sugars content after filtration, using the 3.5-dinitrosalicylic acid (DNS) method by spectrophotometer at 546 nm, using glucose as standard [24].

The results were showed in units, where one enzymatic unit (U) is defined as a quantity of enzyme which is able to release 1 μmol of reducing sugar per hour under the conditions of the experiment. Equation (1) was used for the calculation of the enzymatic activity:

$$\mathrm{EA} = \mathrm{RS} \cdot \frac{v_e}{E} \cdot \frac{1}{0.18 \cdot t}, \quad (1)$$

where EA is enzymatic activity (U/g or U/mL); RS is concentration of reducing sugars (mg/mL); v_e is volume of extract; E is volume of commercial cellulase (mL) or fermented bran mass (g); t is time of the reaction (h); 0.18 mg/μmol of glucose is released.

2.5. Statistical Analysis. The results of the enzymatic activity obtained in the planning were analyzed through analysis of variance (ANOVA), with the estimated effects and regression coefficients being obtained.

3. Results and Discussion

3.1. Formation of Reducing Sugars and Enzymatic Activity during Saccharification of the Substrates. Figures 1 to 5 present the reducing sugars concentrations formed and the activities of total cellulase during saccharification of the substrates filter paper (FP), corncob (C), and eucalyptus sawdust (ES) by using the cellulolytic complex (CC) obtained by fermentation in solid state and the commercial enzyme (CE).

The cellulolytic complex behavior was similar in all substrates studied during the saccharification period. This behavior was not observed for the commercial cellulase, which presented low conversion values when eucalyptus sawdust was used. Therefore, it was verified that the commercial enzyme has different degrees of specificity among substrates, while the cellulolytic complex did not present difference of specificity among the substrates, since no considerable differences in the values of enzymatic activity among the available substrates were presented (Figures 1(b)–4(b)). To the commercial enzyme, the corncob was the substrate which released greater quantities of reducing sugars, under experimental conditions of the temperature 40°C and pH of 4.4 and 5.2.

It was verified that the greatest enzymatic activities were obtained in initial times of saccharification, regardless of the source of enzyme used (cellulolytic complex or commercial cellulase). A high decrease in enzymatic activity was observed until 12 h of reaction, with later stabilization (Figures 1 to 5). For this reason, until 12 h of saccharification, the reducing sugars formation showed gradual increase, remaining stable after this period. This may be explained by the thermal denaturation of the enzymes and also by the influence of substrate concentration on the enzymatic activity, which according to Michaelis and Mentem predicts that the reaction rates increase because of the substrate concentration until a limit from which it passes to be constant [25, 26]. These results demonstrate that it is not feasible to continue the process of saccharification after 12 h of reaction, because of

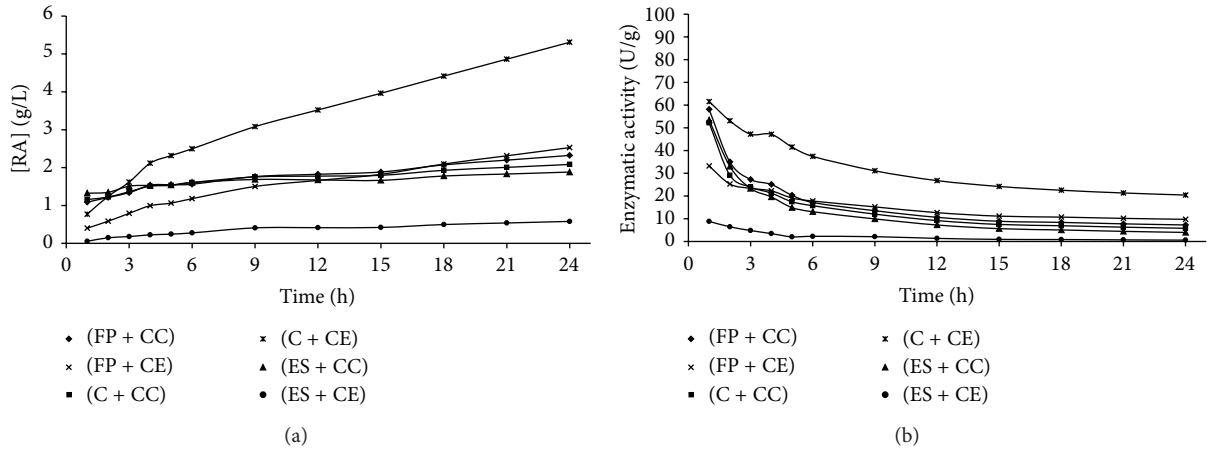

Figure 1: Concentration of reducing sugars formed (a) and enzymatic activity (b) during the time of saccharification, under experimental conditions of the temperature 40°C and pH of 4.4 (Experiment 1), where FP is filter paper, C is corncob, ES is eucalyptus sawdust, CC is cellulolytic complex, and CE is commercial enzyme.

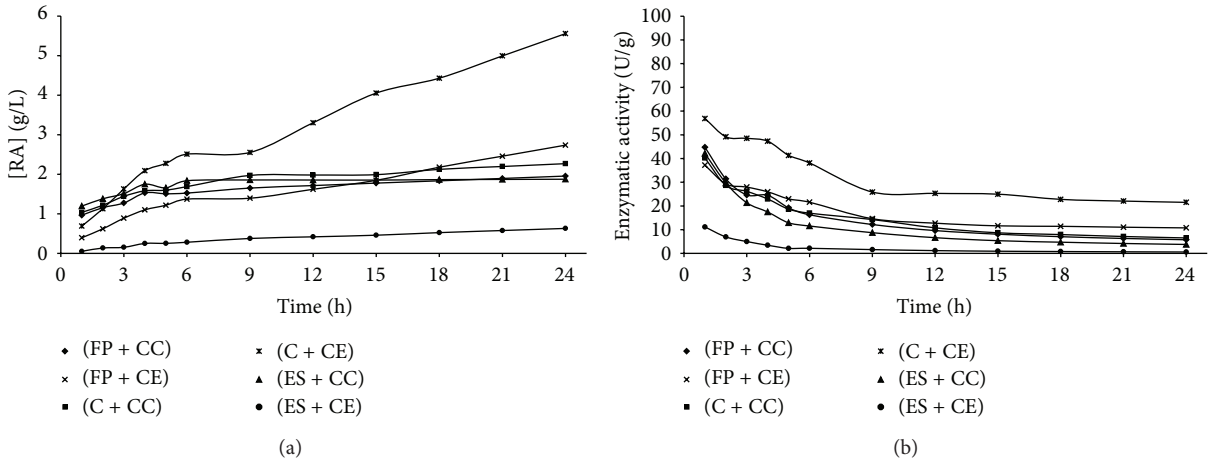

Figure 2: Concentration of reducing sugars formed (a) and enzymatic activity (b) during the time of saccharification, under experimental conditions of the temperature 40°C and pH of 5.2 (Experiment 2), where FP is filter paper, C is corncob, ES is eucalyptus sawdust, CC is cellulolytic complex, and CE is commercial enzyme.

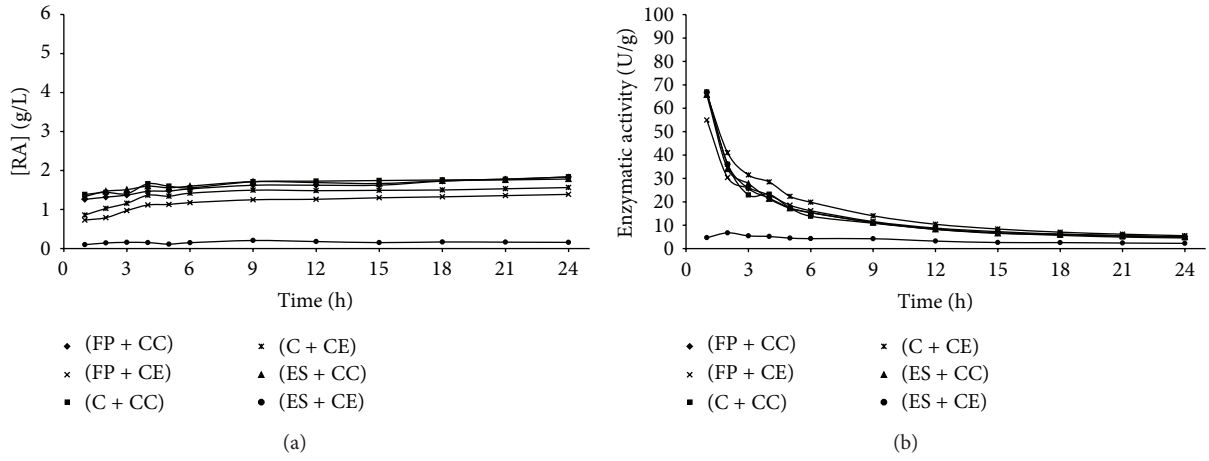

Figure 3: Concentration of reducing sugars formed (a) and enzymatic activity (b) during the time of saccharification, under experimental conditions of the temperature 60°C and pH of 4.4 (Experiment 3), where FP is filter paper, C is corncob, ES is eucalyptus sawdust, CC is cellulolytic complex, and CE is commercial enzyme.

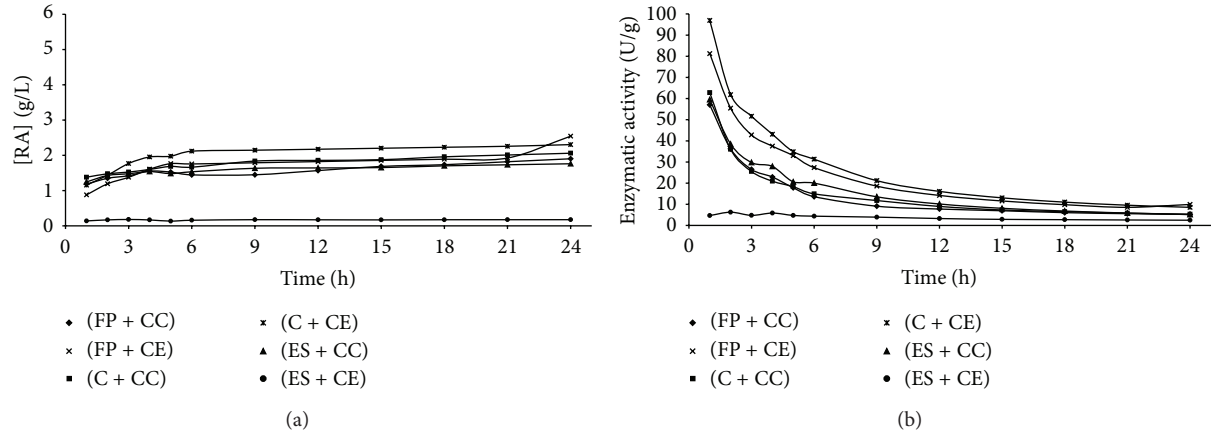

Figure 4: Concentration of reducing sugars formed (a) and enzymatic activity (b) during the time of saccharification, under experimental conditions of the temperature 60°C and pH of 5.2 (Experiment 4), where FP is filter paper, C is corncob, ES is eucalyptus sawdust, CC is cellulolytic complex, and CE is commercial enzyme.

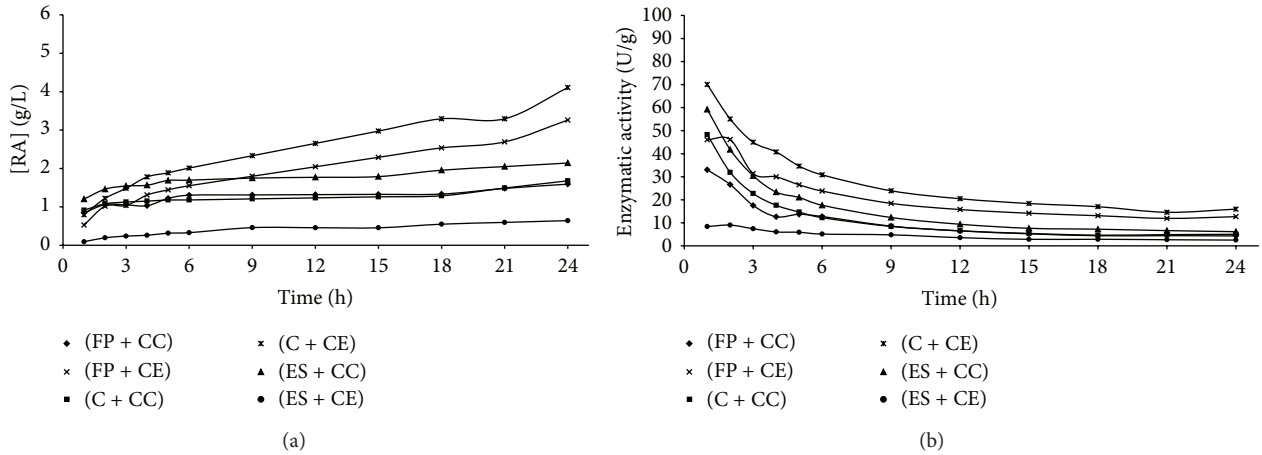

Figure 5: Concentration of reducing sugars formed (a) and enzymatic activity (b) during the time of saccharification, under experimental conditions of the temperature 50°C and pH of 4.8 (Experiment 5), where FP is filter paper, C is corncob, ES is eucalyptus sawdust, CC is cellulolytic complex, and CE is commercial enzyme.

the reduction of the productivity in this period. Table 1 shows the results of the enzymatic activity in 12 h, obtained in saccharification of the filter paper, eucalyptus sawdust, and corncob, by using the cellulolytic complex obtained via SSF.

The maximum enzymatic activity of the cellulolytic complex on filter paper was shown in Experiment 1 (10.634 U/g), with temperature of 40°C and pH 4.4; thus it did not show significant difference ($P > 0.05$) relative to Experiment 2 (9.629 U/g), and this demonstrates that at the lower level of temperature (40°C) the effect of the pH variation was not significant. The same can be observed in Experiments 3 and 4 (60°C), in which the values of enzymatic activity do not show significant difference ($P > 0.05$) with variation of pH, with values of 8.421 U/g and 7.762 U/g, respectively. The results of the enzymatic activity obtained in the central points, performed under conditions mentioned in the literature as great conditions for cellulase action, do not appear to be the best actuation conditions of the cellulolytic complex on the filter paper. So, it can be observed that in one substrate of simple degradation (pure cellulose) the reaction is favored in the lower level of temperature (40°C).

The cellulolytic complex action on eucalyptus sawdust showed maximum enzymatic activity in the lower level of temperature (40°C) and higher level of pH (5.2), with value of 10.146 U/g. These conditions show no significant difference ($P > 0.05$) of the experiments of central points (50°C and pH 4.8).

The saccharification of the corncob substrate by the cellulolytic complex was favored under temperature of 40°C and pH 5.2 and this condition showed significant difference ($P < 0.05$) from the others. According to Marangoni [27], the enzymes present optimal ranges in determined temperature and pH conditions; thus they are characterized by their high specificity. The effect of the pH on the enzymatic activity is due to variations in the ionization state of the components of the system with the pH variation. As enzymes are proteins,

Table 2: Enzymatic activity (U/mL) of the commercial cellulase under the conditions of pH and temperature tested in the 2^2 Full Factorial Design with three central points.

Experiment	T (°C)	pH	Substrate		
			Filter paper	Eucalyptus sawdust	Corncob
1	40	4.4	12.807^{bc}	3.276^{d}	26.87^{b}
2	40	5.2	13.563^{cd}	3.272^{d}	25.308^{b}
3	60	4.4	8.805^{a}	1.369^{b}	10.423^{a}
4	60	5.2	11.315^{b}	1.181^{a}	16.099^{a}
5	50	4.8	15.771^{e}	3.692^{e}	25.456^{b}
6	50	4.8	15.419^{de}	2.914^{c}	26.281^{b}
7	50	4.8	15.528^{de}	3.121^{d}	24.310^{b}

In the same column, different letters mean statistical difference at 5% of significance.

they contain many ionizable groups; hence, the catalytic activity is restrict to a small level of pH.

Annamalai et al. [28] in order to study enzymatic saccharification pretreated rice straw by cellulase produced *Bacillus carboniphilus* CAS 3 utilizing lignocellulosic wastes found that the optimum temperature, pH, and NaCl for enzyme activity were determined as 50°C, 9, and 30% and more than 70% of its original activity was retained even at 80°C, 12, and 35%, respectively. In view of that, the authors suggest that higher temperature, pH, and halo stability of the purified cellulase could be useful for harsh industrial and various biotechnological applications.

Corncob and eucalyptus sawdust substrates show the lowest enzymatic activities in the experiments corresponding to temperature of 60°C. It is verified that the cellulolytic complex obtained a similar behavior in all substrates used, since this enzymatic form has greater performance in temperature between 40°C and 50°C and pH between 4.8 and 5.2. Gokhale et al. [29] observed that the enzymatic activity of cellulases increases gradually until temperature of 50°C and it reduces drastically in the temperature of 60°C, since there is loss of activity in higher temperatures because of the instability of the enzyme molecule. They also verified that the activity reduces when the pH is over 5.1, since the ionizable groups present in the structure of the enzymes make part of the catalytic site. By pH variations of medium, changes occur in its ionic form, resulting in change in the enzymes activity because of the reduction of its specificity.

By comparing maximum enzymatic activities obtained in the experiments of the FFD with the three substrates studied and by using, as source of enzymes, the cellulolytic complex obtained via SSF, it was verified that there was no significant difference ($P > 0.05$) between the averages of the enzymatic activity through the Tukey test at 5% of significance. This demonstrates that the delignification of the eucalyptus sawdust and corncob was efficient, since these substrates are complex, containing high amount of lignin in their original composition (25%), because the enzyme performed in a similar way to the substrate filter paper, presenting a simple composition (pure cellulose) in it.

Table 2 shows the results of the enzymatic activity of the commercial cellulase in the saccharification of the substrates filter paper, eucalyptus sawdust, and corncob.

Maximum enzymatic activities of the commercial cellulase on filter paper were obtained in the experiments of the central points (5, 6, and 7) with maximum value of 15.771 U/mL, at 50°C and pH 4.8, and there was no significant difference between them and Experiment 2 (40°C and pH 5.2), with value of 13.563 U/mL, as it can be observed in Table 2. In the saccharification of the eucalyptus sawdust, the best enzymatic activity was obtained in Experiment 5 (central point), with value of 3.692 U/mL, presenting significant difference from the other experiments ($P < 0.05$).

The commercial cellulase showed greater enzymatic activity in Experiment 1 of 26.787 U/mL using corncob as substrate; however, it did not present significant difference ($P > 0.05$) from Experiment 2, demonstrating that the pH did not influence the activity of this enzyme in intervals tested and at 40°C. The commercial cellulase activity decreases for all substrates with the transition from level −1 (40°C) to +1 (60°C). According to Marangoni [27], the temperature influence on the enzyme activity is represented in terms of activity or rate of reaction. With the increase of temperature an increase of the enzyme activity is observed until a point where the high temperature causes a thermal denaturation and the loss of the enzyme biological activity happens.

Comparing the averages of maximum enzymatic activities obtained in experiments of the FFD with three substrates studied and using the commercial cellulase, through the Tukey test at 5% of significance (15.771 U/mL for the filter paper, 3.692 U/mL for eucalyptus sawdust, and 26.787 U/mL for corncob), it was verified that there was significant difference ($P < 0.05$) between the averages obtained.

The commercial cellulase showed greater specificity with relation to the corncob and then with relation to the filter paper, and it was less specific for eucalyptus sawdust, showing maximum enzymatic activity value for this substrate, approximately 90% lower than the more specific substrate.

According to Sun and Cheng [30], the action of the enzymes may be affected because of the heterogeneity of many lignocellulolytic substrates, commonly used in biochemical processes, since they present varied amounts of cellulose, hemicellulose, and lignin in their biomass composition.

When comparing both forms of cellulase enzyme used, it is observed that the cellulolytic complex from *Trichoderma*

Table 3: Analysis of variance and effects estimated from variables pH and temperature on the enzymatic activity in the experiments of the Full Factorial Design 2^2 with three central points.

Substrates	Source of variation	Cellulolytic complex		Commercial enzyme	
		Effect estimated	Level of significance $P < 0.05$	Effect estimated	Level of significance $P < 0.05$
Filter paper	X_1	−2.040	0.322	−1.225	0.673
	X_2	−0.832	0.663	2.745	0.373
	$X_1 \cdot X_2$	0.173	0.926	2.674	0.384
Eucalyptus sawdust	X_1	−2.250	0.203	−1.972	0.078
	X_2	0.640	0.676	−0.069	0.932
	$X_1 \cdot X_2$	−1.265	0.429	−0.119	0.883
Corncob	X_1	−1.361	0.005	−12.787	0.059
	X_2	1.153	0.009	2.098	0.665
	$X_1 \cdot X_2$	−0.432	0.105	3.578	0.474

viride showed lower enzymatic activities than the commercial cellulase in saccharification of the filter paper (approximately 30% lower) and the corncob (approximately 50% lower) and higher activities for the eucalyptus sawdust substrate, which could be attributed to better endoglucanases and cellobiohydrolases produced by *T. viride* [31]. The cellulase complex secreted by filamentous fungi consists of three major enzyme components, an endo-1,4-β-glucanase (EC 3.2.1.4), a 1,4-β-D-cellobiohydrolase (EC 3.2.1.91), and a 1,4-β-glucosidase (EC 3.2.1.21), which act synergistically. Although *T. reesei* produces cellobiohydrolases and endoglucanases in high quantities, it is deficient in β-glucosidase [32]. The results obtained were satisfactory, because the cellulolytic complex used was the gross product obtained by fermentation in solid state (fermented bran), since it was not submitted to the purification or genetic modification processes of microorganisms.

According to Le Ngoc Huyen et al. [33] the sustainability of ethanol production from lignocellulosic biomass would imply reduction in the consumption of chemicals and/or energetic means but also valorization of the lignocellulosic by-product remaining from enzymatic saccharification. To use lignocellulose as a feedstock, however, pretreatment is necessary to achieve industrially relevant rates of enzymatic saccharification. The pretreatment and enzymatic saccharification processes are costly and the outcomes are not easily predictable. A fundamental understanding of how pretreatment impacts enzyme-substrate interactions, for example, cellulase access to cellulose, can improve the predictability of process outcomes towards overall cost reductions [34].

Table 3 shows the analysis of variance and the effects estimated from variables pH and temperature on the enzymatic activity of the cellulolytic complex and the commercial cellulase, using different substrates in saccharification.

The analysis of variance (Table 3) shows that the enzymatic activity of the cellulolytic complex did not have significant influence ($P > 0.05$) from variables pH and temperature in saccharification of substrates filter paper and eucalyptus sawdust. But as for the corncob, variables temperature and pH were significant ($P < 0.05$). The temperature showed linear effect on the enzymatic activity (−1.361 U/g); that is, by varying the temperature of level +1 (60°C) to −1 (40°C), the enzymatic activity of the cellulolytic complex is favored, while variable pH showed positive linear effect (1.153 U/g); therefore, varying the pH from lower level (4.4) to higher level (5.2), an increase in the enzymatic activity occurs.

The enzymatic activity of the commercial cellulase on substrates filter paper and eucalyptus sawdust was not significantly influenced by variables pH and temperature ($P > 0.05$). With relation to substrate corncob, variable temperature influenced significantly, considering a confidence level of 90% ($P = 0.06$) in the enzymatic activity of the commercial cellulase, presenting a negative linear effect (−12.787 U/mL); that is, by transition from the temperature of the lower level, an increase in the catalytic reaction rate occurred.

4. Conclusions

The enzymes of the cellulolytic complex and the commercial cellulase present better activity and stability between 40°C and 50°C, and the enzymatic activity is not significantly influenced at pH (4.4–5.2). Considering the effect of the temperature on the enzymatic activity, the enzymes of the cellulolytic complex are less affected by the increase of temperature than the commercial cellulase enzyme. The cellulolytic complex shows high specificity for pure substrate as well as for complex substrates such as delignified corncob and eucalyptus. On the other hand, the commercial cellulase is more specific to corncob, followed by the pure substrate (filter paper). The results obtained demonstrate that fungi *Trichoderma viride* has cellulolytic potential to be used in bioprocesses that aim at obtaining enzymes for later use for bioconversion of cellulose into glucose. This produced enzyme shows viability in comparison with the commercial cellulase enzyme. The synthesis of cellulases by microorganisms from lignocellulosic residues is a process of great interest, representing the search for renewable sources to replace the fossil energetic matrix.

Conflict of Interests

The authors declare that there is no conflict of interests regarding the publication of this paper.

Acknowledgment

Financial support for this research was received from the Foundation Support Research of Rio Grande do Sul (FAPERGS, Notice PROCOREDES).

References

[1] C. Menezes, I. Silva, and L. Durrant, "Bagaço de cana: fonte para produção de enzimas ligninocelulolíticas," *Estudos Tecnológicos em Engenharia*, vol. 5, no. 1, pp. 68–78, 2009.

[2] V. F. N. Silva, P. V. Arruda, M. G. A. Felipe, A. R. Gonçalves, and G. J. M. Rocha, "Fermentation of cellulosic hydrolysates obtained by enzymatic saccharification of sugarcane bagasse pretreated by hydrothermal processing," *Journal of Industrial Microbiology & Biotechnology*, vol. 38, no. 7, pp. 809–817, 2011.

[3] J. X. Heck, P. F. Hertz, and M. A. Z. Ayub, "Cellulase and xylanase production by isolated amazon *Bacillus* strains using soybean industrial residue based solid-state cultivation," *Brazilian Journal of Microbiology*, vol. 33, no. 3, pp. 213–218, 2002.

[4] C. Sánchez, "Lignocellulosic residues: biodegradation and bioconversion by fungi," *Biotechnology Advances*, vol. 27, no. 2, pp. 185–194, 2009.

[5] V. S. Bisaria, "Bioprocessing of agro-residues to glucose and chemicals," in *Bioconversion of Waste Materials to Industrial Products*, M. A. Martin, Ed., pp. 187–223, Elsevier, London, UK, 1991.

[6] M. S. Akhtar, M. Saleem, and M. W. Akhtar, " Saccharification of lignocellulosic materials by the cellulases of *Bacillus subtilis*," *International Journal of Agriculture & Biology*, vol. 3, no. 2, pp. 199–202, 2001.

[7] S. P. Gautam, P. S. Bundela, A. K. Pandey, Jamaluddin, M. K. Awasthi, and S. Sarsaiya, "Optimization of the medium for the production of cellulase by the *Trichoderma viride* using submerged fermentation," *International Journal of Environmental Sciences*, vol. 1, no. 4, pp. 656–665, 2014.

[8] R. K. Sukumaran, R. R. Singhania, G. M. Mathew, and A. Pandey, "Cellulase production using biomass feed stock and its application in lignocellulose saccharification for bio-ethanol production," *Renewable Energy*, vol. 34, no. 2, pp. 421–424, 2009.

[9] R. N. Maeda, C. A. Barcelos, L. M. M. S. Anna, and N. Pereira, "Cellulase production by *Penicillium funiculosum* and its application in the hydrolysis of sugar cane bagasse for second generation ethanol production by fed batch operation," *Journal of Biotechnology*, vol. 163, no. 1, pp. 38–44, 2013.

[10] M. Karmakar and M. M. Ray, "Extra cellular endoglucanase production by *Rhizopus oryzae* in solid and liquid state fermentation of agro wastes," *Asian Journal of Biotechnology*, vol. 2, no. 1, pp. 27–36, 2010.

[11] T. L. Ogeda and D. F. S. Petri, "Hidrólise Enzimática de Biomassa," *Química Nova*, vol. 33, no. 7, pp. 1549–1558, 2010.

[12] A. Pandey, C. R. Soccol, and D. Mitchell, "New developments in solid state fermentation. I-bioprocesses and products," *Process Biochemistry*, vol. 35, no. 10, pp. 1153–1169, 2000.

[13] S. R. Couto and M. Á. Sanromán, "Application of solid-state fermentation to food industry—a review," *Journal of Food Engineering*, vol. 76, no. 3, pp. 291–302, 2006.

[14] X. Liming and S. Xueliang, "High-yield cellulase production by *Trichoderma reesei* ZU-02 on corn cob residue," *Bioresource Technology*, vol. 91, no. 3, pp. 259–262, 2004.

[15] M. Chen, L. Xia, and P. Xue, "Enzymatic hydrolysis of corncob and ethanol production from cellulosic hydrolysate," *International Biodeterioration & Biodegradation*, vol. 59, no. 2, pp. 85–89, 2007.

[16] S. Lee, Y. Jang, Y. M. Lee et al., "Rice straw-decomposing fungi and their cellulolytic and xylanolytic enzymes," *Journal of Microbiology and Biotechnology*, vol. 21, no. 12, pp. 1322–1329, 2011.

[17] I. Ahmed, M. A. Zia, and H. M. N. Iqbal, "Bioprocessing of proximally analyzed wheat straw for enhanced cellulase production through process optimization with *Trichoderma viride* under SSF," *International Journal of Biological and Life Sciences*, vol. 6, no. 3, pp. 164–170, 2010.

[18] S. A. Jabasingh, "Response surface methodology for the evaluation and comparison of cellulase production by *Aspergillus nidulans* SU04 and *Aspergillus nidulans* MTCC344 cultivated on pretreated sugarcane bagasse," *Chemical and Biochemical Engineering Quarterly*, vol. 25, no. 4, pp. 501–511, 2011.

[19] S.-Y. Leu and J. Y. Zhu, "Substrate-related factors affecting enzymatic saccharification of lignocelluloses: our recent understanding," *Bioenergy Research*, vol. 6, no. 2, pp. 405–415, 2013.

[20] M. M. Aguiar, L. F. R. Ferreira, and R. T. R. Monteiro, "Use of vinasse and sugarcane bagasse for the production of enzymes by lignocellulolytic fungi," *Brazilian Archives of Biology and Technology*, vol. 53, no. 5, pp. 1245–1254, 2010.

[21] T. K. Ghose, "Measurament of cellulase activities," *Pure and Applied Chemistry*, vol. 59, no. 2, pp. 257–268, 1987.

[22] C. J. Yeoman, Y. Han, D. Dodd, C. M. Schroeder, R. I. Mackie, and I. K. O. Cann, "Thermostable enzymes as biocatalysts in the biofuel industry," in *Advances in Applied Microbiology*, vol. 70, chapter 1, pp. 1–55, Academic Press, New York, NY, USA, 2010.

[23] Y.-H. P. Zhang, M. E. Himmel, and J. R. Mielenz, "Outlook for cellulase improvement: screening and selection strategies," *Biotechnology Advances*, vol. 24, no. 5, pp. 452–481, 2006.

[24] G. L. Miller, "Use of dinitrosalicylic acid reagent for determination of reducing sugar," *Analytical Chemistry*, vol. 31, no. 3, pp. 426–428, 1959.

[25] S. M. Linton and P. Greenaway, "Presence and properties of cellulase and hemicellulase enzymes of the gecarcinid land crabs *Gecarcoidea natalis* and *Discoplax hirtipes*," *The Journal of Experimental Biology*, vol. 207, no. 23, pp. 4095–4104, 2004.

[26] A. L. Lehninger, D. D. L. Nelson, and M. M. Cox, *Lehninger Principles of Biochemistry*, W. H. Freeman, New York, NY, USA, 2005.

[27] A. G. Marangoni, *Enzyme Kinetics: A Modern Approach*, John Wiley & Sons, New York, NY, USA, 2003.

[28] N. Annamalai, M. V. Rajeswari, and T. Balasubramanian, "Enzymatic saccharification of pretreated rice straw by cellulase produced from *Bacillus carboniphilus* CAS 3 utilizing lignocellulosic wastes through statistical optimization," *Biomass and Bioenergy*, vol. 68, pp. 151–160, 2014.

[29] A. A. Gokhale, J. Lu, and I. Lee, "Immobilization of cellulase on magnetoresponsive graphene nano-supports," *Journal of Molecular Catalysis B: Enzymatic*, vol. 90, pp. 76–86, 2013.

[30] Y. Sun and J. Cheng, "Hydrolysis of lignocellulosic materials for ethanol production: a review," *Bioresource Technology*, vol. 83, no. 1, pp. 1–11, 2002.

[31] T. Q. Lan, D. Wei, S. T. Yang, and X. Liu, "Enhanced cellulase production by *Trichoderma viride* in a rotating fibrous bed bioreactor," *Bioresource Technology*, vol. 133, pp. 175–182, 2013.

[32] F. Xu, J. Wang, S. Chen et al., "Strain improvement for enhanced production of cellulase in *Trichoderma viride*," *Applied Biochemistry and Microbiology*, vol. 47, no. 1, pp. 53–58, 2011.

[33] T. Le Ngoc Huyen, M. Queneudec T'Kint, C. Remond, B. Chabbert, and R.-M. Dheilly, "Saccharification of Miscanthus x giganteus, incorporation of lignocellulosic by-product in cementitious matrix," *Comptes Rendus—Biologies*, vol. 334, no. 11, pp. 837.e1–837.e11, 2011.

[34] N. Karuna, L. Zhang, J. H. Walton et al., "The impact of alkali pretreatment and post-pretreatment conditioning on the surface properties of rice straw affecting cellulose accessibility to cellulases," *Bioresource Technology*, vol. 167, pp. 232–240, 2014.